TRANSCRIPTIONAL PROPERTIES OF MEOX2

BY

Mona M.T. Friesen

A Thesis submitted to
the Faculty of Graduate Studies
In Partial Fulfillment of the Requirements for the Degree of

MASTER OF SCIENCE

Department of Biochemistry and Medical Genetics
Faculty of Medicine
University of Manitoba
Division of Stroke and Vascular Disease
St. Boniface General Hospital Research Centre
Winnipeg, Manitoba

TRANSCRIPTIONAL PROPERTIES OF MEOX2

BY

Mona M.T. Friesen

A Thesis submitted to
the Faculty of Graduate Studies
In Partial Fulfillment of the Requirements for the Degree of

MASTER OF SCIENCE

Department of Biochemistry and Medical Genetics
Faculty of Medicine
University of Manitoba
Division of Stroke and Vascular Disease
St. Boniface General Hospital Research Centre
Winnipeg, Manitoba

THE UNIVERSITY OF MANITOBA

FACULTY OF GRADUATE STUDIES

*****

COPYRIGHT PERMISSION

"Transcriptional Properties of Meox2"

BY

Mona M.T. Friesen

A Thesis/Practicum submitted to the Faculty of Graduate Studies of The University of Manitoba in partial fulfillment of the requirement of the degree

Of

MASTER OF SCIENCE

TABLE OF CONTENTS

ABSTRACT

Meox2 induces cell cycle arrest and it is postulated that Meox2 is required for maintaining adult vascular smooth muscle cells (VSMCs) in a quiescent state. Upon vascular injuries, such as atherosclerosis, VSMCs transform from a quiescent, contractile phenotype to a proliferative phenotype. Downregulation of Meox2 expression is observed during this phenotypic transformation.

Currently, direct Meox2 downstream targets are unknown. However, we hypothesize that Meox2 can act as a transcription factor. The aim of this investigation was to examine the transcriptional properties of Meox2.

Our results demonstrated that Meox1 and Meox2 do not require binding to DNA to activate the *p21* promoter. Conversely, *Bapx1* promoter activation is dependent on Meox2-DNA interaction. This study is the first to report that the Meox1 and Meox2 proteins regulate the same downstream target genes and that the mechanism of this regulation is promoter-specific.

ACKNOWLEDGEMENTS

The following work could not have been accomplished without the help and support of many people and organizations. First of all, I am very grateful for the training I have received from my advisor, Dr. Jeffrey Wigle. I also appreciated the contributions of all the Wigle lab members to this work and their friendship over the years. My committee members have also been very instrumental in ensuring my success in the Masters program: Thank you very much to Dr. Nasrin Mesaeli and Dr. David Eisenstat for your suggestions and support. I have also been fortunate to have received funding and scholarships from various organizations during the course of my studies, including the Manitoba Health Research Council, the Department of Biochemistry and Medical Genetics and the University of Manitoba Students Union. I would also like to extend special thanks to the members of the Division of Stroke and Vascular Disease and the St. Boniface General Hospital Research Centre.

De plus, j'aimerais remercier mon cher Eric. Sans toi je n'aurai pas pu poursuivre ce programme jusqu'à ça fin. Tu as été la avec moi a chaque étape, ton encouragement et ton amour m'ont souvent porté a travers les temps les plus difficiles. Je te remercie infiniment.

LIST OF FIGURES

LIST OF TABLES

LIST OF ABBREVIATIONS

AD = Activation domain
Ad-*Meox2* = Adenovirus construct encoding Meox2
Ang II = (Angiotensin II)
ASK1 = Apoptosis signalling regulating kinase
BrdU = 5-bromo-2-deoxyuridine
CDK = Cyclin dependent kinase
CDKI = Cyclin dependent kinase inhibitor
Cip1 = Cdk-interacting protein 1
CNP = C-Type Natriuretic Peptide
d.p.c = Days post coitus
DBD = DNA binding domain
EGFP = Enhanced green fluorescent protein
EMSAs = Electrophoretic mobility shift assays
Eng = Engrailed
FACS = Fluorescent activated cell sorting
HEK293 = Human embryonic kidney cells
HUVECs = Human umbilical vein endothelial cells
IPTG = Isopropyl-beta-D-thiogalactopyranoside
MBP = Maltose binding protein
MEFs = Mouse embryonic fibroblasts
Mt = Mutant
NIH/3T3 = Mouse fibroblast cell line
NLS = Nuclear localization sequence
Pax = Paired box homeobox gene
Pax3 = Paired box protein
PBS = Phosphate buffered saline
PBS-T = Phosphate buffered saline with Tween
PCNA = Proliferating cellular nuclear antigen
Rb = Retinoblastoma
RD = Repressor domain
shh = Sonic hedgehog
TBS = Tris buffered saline
TBS-T = Tris buffered saline with Tween
TUNEL = TdT-mediated dUTP-fluorescein nick-end labeling
VEGF = Vascular Endothelial Growth Factor
VSMCs = Vascular smooth muscle cells
WAF1 = Wild-type p53-activated fragment

A) LITERATURE REVIEW

I) Cardiovascular disease

Adult vascular smooth muscle cells (VSMCs) are normally quiescent, contractile cells but these cells can undergo a phenotypic switch and adopt a synthetic (less differentiated), proliferative phenotype. This phenotype switch occurs during natural biological processes such as embryonic development, responses to injury, or vessel remodeling induced by changes in tissue demands [1]. Increases in VSMC proliferation contributes to the progression of many pathological conditions such as atherosclerosis, hypertension, post-angioplasty restenosis and coronary artery transplant vasculopathy [1, 3-6]. In vasculoproliferative diseases such as restenosis, VSMC growth contributes to the stenosis of the blood vessel by forming the neointimal layer [4, 5].

The mechanisms that induce the VSMC phenotypic switch vary due to the heterogeneous nature of blood vessels within the body [1]. Signaling by both autocrine molecules such as platelet derived growth factor, fibroblast growth factor, epidermal growth factors, angiotensin II and paracrine molecules (i.e. nitric oxide and endothelin-1) secreted by adjacent endothelial cells, monocytes, fibroblasts and dendritic cells play a role in mediating the phenotypic switch [1]. As well, stimuli such as hypoxia, mechanical forces and reactive oxygen species are involved in the activation of VSMCs [1, 7-10]. A better understanding of how these signals converge to regulate VSMC cell cycle progression is identifying potential new therapeutic targets for use in the treatment of vasculoproliferative diseases. Conventional therapies largely treat the symptoms which result from an established vascular lesion rather than by targeting the underlying mechanisms involved in lesion formation [3]. Furthermore, understanding how the cell

cycle is regulated in VSMCs may also be a useful approach to prevent the vascularization of tumors which is crucial for both tumor growth and dissemination [11, 12].

Cardiomyocytes proliferate at a very low rate in the healthy adult and this low rate of proliferation cannot be induced sufficiently to regenerate the cardiac muscle lost following insults such as a myocardial infarction [13]. An understanding of how the cell cycle is controlled in cardiomyocytes could provide the basis for the development of therapies aimed at myocardial reconstitution [14-17]. Manipulating the function or level of molecules that either promote cell cycle entry or the down-regulation of molecules that inhibit cell cycle entry would be beneficial for repairing the damaged myocardium [14-17].

II) The cell cycle

1. Five phases

The cell cycle is a tightly regulated process by which a cell grows, duplicates its genomic DNA and separates into two identical daughter cells. The cell cycle includes five stages; three Gap phases (G-phases), the S-phase and the M-phase (Figure 1). Quiescent cells in the G_0 gap phase enter the G_1 phase following stimulation by mitogens or growth factors. During the G_1 phase, cells synthesize the mRNA and proteins required for duplicating their DNA during the S-phase. In the following phase, G_2, cells produce the mRNA and protein necessary for the M-phase (mitosis). Mitosis includes karyokinesis and cytokinesis, the separation of the DNA and the daughter cells respectively.

2. Cell cycle checkpoints

Transitions through the different phases of the cell cycle are regulated by several checkpoints. These checkpoints ensure that the environment is favorable for replication by assessing positive and negative signals. Also, they ensure the sequential order of events by establishing that each step is finished before the next step begins and that DNA is faithfully replicated [18, 19]. Transition past these checkpoints is controlled by positive and negative regulators. Positive regulation is provided by the association of cyclins with, and the activation of, their respective cyclin dependent kinases (CDKs) (see Figure 1). CDK levels are constant during the different phases of the cell cycle. However, the activity of these molecules is regulated by phosphorylation and dephosphorylation by CDK-activating kinases and phosphatases respectively [20-22]. Previously, it was believed that CDKs must bind cyclins in order to be activated. Cyclin protein levels are regulated by their synthesis, degradation and nuclear transport and they exhibit a cyclic expression pattern during the cycle. [3, 23]. The activated cyclin-CDK complexes then phosphorylate other effector molecules such as histones and the retinoblastoma (Rb) pocket-proteins [3]. Recent results suggest that CDKs can also be positively regulated by cell-type specific proteins other than cyclins. Examples of such proteins are the Speedy/Ringo proteins and p35 [24-27]. These proteins do not share any homology with the cyclins but can selectively bind specific CDKs and activate them independent of cyclin binding [25, 28].

For example, the association of cyclinD-CDK4 and cyclinE-CDK2 in G_1 leads to the phosphorylation of hypo-phosphorylated Rb. Hypo-phosphorylated Rb binds to and inactivates the E2F transcription factors. Phosphorylation of Rb disassociates the Rb-E2F

complex and the free E2F then binds and activates the promoters of genes needed for entry into S-phase [29].

Negative regulation of the cell cycle is provided by CDK inhibitors (CDKIs) such as $p21^{WAF1/CIP1}$ (referred to as p21 throughout the remainder of this thesis), $p27^{kip1}$ and $p57^{kip2}$. These molecules bind and inactivate the cyclin-CDK complex [30]. p21 was initially identified using cDNA subtractive hybridization of cells either expressing or not-expressing the transcription factor and tumor suppressor protein p53 [31]. Analysis of the *p21* promoter revealed that it contained two p53 consensus binding sites and electrophoretic mobility shift assays (EMSAs) showed that the p53 protein could indeed bind to these sites [31, 32]. Other transcription factors have also been shown to regulate *p21* expression. GATA-6 and Meox2 induce *p21* and subsequently induce a p21 dependent cell cycle arrest. However, they both act independently of p53 [33-35].

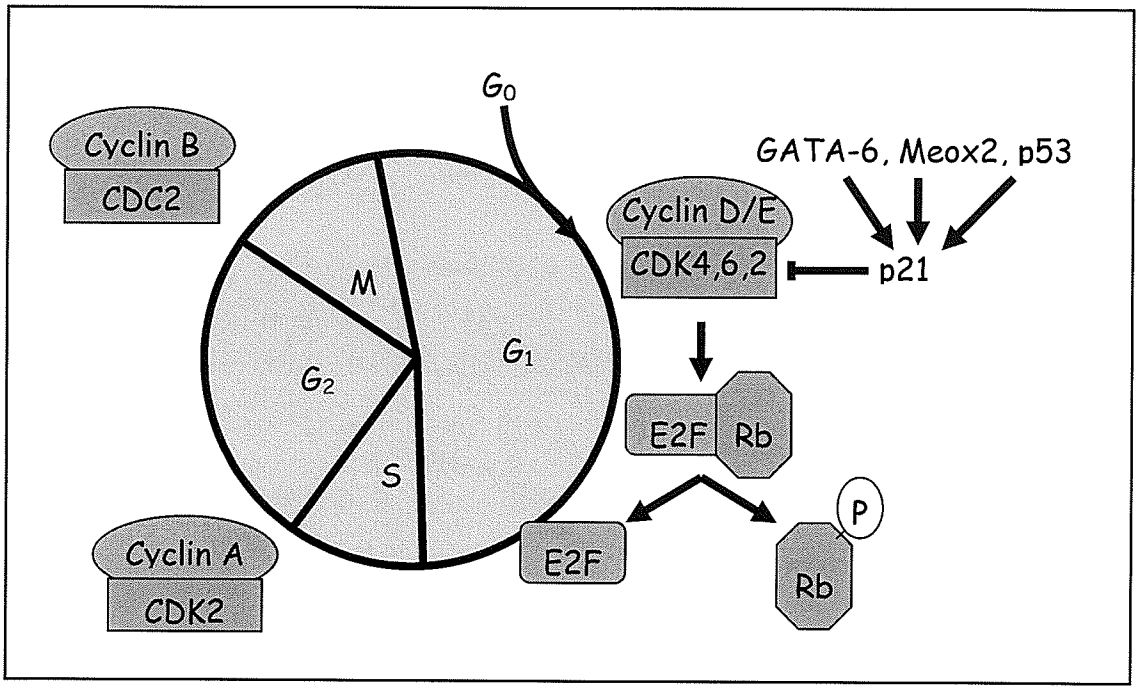

Figure 1: Cyclin regulation of cell cycle progression
Transition through the cell cycle is regulated by the association of specific cyclins with CDKs. Progression through the G_1 phase initially requires the interaction of cyclin D with CDKs 4 and 6 and later the association of cyclin E with CDK2. The p21 CDKI, which is induced by several transcription factors including Meox2, can block transition to the S phase of the cell cycle.

III) Homeobox Genes

1. Isolation and molecular characterization

Several genes, called homeotic genes, were found to cause transformations of one segment or organ to another in insects (homeotic transformations) [36-38]. Subsequent analysis revealed that these genes have a conserved protein coding sequence, the homeobox, which is also well conserved in orthologous genes in other species [39]. The homeobox, first described in 1984, codes for a 60 amino-acid segment (homeodomain) that is able to recognize and bind to specific DNA sequences [2, 39]. This conserved motif is composed of three major helices and a fourth small helix (Figure 2). Helices I and II are separated by a loop whereas helix II and III are separated by a turn [2]. The helix-turn-helix motif, formed by helices II and III, resembles a DNA bindng motif found in many prokaryotic proteins such as the lactose and tryptophan repressors [40, 41]. However, the overall structure of the homeodomain is unique to eukaryotes [42]. Helices III and IV lie within the major groove of the DNA double helix and make intermolecular contacts with the DNA [2, 42]. Conserved residues in this domain are important for the overall three dimensional structure whereas the non-conserved residues convey binding specificity [42]. As a result, homeodomain proteins interact with specific DNA operators through their homeodomain whereas this region and other regions of homeodomain proteins mediate protein-protein interactions with accessory proteins important for transcriptional regulation, nuclear import and protein turnover [42-46].

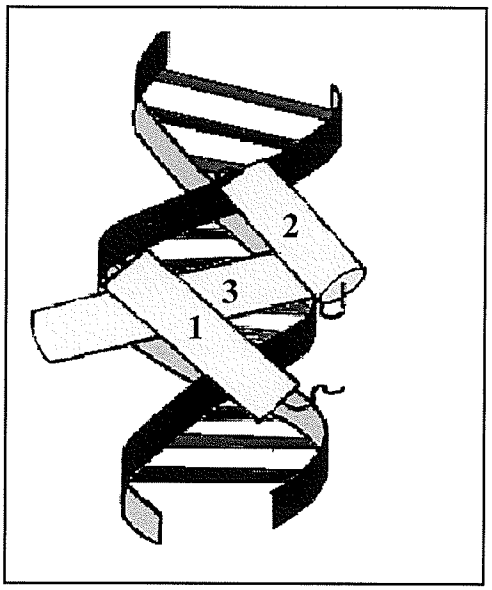

Figure 2: The Homeodomain
The homeodomain is a conserved motif composed of 4 helices. The structure includes a loop between helices 1 and 2 as well as a turn between helices 2 and 3. Helices 3 and 4 are separated by few residues and are often schematically drawn as a single helix, as in the adjacent diagram. Helices 3 and 4 lie in the major groove and interact with the DNA nucleotides [2].
(Image adapted from http://www.uic.edu/classes/bios/bios100/lecturesf04am/lect15.htm University of Illinois at Chicago)

2. Role of homeobox genes in human development and disease

Although homeobox genes were first identified in *Drosophila* [39] they have since been identified in fungi, plants and other eukaryotes [2]. In vertebrates, many homeobox genes are localized in genomic arrays called Hox clusters. Humans and other vertebrate species have four Hox clusters (A-D) that each contain 9-11 genes [47, 48]. The expression pattern of these genes along the anterior-posterior body axis of many different organisms (humans, fly, mice, zebrafish, etc) is collinear with their position in the genome [48]. Non-clustered homeobox genes (Para Hox) form families that are characterized by similarities within their homeodomain sequences as well as the presence of conserved domains flanking the homeodomain [49]. Examples of these families include the *Lim, Pax* and *Six* families that contain LIM, paired box (PAX) and SIX domains, respectively, in addition to their homeodomains [43, 49].

3. Cellular role of homeobox genes

Homeodomain proteins regulate many diverse cellular processes including differentiation, proliferation, apoptosis, migration and overall body patterning [47, 50]. Deregulated homeodomain protein expression has been implicated in different pathological conditions such as vascular disease and the development/progression of cancer [47, 51, 52]. Alterations in homeodomain protein expression can take many forms including the reactivation of developmental genes, the silencing of genes usually expressed in the adult and the activation of genes not normally expressed in a given tissue [49].

IV) Mesenchyme homeobox genes

1. Conservation of *Meox* genes during evolution

Murine *Meox1* (Mesenchyme Homeobox Gene), the first orthologue identified, encodes a 254 amino acid protein [53]. *Meox2,* the only other *Meox* homeobox family member identified, is slightly larger at 303 amino acids and has a predicted molecular weight of 33.6 kDa [54]. These proteins are 95% identical and 100% similar in their homeodomain sequences but have significantly diverged in regions which surround their homeodomains (Figure 3) [53, 54]. The *Meox1/2* genes share a similar genomic organization which includes three exons and two introns and they are not linked to any of the Hox clusters [53-55]. Meox2 also contains a region rich in histidine and glutamine residues known as a CAX repeat (Figure 4) [54, 55]. Similar sequences, also called *opa* sequences, have been shown to be important in the transactivation function of other transcription factors such as HB24, Notch and HOX-11, although its function in Meox2 is still unknown [56-58]. In our lab we have found that Meox2 is a stronger transcriptional

activator in the Gal4 Yeast Two Hybrid system than a Meox2 construct with the CAX repeat deleted [59]. Meox2 is very well conserved across evolution which implies that its function has also been conserved (Figure 5) [53, 55, 60-65] .

```
mMeox2  MEHPLFGCLRSPHATAQGLHPFSQSSLALHGRSDHMSYP----ELSTSSSSCIIAGYPNE 56
mMeox1  MDPVANSCVRNPQPPAPVWGCLRNPHSEDSSASGLSHYPPTPFSFHQKSDFPATAAYPD- 59
        *:    .*:*.*:..*     : :.     . *.   **    .:  .*.    *.**:

mMeox2  EGMFASQHHRGHHHHHHHHHHHHQQQQHQALQSNWHLPQMSSPPSAARHSLCLQPDSGGP 116
mMeox1  --FSASCLAATPHSLPRTERIFNEQHPAFPQTPDWHFP-----ISEAGQRLNLGP-AGSA 111
        : **      *   : .: .::*:   .  .:**:*      * * : * * * :*..

mMeox2  PELGSSPPVLCSNSSSLGSSTPTGAACAPGDYGRQALSPADVEKRSGSKRKSDSSDSQE- 175
mMeox1  REMGAGSPGLVDGTAGLGEDCMVLGTIAN----------ETEKKS-SRRKKERSDNQEN 159
        *:*:..* * ..::.**..  . .: *            :.**:* *:**.: **.**

mMeox2  GNYKSEVNSKPRKERTAFTKEQIRELEAEFAHHNYLTRLRRYEIAVNLDLTERQVKVWFQ 235
mMeox1  GGGKPEGSSKARKERTAFTKEQLRELEAEFAHHNYLTRLRRYEIAVNLDLSERQVKVWFQ 219
        *. *.* .**.**********:**************************:*********

mMeox2  NRRMKWKRVKGGQQGAAAREKELVNVKKGTLLPSELSGIGAATLQQTGDSLANEDSRDSD 295
mMeox1  NRRMKWKRVKGGQ---------------PVSPQEQD-------REDGDSAASP------ 250
        *************                .: *.* .       :: *** *.

mMeox2  HSSEHAHL 303
mMeox1  -SSE---- 253
         ***
```

Figure 3: Alignment of murine Meox1 and Meox2 protein sequences
Murine Meox1 (mMeox1, Accession # A49122) and Meox2 (mMeox2, Accession # P32443) are 95% identical in their homeodomains (green) and their predicted nuclear localization signals (orange) but they are not conserved outside of these regions. The CAX repeat present in Meox2 (red) is absent in Meox1.

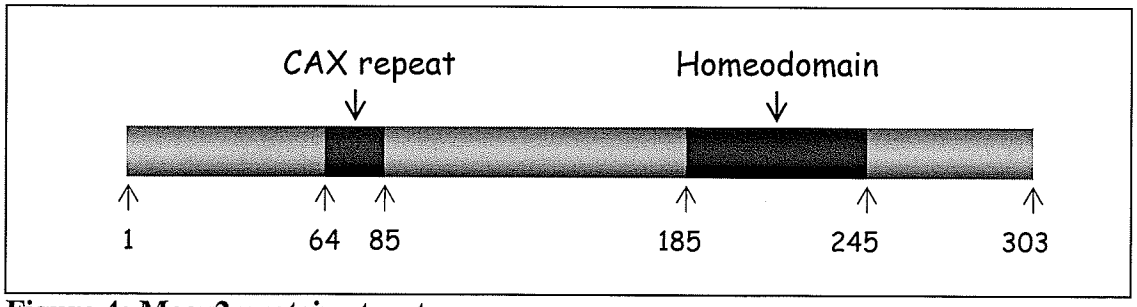

Figure 4: Meox2 protein structure
Meox2 contains a histidine/glutamine rich region called a CAX repeat (red) between residues 64 and 85 and a 60 amino acid homeodomain sequence (green) between residues 185-245.

Figure 5: Sequence conservation of Meox2 during evolution
ClustalW alignment between four Meox2 orthologues. There is a 100% sequence identity in the homeodomain region (green) between mMeox2 (murine, Accession # P32443), hMeox2 (human, Accession# A56837), cMeox2 (chicken, Accession # CAC42831) and xMeox2 (Xenopus, Accession # P39021). Overall there is 86% identity between the four orthologous sequences. Red, CAX repeat; Orange, predicted Nuclear Localization signal (NLS); Green, Homeodomain

2. Meox1 and Meox2 expression during embryogenesis

i) Meox1 expression in the somites

Meox1 RNA transcripts and protein are first detected in the mouse mesoderm at 7.0-7.5 days post coitus (d.p.c) and are later expressed in pre-somitic mesoderm,

epithelial somites, differentiating somites, intermediate and lateral plate mesoderm [53, 66]. By 11.5 d.p.c, Meox1 is found in the dermatome and sclerotome of the differentiating somites but not the myotome [66]. During organogenesis, *Meox1* is expressed in populations of differentiating cells or cells that are undergoing an epithelial-mesenchymal transformation [53]. Such organs include lateral plate derivatives such as the heart, kidney and loose connective tissues [53].

ii) Meox2 expression in the somites

Meox2 mRNA expression starts at a later timepoint in development than *Meox1* and has been detected starting at 8.0 d.p.c of mouse development [53, 67] and the protein can be detected at 9.0 d.p.c [66]. However, transgenic Cre recombinase expression under the control of the *Meox2* promoter has been detected in the epiblast suggesting that Meox2 may be expressed earlier than what has currently been detected [68]. *In situ* hybridization shows that *Meox2* is first expressed in the epithelial somite and later it becomes restricted to the sclerotome of differentiating somites [53, 69]. In chick somites *Meox2* mRNA expression is not as restricted and was detected in the dorsal and ventral lips of the dermomyotome as well as in the sclerotome [69]. These differences in expression are likely due to the different sensitivities of the methods used since Candia *et al.* (1997) repeated their analysis using immunohistochemistry with an anti-Meox2 antibody rather than *in situ* hybridization and were unable to detect differences between mouse and chick expression nor were they able to identify a restriction of Meox2 to the sclerotome in the mouse. Expression of Meox2 persists in migrating myoblasts, which originate from the somites, during the formation of the ribs, vertebrae and limb buds [67].

Meox2 is also expressed in several smooth muscle cell lineages including the stomach, posterior pharynx, esophagus, diaphragm, bladder and lungs [67].

iii) Meox2 expression during cardiogenesis

Lateral plate derivatives, such as the developing cardiovascular system, express Meox2 [54, 64, 67]. Its expression is first detected in a few nuclei of cardiomyocytes and cells composing the heart vasculature at stage 33 of chick (*Gallus gallus*) heart development and in several nuclei during stages 35 through to 41 [64]. By these stages the cardiomyocytes have a decreased proliferation potential and most of the specialized structures of the heart have been formed [64]. Biphasic *Meox2* mRNA transcript production and protein expression have been observed in the developing mouse heart [67]. The first wave of Meox2 protein expression starts at the early heart tube (8-8.5 d.p.c) and peaks at 12.5 d.p.c in the atria and ventricles but falls to undetectable levels by 13.5 d.p.c [67]. Immunohistochemistry shows that Meox2 is localized predominantly to perinuclear and cytoplasmic regions during these early time points of expression [67]. Meox2 is re-expressed in the nuclei of some ventricular cardiomyoctyes at 15.5 d.p.c [67]. At this stage Meox2 is located in the correct cellular compartment to act as a transcription factor. Meox2 continues to be expressed in the adult myocardium [54].

Forced early expression of exogenous *Meox2* in the cardiomyocytes of the developing heart results in a perturbed heart morphology such as smaller, underdeveloped atria and ventricles [64]. This effect of Meox2 on cardiac development is likely due to its inhibitory effect on cellular proliferation [64, 69].

iv) Meox2 is required for Pax activation during limb muscle development

Mice nullizygous for *Meox2* (*Meox2* -/-) display variable penentrance of limb muscle defects [70]. Several forelimb muscles are completely missing such as the *musculus deltoideus*, *m. teres major* and *m. biceps brachii*, among others [70]. In the hindlimb the decreased muscle mass is largely due to the formation of a smaller *m. gastrocnemius* [70]. Although the loss of Meox2 function is not embryonic lethal, most animals die before weaning [70]. 10% of the null animals also displayed cleft palates which is a defect that has been identified with mutations in the paired box protein Pax3 [70, 71].

Since the *Meox* genes have overlapping expression patterns and functions during embryonic development with those of *Pax1* and *Pax3*, the relationship between these homeobox genes was studied [70, 72]. A population of migrating myoblasts, originating from the dermomyotome, co-express Meox2 and Pax3 as they migrate to the limb bud in 9.75 d.p.c embryos [69, 70]. Meox1, which is expressed in the dermomyotome, is not expressed in these migrating myoblasts [70]. Further evidence supporting a functional role for Meox2 in the migration of these cells is the observation that expression of Pax3 was decreased in the migrating myoblasts in the *Meox2* -/- mice [70]. Using the yeast two-hybrid approach and GST-Pull down assays it was also found that Meox and Pax proteins could bind to each other. Specifically, Meox1 preferentially bound to Pax1 and Meox2 preferentially bound to Pax3 [72]. These interactions are largely mediated through the homeodomain of the Meox1/2 proteins [72]. Regions outside the homeodomain must be important for the specificity of the interactions since the homeodomains of the Meox proteins are essentially identical.

3. Meox1 and Meox2 expression in the adult

Meox2 expression in the adult has only been detected in the cardiovascular system, heart and highly vascularized tissues such as the lungs and kidneys [54]. Expression of *Meox2* in primary vascular smooth muscle cells can be detected by Northern blot analysis. However, this expression is lost in transformed vascular smooth muscle cell lines such as A7r5s, and A10s [54]. *Meox2* RNA transcripts and protein are also detected in primary cultured endothelial cells such as HUVECs [35]. Currently, there are no reports of *Meox1* expression in the adult.

4. Meox2 regulation of cell cycle progression

i) Induction of a G_0/G_1 cell cycle arrest

Meox2 expression is regulated similarly to that of proteins of the growth arrest specific (GAS) and growth arrest and DNA-damage inducible (GADD) protein families [73-76]. GAS and GADD proteins are highly expressed in either quiescent cells or under conditions that promote growth arrest. Their expression is down-regulated in mitogen stimulated and proliferating cells [74, 77, 78]. This pattern of expression suggests that Meox2 may function as a negative regulator of cell cycle progression. Specifically, *Meox2* has been shown to be highly expressed in quiescent primary VSMCs and down-regulated upon stimulation with growth serum or specific mitogens such as PDGF-AB (Platelet derived growth factor) and PDGF-BB [54]. Decreased *Meox2* levels correlated with increases in ^{3}H-thymidine uptake, a measure of DNA synthesis [54].

Microinjection of recombinant glutathione S-transferase (GST)-Meox2 into quiescent cells was sufficient to prevent mitogen-stimulated S-phase entry in primary rat VSMCs, BALB/c 3T3s (mouse fibroblast cell line) and human VSMCs [34]. However

microinjected recombinant Meox2 was unable to arrest cycling cells indicating that Meox2 acts only at a specific phase in the cell cycle. Specifically, the block of the cell cycle mediated by Meox2 can only be seen if it is injected before or in the first 12 hours following serum stimulation, suggesting that Meox2 cannot reverse the decision of a committed cell to divide [34]. Further evidence of the ability of Meox2 to inhibit cell cycle progression was obtained when primary human and rat VSMCs were largely prevented from entering S-phase when transduced with a replication defective adenovirus construct encoding rat *Meox2* (Ad-*Meox2*) [34]. Flow cytometry and time course studies showed that Meox2 arrested cells in the G_0/G_1 phase of the cell cycle [34, 54]. Also, only 30% of embryonic chicken cardiomyocytes transduced with an adenovirus encoding chick *Meox2* were positive for PCNA (Proliferating cellular nuclear antigen) expression by immunocytochemistry compared to 40-48% of the cells in *β-Gal* transduced controls 48 hours after transduction [64]. Accordingly, [^{3}H]thymidine incorporation by VSMCs and HUVECs of Ad-*Meox2* infected cells decreased in a dose-dependent manner [35, 79]. Work supporting Meox2's anti-proliferative effect *in vivo* was that embryonic chick myoblasts that were positive for Meox2 were also negative for 5-bromo-2-deoxyuridine (BrdU) incorporation [69].

Furthermore, it seems that Meox2 expression is regulated by Angiotensin II (Ang II) and C-Type Natriuretic Peptide (CNP), which positively and negatively influence vascular growth, respectively [80, 81]. Ang II treatment reduced Meox2 expression whereas CNP increased Meox2 expression [80]. DNA microarray analysis has also identified *Meox2* as being an Ang II responsive gene [82]. Mechanistic studies have shown that this Ang II regulation is mediated through the Erk1+2 mitogen-activated protein kinase pathway [81].

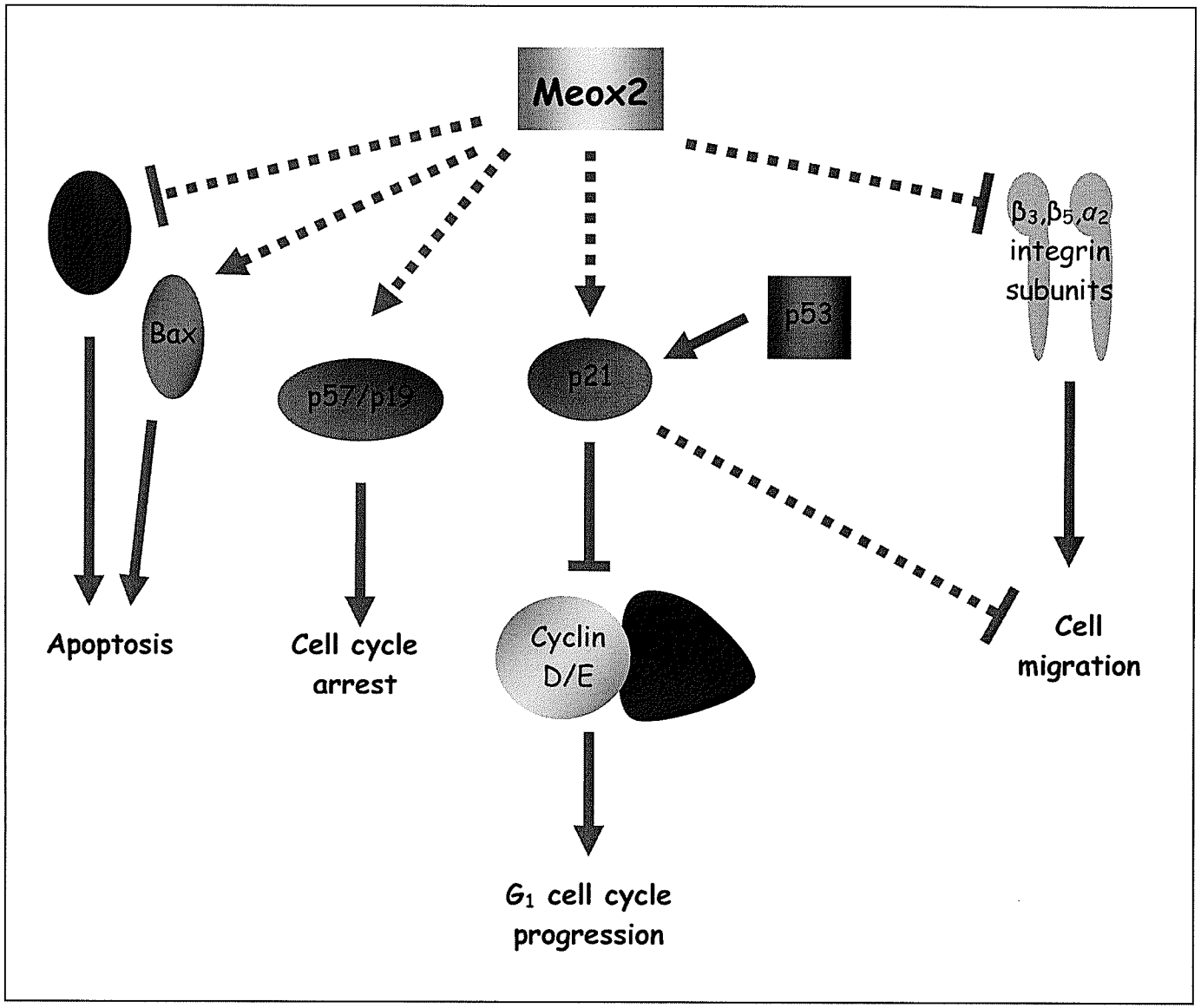

Figure 6: Meox2 involvement in cellular processes
Meox2 expression induces apoptosis and cell cycle arrest. The p21 CDKI is necessary for Meox2 induction of G_0/G_1 cell cycle arrest. Other CDKIs such as p57 and p19 have been shown to be up-regulated by Meox2 but their role in Meox2 induced cell cycle arrest has not been elaborated. Meox2 expression also inhibits cell migration. This effect may be mediated through Meox2's down-regulation of the β_3, β_5 and α_2 integrin subunits. Meox2 also affects Bax and Bcl2 levels post-transcriptionaly in order to induce apoptosis.

ii) Requirement of the CDKI p21

Since Meox2 induces cell cycle arrest in G_1, a timepoint where p21 is known to act, the co-expression of these proteins in VSMCs was examined. Both proteins are expressed and localized to the nucleus in quiescent cells, as well, both are down-regulated upon serum stimulation [34]. Upon *Meox2* transduction, p21 levels are up-regulated in a variety of cells, including HUVECs, human, rat and rabbit VSMCs (Figure 6) [34, 35]. Using luciferase promoter assays in MEFs (*p53*-/-), it was shown that the full length Meox2 was able to induce expression from the human *p21* 2.4 kb promoter construct 3.4 fold whereas the homeodomain-deleted version of Meox2 did not activate transcription [34]. Meox2-mediated activation of the *p21* promoter was also demonstrated in HUVECs by luciferase assays where it activated the promoter 7 fold [35]. Cdk2 kinase activity is decreased following Meox2 expression in both human and rat VSMCs, further establishing p21 as being a mediator of Meox2 induced cell cycle arrest. Meox2 cannot arrest the cell cycle progression of *p21* -/- fibroblasts indicating that p21 is essential for Meox2 regulation of cellular proliferation [34].

iii) Involvement of other CDKIs

Recently, data from adenoviraly infected cultured endothelial cells has revealed that two other cyclin dependent kinase inhibitors (CDKIs), $p19^{INK4d}$ and $p57^{Kip2}$, are up-regulated following Meox2 overexpression (Figure 6) [83]. p19 belongs to the INK4 class of CDKIs that arrest cells in the G_1 phase of the cell cycle by binding and inhibiting CDK4 and CDK6 [84]. On the other hand, $p57^{Kip2}$ interacts with a variety of cyclin and CDK complexes including many formed with CDK2/4 and the mitotic cyclinB-Cdc2 complex and may arrest cells in these phases [85, 86]. $p57^{Kip2}$ is ubiquitously expressed

during early development and its deletion results in embryonic/neonatal lethality, further supporting its crucial role during embryogenesis [86-88].

5. Meox2 induction of apoptosis

Meox2-mediated block of VSMC growth is not entirely due to its ability to block proliferation but also due, in part, to its ability to induce apoptosis. Quiescent cells that were transduced with Ad-*Meox2* followed by serum stimulation morphologically appeared to be undergoing apoptosis 48 hours post-stimulation [89]. The morphological changes included cytoplasmic blebbing, chromatin condensation and DNA nicking as identified by TdT-mediated dUTP-fluorescein nick-end labeling (TUNEL) [89]. Furthermore, increased pro-apoptotic Bax and decreased protective Bcl-2 protein levels were detected, whereas their transcript levels were not changed [89]. These experiments suggest that Meox2 may be acting by a post-transcriptional mechanism to induce apoptosis. This apoptotic function was also independent of cell cycle activity as shown using specific cell phase inhibitors such as rapamycin (G_1 phase), hydroxyurea (G_1/S phase), aphidicolin and mimosine (S phase) [89]. In contrast to Meox2 induced cell cycle arrest, Meox2 was able to induce apoptosis in both *p21-/-* MEFs and 10.1 MEFs (*p53-/-*) [89]. Therefore it seems that alternative pathways are used by Meox2 to induce apoptosis and to induce a G_0/G_1 cell cycle arrest although both are dependent on the Meox2 homeodomain (Figure 6). The pro-apoptotic effect of Meox2 was supported by *in vivo* work which showed that transduction of rat carotid arteries with Ad-*Meox2* led to an increase in TUNEL labeling of VSMC when compared to arteries that were transduced with a control virus [90].

6. Meox2 block of cellular migration

Transduction of *Meox2* into VSMCs *in vitro* decreased their ability to migrate towards the chemotactic factor PDGF-BB [91]. Using knockout MEFs, it was demonstrated that this effect was dependent on either p21 expression or cell cycle arrest and independent of p53 expression [91]. Although cell cycle arrest is necessary for Meox2-mediated inhibition of migration, cell cycle arrest itself is not sufficient to inhibit the migration of VSMCs [91]. Therefore, Meox2 must be altering the expression or function of genes other than *p21* in order to block VSMC migration. Since integrins have been shown to be important in controlling VSMC migration, their expression was compared between control and *Meox2* overexpressing cells. Fluorescent activated cell sorting (FACS) and western blot analyses showed that both β_3 and β_5 integrin subunits were expressed at lower levels in Ad-*Meox2* treated rat VSMCs (Figure 6) [91]. Also, when rat carotid arteries were injured with a catheter, an operation shown to decrease *Meox2* expression, β_3 and β_5 integrins were up-regulated [91, 92]). Ad-*Meox2* treatment of arteries during vessel injury was sufficient to inhibit this enhanced expression and thereby reduce VSMC migration and neointima formation [91]. Similarly, Markmann *et al.* showed that VSMCs derived from porcine aortic tissue are refractory to serum stimulated increases in α_2 integrin expression following transduction with an adenovirus construct encoding the porcine *Meox2* gene [65].

7. Meox2 as a possible therapeutic target

In response to the endothelial denudation which is caused by balloon injury, VSMCs transform from a contractile, quiescent state to a proliferative, synthetic phenotype [1, 3-5]. In a rat model of carotid artery injury, *Meox2* mRNA was decreased

2 hours after injury, reaching a minimal level of expression at 4 hours post-injury and only returning to basal levels of expression after 7 days [92]. This decrease in *Meox2* expression in the injured artery has been hypothesized to be partially responsible for the phenotypic change that occurs in VSMCs. This role for Meox2 is based on its

1) down-regulation as VSMCs re-enter the cell cycle [92]
2) transcriptional inhibition of genes needed for the synthetic phenotype such as the α2 integrin subunit [65]
3) transcriptional activation of CDKIs such as *p21*, *p19* and *p57* [34, 35, 83].

The ability of VSMCs to de-differentiate, re-enter the cell cycle and migrate to form a neointima was inhibited by Ad-*Meox2* transduction, resulting in decreased luminal narrowing in response to vessel injury [34, 79, 90, 91]. Closer inspection of the treated vessels revealed that the Ad-*Meox2* treated vessels had reduced PCNA expression versus Ad-*β-gal* and saline treated controls 3 days post-injury [90]. At 7 and 14 days post-injury, large differences in apoptosis between the Ad-*Meox2* transduced vessels and controls were detected [90]. Taken together, these results suggest that after vessel injury Meox2 initially acts to inhibit VSMC hyperplasia during neointima formation by blocking the cell cycle, but later Meox2 inhibits hyperplasia by inducing apoptosis. Gene therapies aimed at increasing the expression of Meox2 in VSMCs that are stimulated to re-enter the cell cycle could potentially block their growth and thus inhibit the pathogenesis of diseases such as atherosclerosis and post-angioplasty restenosis.

In vitro work with HUVECs showed that adenoviral delivery of *Meox2* is able to inhibit tube formation on matrigel upon treatment with Vascular Endothelial Growth Factor (VEGF) [35]. This anti-angiogenic effect of Meox2 is likely mediated through Meox2 inhibiting the binding of the pro-angiogenic NF-$\kappa\beta$ transcription factor to its target

DNA sequences [83]. How Meox2 inhibits NF-$\kappa\beta$ DNA binding remains to be elucidated. However, microarray data supports a role for Meox2 inhibition of NF-κB binding. Many NF-$\kappa\beta$ responsive genes are down-regulated when Meox2 is over-expressed in endothelial cells [83]. Interestingly, cross-talk between homeodomain proteins and NF-$\kappa\beta$ has previously been shown [93, 94]. Hepatitis B virus X-associated protein (a plant homeodomain protein) has been shown to physically interact with NF-$\kappa\beta$ negatively affecting the ability of NF-$\kappa\beta$ to bind its target DNA sequences [94]. This anti-angiogenic potential of Meox2 could be used to inhibit the angiogenesis associated with tumor growth or diabetic retinopathy.

V) p21 Cyclin Dependent Kinase Inhibitor

1. Isolation and characterization of p21

p21 was identified separately in two laboratories [31, 95]. In one case, it was named Wild-type p53-activated fragment (WAF1) since its transcription was shown to be regulated by p53 directly binding to its promoter [31]. Simultaneously, another laboratory isolated a 21 kDa protein called Cdk-interacting protein 1 (Cip1) that was able to bind cyclin complexes containing cyclin A, cyclin D1, cyclin E, and Cdk2 proteins [95].

2. The role of p21 in regulating apoptosis

p21 has since been shown to interact with proteins such as pro-caspase 3, caspase 8 and ASK1 (apoptosis signalling regulating kinase) thereby having an anti-apoptotic effect [96-99]. Furthermore, cleavage by activated caspase 3 and other caspases that recognize the DEVD amino-acid sequence led to p21 being cleaved into a p15 fragment

and to cell death in LIM 1215 colorectal cancer cells [96, 100]. In some instances, p21 expression has been shown to be necessary for the induction of apoptosis as seen with hRAD50 expression in colon carcinoma cells [101]. Whether p21 is pro or anti-apoptotic warrants further studies and will likely depend on the particular cell type or tissue being studied.

3. The role of p21 in modulating the cell cycle

Regarding p21's regulation of the cell cycle, there is emerging evidence demonstrating that p21 can also positively regulate cell cycle progression in contrast to the initial dogma that this protein was acting as a brake on the cell cycle [102-104]. The subcellular localization and the concentration of the protein as well as the cell type are partially responsible for this difference in p21 regulation of the cell cycle [29, 102, 104, 105]. For example, cytoplasmic p21 promotes cell cycle progression and this effect cannot be explained by simple loss of its function in the nucleus since the effect of cytoplasmic p21 differs from when p21 expression is completely lost [102]. Also, binding of p21 to Cdk4/6 is beneficial for the activity of these CDKs, whereas the binding of p21 to Cdk2 results in the loss of Cdk2 activity and cell cycle arrest [29, 95, 104].

4. Regulation of *p21* transcription by homeodomain proteins

i) Cdx2 and HoxA10

The *p21* promoter has three TAAT homeodomain consensus binding sequences, between nucleotides -444 to -465 relative to the transcriptional start site, which can be bound by the Cdx2 and HoxA10 homeodomain proteins [106, 107]. Cdx2 activation of the *p21* promoter was illustrated using luciferase assays. However, the observed level of

activation varied between the cell types studied [107]. A p53 independent activation of this promoter by Cdx2 was shown using *p53* null cells and this was further supported by evidence that Cdx2 directly bound to the TAAT sites within the promoter as was shown by EMSAs [107]. Similarly, HoxA10 has been shown to bind and activate the *p21* promoter up to 50 fold depending on the cell line used [106]. This HoxA10 dependent activation of *p21* transcription required the presence of the homeodomain further supporting direct binding between the promoter sequence and HoxA10 [106].

ii) Meox2

Similar to HoxA10 and Cdx2, Meox2 was also demonstrated to activate the *p21* promoter in both HUVECs and MEFs (*p53-/-)* [108, 109]. Whether this activation was due to Meox2 binding directly to the *p21* promoter, or Meox2 acting as a co-factor, or via Meox2 activating an upstream gene whose product then binds and activates the *p21* promoter, has not been determined. However, a role for Meox2 DNA binding in mediating its regulation of the *p21* promoter has been shown in *p53*-/- MEFs [109]. Although Meox2 induced cell cycle arrest is p21 dependent, the mechanism by which Meox2 activates p21 protein expression has not been established.

VI) Bapx1

1. Role of Bapx1 during sclerotome differentiation

During embryogenesis, cells within the paraxial mesoderm, which flanks the notochord and neural tube, condense and become more tightly associated. These epithelial somites differentiate in an anterior to posterior direction with each subsequent somite budding off from the pre-somitic mesoderm in a highly spatially and temporally

regulated fashion (Figure 7A). The somites then undergo an epithelial to mesenchymal transformation and further differentiate into the sclerotome and the dermomyotome. The ventral component, the sclerotome, gives rise to the vertebrae and the ribs under the influence of sonic hedgehog (shh) signalling. The dorsal component, the dermomyotome, continues to differentiate into the dermatome and myotome, which give rise to the dermis and the skeletal musculature respectively (Figure 7A and 7B). *Meox1* -/- mice have severe defects in the differentiation of the axial skeleton, which is a sclerotome derivative, whereas *Meox2* -/- mice have limb muscle defects, which indicates a problem in myotome differentiation [110]. Since the expression of Meox1 and Meox2 in the somites is largely overlapping, it was predicted that they may have some redundant functions with one Meox family member partially compensating for the loss of the other. This hypothesis was supported by the generation of the *Meox1/2* double knockout mouse which has a much more severe phenotype than the simple additive phenotypes of the individual single knockouts [110].

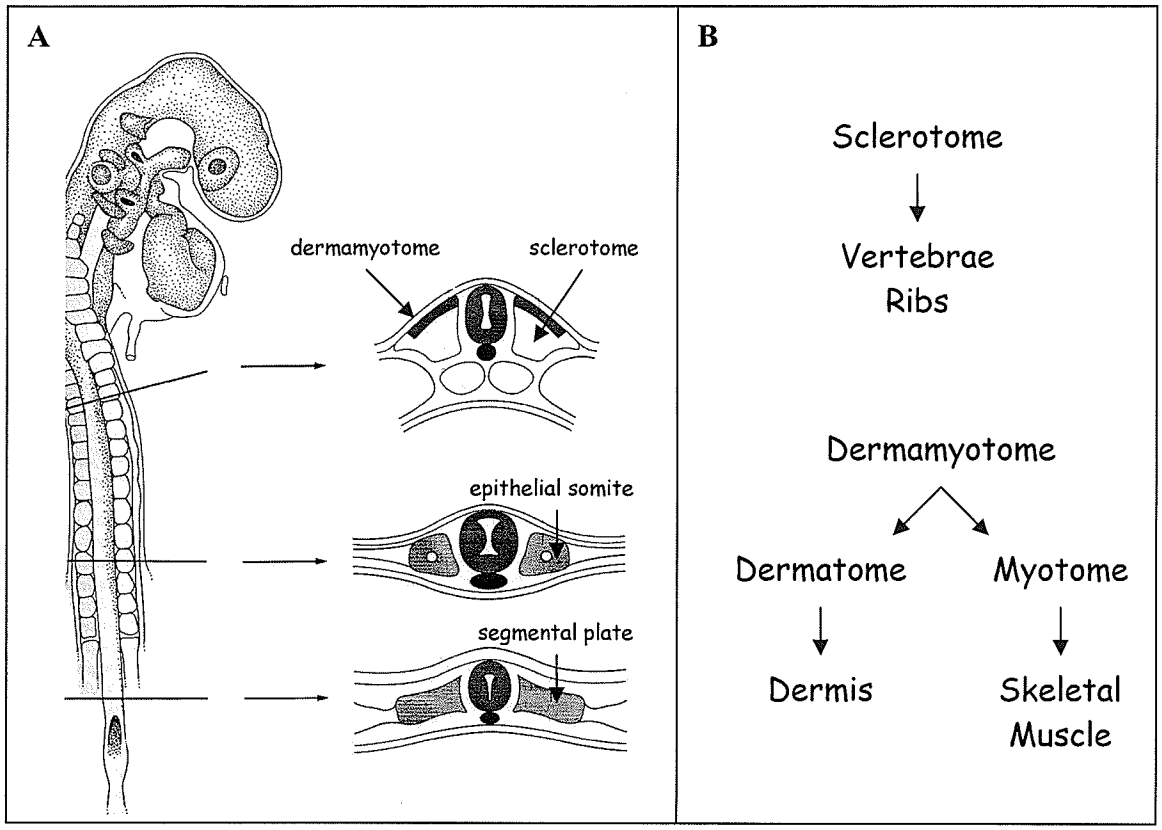

Figure 7: Somitogenesis and the fate of somite cell populations
A) Somitogenesis proceeds from anterior to posterior with subsequent somites budding of the pre-somitic mesoderm to form the epithelial somites. These epithelial somites mature and differentiate into distinct cell populations, the dorsal dermamyotome and ventral sclerotome. B) The fate of sclerotome and dermamyotome cell populations during development. Scleotome derivatives contribute to vertebrae and ribs. The dermamyotome differentiates into dermatome and myotome. Cells of originating from the dermatome give rise to dermis whereas those cells originating from the myotome become skeletal muscles. (Adapted from Essential Developmental Biology 2001, Jonathan, Slack)

Bapx1 and *Nkx3.2* are the murine and human orthologues of the *Drosophila* *Bagpipe* homeobox gene respectively [111]. Bagpipe is expressed in the mesoderm and is required for development of the visceral musculature. As well, it may have a role in the formation of left/right asymmetry during embryonic development [111-114]. *Pax1/9* double knockout mice, *Meox1/2* double knockout mice and *Bapx1* knockout mice have similar axial skeleton defects suggesting that these transcription factors are in the same

developmental cascade [115-118]. The genetic hierarchy of this cascade is being elucidated using a combination of knockout animals, luciferase assays, EMSAs and chromatin immunoprecipitation techniques.

2. *Bapx1* transcriptional regulation

i) Synergistic activation by Pax1/9 and Meox1/2

Pax1 and Pax9 expression is normal in the *Bapx1* -/- mouse indicating that these two paired box genes act upstream of Bapx1 [115]. This is supported by the complete loss of Bapx1 expression in the *Pax1/9* double knockout mice [119]. In these mice, Meox1 and Meox2 expression is not affected, suggesting that the *Meox* genes are either upstream or act in a parallel pathway to the *Pax* genes [119]. Luciferase assays and EMSAs have demonstrated that both Pax and Meox regulate *Bapx1* expression by directly binding to the promoter [117, 119]. In addition, the Meox and Pax proteins are able to synergistically activate *Bapx1* expression since they bind to distinct TAAT motifs in its promoter [117].

ii) Putative genetic hierarchy of *Bapx1* regulation

Meox proteins appear to regulate *Pax* gene expression as illustrated by the altered expression of Pax9 in the posterior somites and Pax1 in the paraxial mesoderm in the *Meox* double knockout mice [110]. The mechanism by which this Meox-mediated regulation occurs has not been established. A further complication in establishing the genetic hierarchy of this transcription factor cascade is that the Pax and Meox proteins bind to each other [72]. The *Meox1/2* double knockout mouse has a more severe phenotype than the *Pax1/9* double knockout or the *Bapx1* single knockout indicating that

Meox1 and Meox2 have functions that are independent of regulating *Pax1/9* and *Bapx1* expression [110]. Whether interactions with other Pax proteins are needed to mediate these effects still needs to be established.

B) RATIONALE

Given that the phenotypic transformation of VSMCs from a contractile quiescent to a synthetic proliferative state contributes to the progression of many cardiovascular diseases, elucidating the molecular changes that occur during this phenotypic transformation will provide a better understanding of this fundamental change and may lead to the identification of new therapeutic targets [1]. A role for Meox2 in maintaining the normal quiescent phenotype in adult VSMCs has been established and its over-expression in rat and rabbit models of balloon injury has prevented the formation of the neointima [54, 79, 92]. An anti-proliferative role for Meox2 in regulating cell cycle progression has been demonstrated *in vivo* and *in vitro* [34, 35, 54, 64, 69, 79]. Finally, Meox2 has been shown to have a pro-apoptotic function in MEFs and VSMCs [89, 90]. Determining how Meox2 mediates these different effects will provide a clearer perspective of how the growth of VSMCS is regulated.

Meox2 has been shown to activate the *p21* promoter but the mechanism of this activation is unknown [34, 35]. Meox2 may be acting as an activator, co-activator or via an indirect mechanism on this promoter. Meox1 may also be able to activate this promoter since its homeodomain is identical to that of Meox2. Ascertaining how the Meox proteins activate the *p21* promoter will provide further evidence of the role of these proteins in controlling the cell cycle of VSMCs. Also, determining whether these homeodomain proteins act either as transcription factors or as co-activators will facilitate the identification of other Meox downstream targets. Direct binding of these proteins to the *Bapx1* promoter has been demonstrated, although the Meox proteins may use different mechanisms of activation on different promoters [117].

We hypothesize that Meox2 acts as a transcription factor, binding to and activating transcription from promoters of genes essential for G_1 cell cycle arrest. We tested the hypothesis that Meox2 and its homologue Meox1 bind the *p21* promoter directly in order to activate transcription.

C) MATERIALS AND METHODS

I) Materials

Dulbecco's Modified Eagle Medium, Lipofectamine 2000 transfection reagent, T4 DNA ligase, Pfx polymerase, Alkaline Phosphatase, Klenow Large Fragment DNA polymerase and most restriction enzymes were purchased from Invitrogen. Plasmid miniprep kits were obtained from either Qiagen or Promega. Plasmid maxiprep and DNA gel extraction kits were purchased from Qiagen. Beetle Luciferin potassium salt was obtained from Promega. The pMal Protein Fusion and Purification System and some restriction enzymes were purchased from New England Biolabs. The Lightshift Chemiluminescent EMSA kit was from Pierce. The Precision Plus Protein Dual Color Standards for SDS-PAGE and the DC Protein Assay kit were obtained from Bio-Rad. The pCMV-Tag4A and pBluescript vectors were purchased from Stratagene. The pGL3-basic, p53-EGFP, pIRES-EGFP and pcDNA3-lacZ vectors were kindly provided by Dr. Mesaeli (St. Boniface Hospital Research Centre, Division of Stroke and Vascular Disease, Winnipeg, MB). The WWP-LUC vector was a generous gift from by Dr. Vogelstein (Howard Hughes Medical Institute & Sidney Kimmel Comprehensive Cancer Center, Baltimore, USA). The pCS2-ENG-N and pCS2-VP16-N vectors were kindly provided by Dr. Kessler (Department of Cell and Developmental Biology, University of Pennsylvania School of Medicine, Philadelphia, USA). Primers, biotinylated primers (5') and the anti-FLAG M2 monoclonal antibody were purchased from Sigma. NIH/3T3 cells and HEK293 cells were purchased from American Type Culture Collection. All other chemicals were of molecular biology grade and were purchased from either Sigma or Fisher.

II) Methods

1. Plasmids and reporter constructs

When DNA was amplified using PCR, the resulting plasmids were sent to the University of Calgary Core DNA & Protein Services to be sequenced to ensure that no inadvertent mutations were incorporated into the amplicon. The pBluescript vector was often used as an intermediate since its multiple cloning site contained many different restriction sites and inserts could be sequenced using the well characterized T7 and T3 sequencing primers. See Table 1 for a complete list of sub-cloning and mutagenesis primers and their corresponding sequences.

i) EGFP tagged Meox1/2 mammalian expression vectors

Mouse *Meox1* (I.M.A.G.E. Clone ID 464899) was PCR amplified using the *Pfx* proofreading polymerase and primers Mx3/Mx4 and human *Meox2* (I.M.A.G.E Clone ID 3917118) was amplified using primers Mx1/Mx2. Both genes were cloned inframe with the enhanced green fluorescent protein (EGFP) of the p53-EGFP vector (Clontech) after the p53 coding sequenced was excised. The resulting Meox1-EGFP and Meox2-EGFP vectors were used in subcellular localization experiments and the initial luciferase assays.

ii) FLAG epitope tagged Meox1/2 mammalian expression vectors

Meox1 and *Meox2* were amplified using *Pfx* polymerase and Mx3/Mx8 and Mx1/Mx5 primer pairs respectively, digested with EcoRI and XhoI and inserted into the similarly digested pCMV-Tag4A vector. The resulting expression vectors were designated 4A-Meox1-FLAG and 4A-Meox2-FLAG. Amplicons including the entire Meox proteins and the FLAG epitope tag were generated (*Meox1-FLAG* (primers Mx3

and Mx10) and *Meox2-FLAG* (primers Mx1 and Mx10)) and cloned into the pBluescript vector for mutagenesis (see mutagenesis section for details). Following mutagenesis, the DNA binding domain (DBD) mutant and homeodomain-deleted (ΔHD) constructs were digested with EcoRI and XhoI and re-introduced into the pCMV-Tag4A vector. The resulting vectors were designated 4A-Meox2-DBD^{mt}-FLAG, 4A-Meox2ΔHD-FLAG, 4A-Meox1-DBD^{mt}-FLAG and 4A-Meox1ΔHD-FLAG.

The *Meox*1 and *Meox2* homeodomains and carboxyl terminal regions were fused to the *VP16* Herpes Simplex Virus activation domain and the *Drosophila Engrailed* repressor domain. Primers Mx14/Mx18 were used to amplify this region from 4A-Meox1-FLAG to create the pCS2-Eng-Meox1 vector, whereas primers Mx15/Mx18 were used to make the pCS2-VP16-Meox1 construct. Similarly, 4A-Meox2-FLAG was the template to create pCS2-Eng-Meox2 (Mx16/18) and pCS2-VP16-Meox2 (Mx17/18). Since the DNA expression vectors for all of Meox constructs used in the luciferase experiments were either p53-EGFP or pCMV-Tag4A, the various chimeric genes were also cloned into the appropriate vectors. The regions encoding the chimeric proteins were excised from the pCS2 vector and cloned into the pCMV-Tag4A vector creating: 4A-Eng-Meox1-FLAG, 4A-Eng-Meox2-FLAG, 4A-VP16-Meox1-FLAG and 4A-VP16-Meox2-FLAG. Similar cloning steps were performed using 4A-Meox2-DBD^{mt}-FLAG as a template in order to create the 4A-VP16-Meox2-DBD^{mt}-FLAG and 4A-Eng-Meox2-DBD^{mt}-FLAG expression constructs.

Table 1: Cloning and mutagenesis primers

Gene	Primer	Sequence	5'/ 3'	Enzyme Site
Meox2	Mx1	GGGAATTCCCGGGATTATCCGAGCTCTG	5'	EcoRI
Meox2	Mx2	GCGGATCCTAAGTGCGCATGCTCTGAG	3'	BamHI
Meox1	Mx3	GCGAATTCGCAGTGGACAGCAGATGGACC	5'	EcoRI
Meox1	Mx4	GCGGATCCCTCTGAACTTGGAGAAGC	3'	BamHI
Meox2	Mx5	GGGCTCGAGTAAGTGCGCATGCTCTGAG	3'	XhoI
Meox1	Mx8	GGCTCGAGCTCTGAACTTGGAGAAGCTGC	3'	XhoI
Meox1+2	Mx10	GCGGATCCTAATACGACTCACTATAGGGC	3'	BamHI
Meox1	Mx11	GGGAATTCATGGATCCAGTGGCCAAC	5'	EcoRI
Meox2	Mx12	GGGAATTCATGGAACACCCGCTCTTTGG	5'	EcoRI
Meox1+2	Mx13	GGTCGACTAATACGACTCACTATAGGGC	3'	SalI
Meox1	Mx14	GGGTCGACCGAGACGGAGAAGAAATCAT	5'	SalI
Meox1	Mx15	GGGTCGACGAGACGGAGAAGAAATCATCC	5'	SalI
Meox2	Mx16	GGGTCGACCGAGGCGGAGAAGCGAAGC	5'	SalI
Meox2	Mx17	GGGTCGACGAGGCGGAGAAGCGAAGC	5'	SalI
Meox1+2	Mx18	GCTCTAGATAATACGACTCACTATAGGGC	3'	XbaI
Meox1	Mx22	CCTTTCTGAGCGGCAGGTCAAAGTCTGGTTCGAA AACCGGAGGATG	5'	*
Meox1	Mx23	CATCCTCCGGTTTTCGAACCAGACTTTGACCTGC CGCTCAGAAAGG	3'	*
Meox2	Mx24	GACAGGTGAAAGTCTGGTTCGAAAACAGGCGGA TGAAGTGGAAGAGGG	5'	*
Meox2	Mx25	CCCTCTTCCACTTCATCCGCCTGTTTTCGAACCA GACTTTCACCTGTC	3'	*
Meox2	Mx28	GCCCTCGAGGCTGTTGACTTCTGACTTG	3'	XhoI
Meox1	Mx30	GCCCTCGAGTTTCTTCTCCGTCTCATTGG	3'	XhoI
Meox2	Mx32	CCCAGGAAAGAAAGGACAGCATTTACCGGTGGA CAGCAAGGAGCTGCGGC		*
Meox1	Mx33	GGAAGGAGAGGACAGCCTTCACCGGGGGTCAGC CTGTGTCCCCACAGGAG		*
p21-promoter	Mx62	CCCCTCGAGGGCCAACAAAGCTGCTGCAACC	5'	XhoI
p21-promoter	Mx63	CCACAAGCTTCTGACTTCGGCAGCTGCTCAC	3'	HindIII
Bapx1 promoter	Mx66	GGAAGCTTGCCCCCCTCAGTTCCAGGATCCGCGC CGAC	3'	HindIII
Bapx1 promoter	Mx67	GGCTCGAGTTGTTCTTCGACTCTGGGCTCCTTCC TAGA	5'	XhoI
p21-promoter	Mx68	CCCTCGAGGGAAATTGCAGAGAGGTGCATCGT	5'	XhoI
p21-promoter	Mx69	CCCTCGAGGCATTGGGTAAATCCTTGCCTGCCA	5'	XhoI
p21-promoter	Mx70	CCCTCGAGCCCTCCTGCAGCACGCGAGAGGTTC	5'	XhoI

* used in PCR-based mutagenesis

4A-Meox1-FLAG and 4A-Meox2-FLAG were used as templates along with the primer sets Mx3/Mx30 and Mx1/Mx28 to PCR amplify (using *Pfx* polymerase) the amino-terminal regions upstream of the homeodomain of *Meox1* and *Meox2*, respectively. These PCR products were used to create the 4A-Meox1-N-term-FLAG and 4A-Meox2-

N-term-FLAG expression vectors. Some of the different recombinant Meox2 proteins constructed for this study are shown in Figure 8.

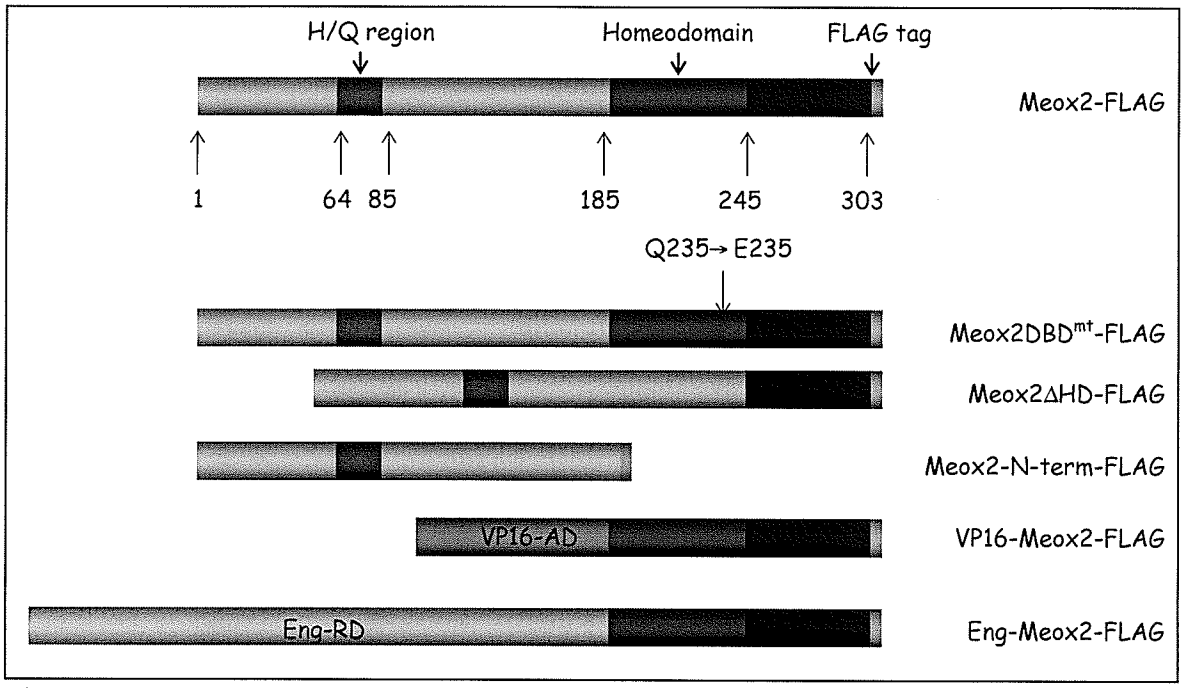

Figure 8: Schematic representation of the Meox2 proteins
PCR-based mutagenesis was used to create Meox2 constructs for use in luciferase reporter assays. Similar constructs were made for Meox1. The Meox2DBD^{mt} has a glutamine residue mutated to a glutamate in the third helix of the homeodomain, shown to be important for interactions with DNA. The Meox2ΔHD has the entire homeodomain removed whereas the Meox2-N-term represents the part of the Meox2 protein encoded 5' to the homeodomain. The VP16 and Eng chimeric proteins have the VP16 activation domain (AD) and the Engrailed (Eng) repressor domain (RD) fused to the homeodomain and carboxyl-terminal regions of Meox2. All proteins have a carboxyl-terminal FLAG epitope (lime). The Meox2 amino-terminal region is shown in blue. The Meox2 carboxyl-terminal region is shown in purple.

iii) *p21* and *Bapx1* promoter luciferase reporter constructs

The pGL3b-p21-2.4 kb reporter construct was created by excising the human *p21* promoter from the WWP-LUC vector using SstI and HindIII and subsequently ligating the promoter into the pGL3-basic vector. The pGL3-basic vector contains a minimal promoter driving expression of the firefly luciferase gene. Transcription of the luciferase reporter gene is either enhanced or repressed depending on which transcription factors

bind to the promoter upstream of the reporter. The pGL3b-p21-850 bp deleted promoter was created by amplifying a truncated *p21* promoter using WWP-LUC as a template and the primers Mx62/Mx63. The pGL3b-p21-500 bp, 400 bp and 200 bp promoters were created by amplifying the *p21* promoter using Mx68, Mx69 and Mx70 (5' primers) respectively and the Mx63 (3' primer). The pGL3-p21-850 bp promoter was used as the template for these PCR reactions.

Mouse genomic DNA was used as a template in order to amplify the *Bapx1* promoter using primers Mx66/Mx67. This PCR product was sequence verified and then sub-cloned into the pGL3-basic vector to yield the pGL3b-Bapx1-900 bp reporter plasmid.

iv) pcDNA3 Meox2 expression vectors

In order to determine if the FLAG tag or the pCMV-Tag4A vectors altered Meox2 function, *Meox2* constructs were cloned into the pcDNA3 vector. pcDNA3-Meox2 was created by excising *Meox2* from the original vector EST clone (I.M.A.G.E Clone ID 3917118) with EcoRI. This excised segment which encodes Meox2 without the FLAG tag was inserted into the EcoRI digested pcDNA3 vector. The direction of insertion was verified by restriction enzyme digestion and sequencing.

To create the pcDNA3-Meox2-FLAG and pcDNA3-Meox2ΔHD-FLAG expression vectors the pcDNA3, 4A-Meox2-FLAG and 4A-Meox2ΔHD-FLAG plasmids were digested with EcoRI followed by removal of the 3' overhangs using Klenow DNA polymerase and KpnI digestion. The pcDNA3 vector was then ligated with the *Meox2-FLAG* and *Meox2ΔHD-FLAG* inserts and screened by restriction enzyme digestion.

v) pMal Meox2 bacterial fusion protein expression vectors

The appropriate 4A-Meox2-FLAG vectors were utilized along with the primer pair Mx12/Mx13 to PCR amplify inserts encoding both *Meox2-FLAG* and the *Meox2-DBD^{mt}-FLAG*. The amplicons were then cloned inframe with the *malE* gene in the pMalc2X vector (NEB). The resulting vectors were designated pMalc-Meox2-FLAG and pMalc-Meox2-DBD^{mt}-FLAG.

2. Site directed mutagenesis and deletions

The splice overlap extension PCR method was utilized in order to generate the Meox1 and Meox2 homeodomain-deleted constructs using the pBluescript vectors as templates [120]. For Meox2, primers Mx32 and Mx10 were used in the first PCR step to generate a product lacking the homeodomain. This product and Mx1 were used in a second PCR amplification step to generate the final amplicon encoding the entire Meox2 protein lacking the homeodomain. Similarly for Meox1, primers Mx33 and Mx10 were employed for generation of the first DNA product followed by a second PCR step with this product and Mx3. The final amplicons were digested with EcoRI and BamHI and ligated into the similarly digested pBluescript vector.

Site-directed mutagenesis was used to produce the Meox1-DBD^{mt} and Meox2-DBD^{mt} constructs [121]. Forward primer Mx22 and reverse primer Mx23 were used to amplify *Meox1* from the pBluescript vector. These primers contained two point mutations that resulted in the incorporation of a BstBI restriction enzyme site in the DNA and a Q to E mutation in the protein sequence. The PCR product was digested with DpnI (recognizes 5'-Gm6ATC methylated and hemimethylated DNA only) to degrade the template and then transformed into DH5α bacteria for blue/white screening. Isolated

plasmids were screened for the desired mutation using a BstBI digestion. Similar steps were followed for *Meox2* except the primers used were Mx24 (forward) and Mx25 (reverse).

3. Cell lines

i) NIH/3T3 mouse fibroblast cell line

NIH/3T3 fibroblasts (mouse) were cultured in DMEM without sodium pyruvate, supplemented with 10% bovine calf serum and 5% penicillin-streptomycin. Cells were incubated at 37°C in a humidified 5% CO_2/95% air tissue culture incubator.

ii) HEK293 human embryonic kidney cell line

Human embryonic kidney cells (HEK293) were grown in DMEM with sodium pyruvate supplemented with 5% fetal bovine serum and 5% penicillin-streptomycin. Cells were incubated at 37°C in a humidified 5% CO_2/95% air tissue culture incubator.

iii) Plasmid DNA transfections

NIH/3T3 and HEK293 cell transfections were performed using the Lipofectamine 2000 reagent following the manufacturer's protocol. Some HEK293 transfections were performed using the Ca^{2+} phosphate method [122] due to their ability to easily take up plasmid DNA. The number of cells, the quantity of plasmid DNA and the incubation times varied for different types of experiments. These details are explained elsewhere in this document.

4. Western Blot Analysis

The DC Protein Assay kit was used to calculate protein concentrations according to the manufacturer's suggested protocol. 6-10 μg proteins and 5 μL Precision Plus Protein Dual Color Standards were run on 10% SDS-PAGE gels followed by immersion transfer at 4°C overnight to a nitrocellulose membrane. Membranes were blocked with 5% milk protein (mp) in Tris-buffered Saline (TBS) for 30 minutes followed by incubation with the primary anti-FLAG M2 monoclonal antibody (Sigma) (0.5 μg/mL in 1X TBS with 5% mp) for 2 hours at 23°C. After 5 washes with Tris-buffered Saline with 0.5% Tween (TBS-T), the nitrocellulose membranes were incubated with goat anti-mouse antibody conjugated to horseradish peroxidase (1:10,000 dilution in 0.25X TBS with 5% mp) for 30 minutes and then rinsed 5 times with TBS-T. Chemiluminescence was detected using the SuperSignal West Dura Extended Duration Substrate (Pierce).

5. Immunocytochemistry

Twenty-four hours post-transfection, cells were washed with Phosphate-buffered Saline (PBS), fixed for 30 minutes in 4% paraformaldehyde, washed 3 times in PBS-T (10 minutes per wash) and then blocked at room temperature for 1 hour (5% goat serum in PBS-T). Cells were incubated with the anti-FLAG M2 monoclonal antibody (4.9 μg/mL in blocking buffer) overnight at 4°C. The following day, cells were washed 3 times with PBS-T. Goat anti-mouse conjugated to Alexa-546 (1:400 dilution in blocking buffer) was utilized as a secondary antibody. Slides were mounted using the Molecular Probes SlowFade ® Antifade Kit with DAPI. Slides were visualized with a Zeiss Axioskop 2 fluorescent microscope equipped with an AxioCam digital camera.

6. Luciferase Reporter Gene Assays

Assays were performed using either the HEK293 cell line or the NIH/3T3 cell line in 6 well tissue culture plates. For the *p21* promoter regulation studies, HEK293 cells were transfected either using the Ca^{2+} phosphate method ($1x10^6$ cells/well) or using Lipofectamine 2000 as per the manufacturer's protocol ($2\text{-}3x10^6$ cells/well), 2μg of pGL3b-p21-promoter constructs and 3μg of the expression plasmid encoding the specific transcription factor being tested or the empty vector control. For *Bapx1* promoter regulation studies, $1.5x10^6$ NIH/3T3 cells were transfected using Lipofectamine 2000 with 0.5μg pGL3b-*Bapx1* promoter and 1μg of the expression plasmid encoding the specific transcription factor being tested or the empty vector control. pcDNA-lacZ (1 μg) was included in the transfections to control for differences in transfection efficiency. For dose response curves, the quantity of transcription factor varied but the total amount of DNA was kept constant by varying the amount of empty vector used in the transfection. The total amount of DNA was kept constant to correct for non-specific effects due to the transfection protocol.

Cell lysates were collected 24 hours post-transfection. Briefly, cells were washed with PBS twice and then NP40 lysis buffer (0.5% NP40, 100 mM Tris, 50mM DTT pH 7.8) was added. Cells were scraped to resuspend and lyse the cells. Supernatants were aliquoted in duplicate for analysis using luciferase and β-Gal assays.

The luciferase assays were performed on a Lumat LB 9507 luminometer using 100μL of luciferase assay buffer (20mM Tricine, 1.07mM $MgCO_3$, 2.67mM $MgSO_4$, 0.1mM EDTA, 33.3mM DTT, 270μM coenzyme A, 470μM luciferin, 530μM ATP) for each 20μL sample and a 20 sec measuring time. β-Gal assays were performed by adding 80μL ddH_2O and 20μL ONPG (4 mg/mL) to 20μL samples of cell lysates. These

samples were incubated at 37°C for 1 hour followed by spectrophotometer readings at 418 nm.

To obtain the relative levels of transcriptional activation *in vitro*, mean values were calculated followed by the division of the luciferase value by the β-Gal value to correct for varying levels of transfection efficiency. Mean basal activation for the empty vector control was fixed to an arbitrary unit of 1 and the activation levels mediated by all the transcription factors were compared to their empty vector controls.

7. Affinity purification of recombinant Meox2-maltose binding protein (MBP) fusion protein

pMAL fusion protein expression vectors were transformed into TBI *E.coli*. Individual colonies were picked into 1L of Rich media supplemented with glucose and ampicillin (100μg/ml) and grown at 37°C until OD600~0.5, after which isopropyl-beta-D-thiogalactopyranoside (IPTG) (0.3 mM) was added to induce fusion protein expression. After the addition of IPTG, cells were cultured at 23°C for a further 6 hours. TBI cells were harvested and then pelleted at 4,000 rpm for 20 minutes, re-suspended in column buffer (20 mM Tris-HCl, 200 mM NaCl, 1mM EDTA) and frozen overnight at -20°C. The following day, samples were thawed at room temperature and sonicated to lyse the cells and to release the protein. The lysed cells were centrifuged at 9,000 rpm for 30 minutes to pellet the insoluble bacterial components and to isolate the supernatant. The supernatant was loaded on a 2.5 x 10 cm amylose resin column and washed with 100 ml column buffer. Column buffer with 10 mM maltose was used to elute the bound protein. Fractions (1 ml) were collected and run on SDS-PAGE gels followed by Coomassie blue

staining or Western blot analysis to determine the fraction containing the eluted fusion proteins of interest.

8. Nuclear Extract Preparation

$3.5x10^6$ NIH/3T3 cells were plated into 175 cm^2 tissue culture flasks. The following day, cells were transfected with 47 μg of plasmid DNA using Lipofectamine 2000. 48 hours post-transfection, cells were rinsed with 1X PBS twice and resuspended by scraping in 1 mL ice cold 1X PBS with 1mM Na orthovanadate. Pellets were collected by centrifuging the cells at 9,000 rpm 4°C for 30 seconds. 400 μL hypotonic buffer (4 mM HEPES, 4 mM NaF, 0.2 mM Na pyrophosphate, 0.2 mM Na orthovanadate, 0.05 mM Na molybdate, 8 mM β-glycerophosphate, 0.2 mM EDTA, 0.2 mM EGTA, 10 μg/mL Leupeptin, 10 μg/mL Aprotonin, 10 μg/mL Pepstatin, 0.5 mM PMSF) was used to resuspend the cells. Addition of 40 μL of 0.5% NP40 buffer and vortexing were used to disrupt the plasma membrane. Following treatment, the lysed samples were centrifuged at 13,000 rpm for 30 sec at 4°C. The supernatant (cytoplasmic fraction) was saved at -20°C for analysis by Western blotting. 80 μL of high salt buffer (1X hypotonic buffer with 20% Glycerol, 0.4 M NaCl) was used to re-suspend the pellet with shaking at 4°C for 1 hour. Subsequently, samples were centrifuged for 20 minutes at 13,000 rpm 4°C and the supernatant (nuclear fraction) was aliquoted and stored at -80°C.

9. Non-radioactive electrophoretic mobility shift assays

i) Probe annealing

For annealing, probes were diluted to 25 pmol in annealing buffer (10mM Tris, 1mM EDTA, 50mM NaCl, pH 8.0). Tubes containing un-annealed probes were set in a 500 ml beaker of boiling H_2O for 10 minutes and then the beaker containing the tubes was allowed to cool to room temperature. Unlabeled probes were aliquoted and stored at -20°C at this 25 pmol concentration. 5' Biotin labeled probes were diluted to 10 fmol with annealing buffer and stored at -20°C.

ii) Assays

Binding reaction components were initially mixed without the labeled probe and incubated at 4°C for 20 minutes. The Biotin labeled probe (see Table 2) was then added and reactions were incubated an additional 30 minutes at 4°C. Reactions were in 1X binding buffer (Pierce) with 1 ug poly dI-dC, 4 ug nuclear extracts, 30 fmol biotinylated probe and 10% glycerol. 20 pmol unlabeled wild-type and mutant probes were used in cold competition assays and 9.8 μg anti-FLAG antibody was used for supershifts. 1X TBE (450 mM Boric acid, 450 mM Tris, 10 mM EDTA pH 8.3) 6% Acrylamide gels were run for approximately 2 hours at 100V followed by immersion transfer to a charged nylon membrane at 100V for 60 minutes. Cross-linking of proteins to the membrane and membrane blotting with streptavidin-linked horseradish-peroxidase were performed according to the manufacturer's recommended protocol (Pierce Lightshift kit).

Table 2: EMSA probes

Promoter	Probe name	Sequence
Bapx1	B7	5'GTAGAGTGATTTTAATTATCAGATTACTTCA-3'
Bapx1	B7mut	5'GTAGAGTGATTTTACCCCTCAGATTACTTCA-3'
Bapx1	B5	5'GTAGAGTGATTTTAATTATCAGATTACTTCAGTAAAGAGCATTA GCAGAGAA-3'

D) RESULTS

I) Expression of epitope tagged Meox proteins in NIH/3T3 and HEK293 cells

The expression of the various Meox proteins and their subcellular localization in NIH/3T3 cells was analyzed by immunocytochemistry 24 hours post-transfection using an anti-FLAG monoclonal antibody. A sufficient commercial antibody to the Meox proteins has not been found. Many cells expressing Meox1-FLAG and Meox2-FLAG demonstrated protein localization or close association with the nuclei (Figure 9A -9D). Meox2ΔHD-FLAG and Meox2-N-term-FLAG were localized to the cytoplasm and excluded from the nuclei (Figure 9E and 9F). Interestingly, the DBD mutant version of Meox2-FLAG is largely localized to the cytoplasm as well (Figure 9G). In a minority of cells Meox2-DBD^{mt}-FLAG is localized to the nuclei (Figure 9G arrowhead). The ENG-Meox2-FLAG and VP16-Meox2-FLAG chimeric proteins contain repressor and activator domains fused to the Meox2 HD and carboxyl-terminal region (Figure 8). ENG-Meox2-FLAG was largely localized to the nuclei of the NIH/3T3 cells as seen by co-localization with the nuclear DAPI stain (Figure 9H and 9I). VP16-Meox2-FLAG was more diffusely localized within both the cytoplasm and nuclei of cells (Figure 9J and 9K). This fusion protein is smaller in size compared to all other Meox proteins (excluding the amino-terminal fragment) and thus diffusion through the nuclear pore complex would be enhanced [123].

The subcellular localization of Meox2-FLAG and Meox1-FLAG was unchanged 48 hours after transfection (data not shown). Several attempts at determining the localization of Meox2-DBD^{mt}-FLAG and Meox2ΔHD-FLAG at this timepoint were unsuccessful. At this timepoint, very few cells expressing the Meox deletion constructs

were observed and those cells that were stained with the anti-FLAG antibody appeared to be apoptotic (data not shown).

The subcellular localization of the Meox proteins were also analyzed in HEK293 cells and similar results as in those seen in the experiments using the NIH/3T3s were obtained. Alterations in subcellular distribution were less apparent due to the larger nuclei and rounded up appearance of the HEK293 cells following transfection (data not shown). Western blots of HEK293 cellular extracts from *Meox* transfected cells were also performed to ensure that similar levels of ectopic protein expression were achieved for the different expression constructs (Figure 10). Although quantification was not performed, all Meox proteins visually appeared to be expressed at similar levels in this cell type and in NIH/3T3 cells (data not shown).

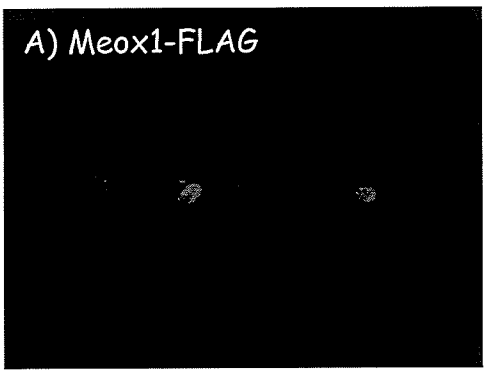
A) Meox1-FLAG


B) Meox1-FLAG


C) Meox2-FLAG

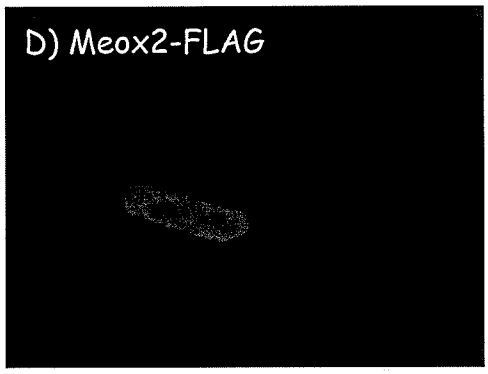
D) Meox2-FLAG


E) Meox2ΔHD-FLAG

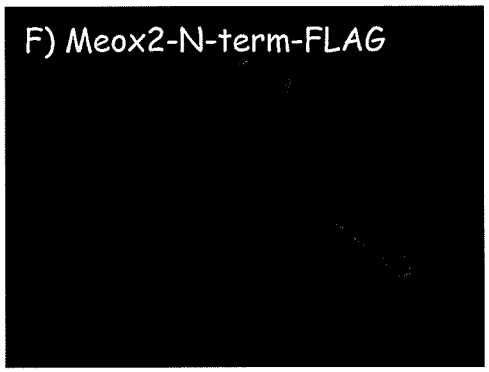
F) Meox2-N-term-FLAG


G) Meox2DBD^{mt}-FLAG

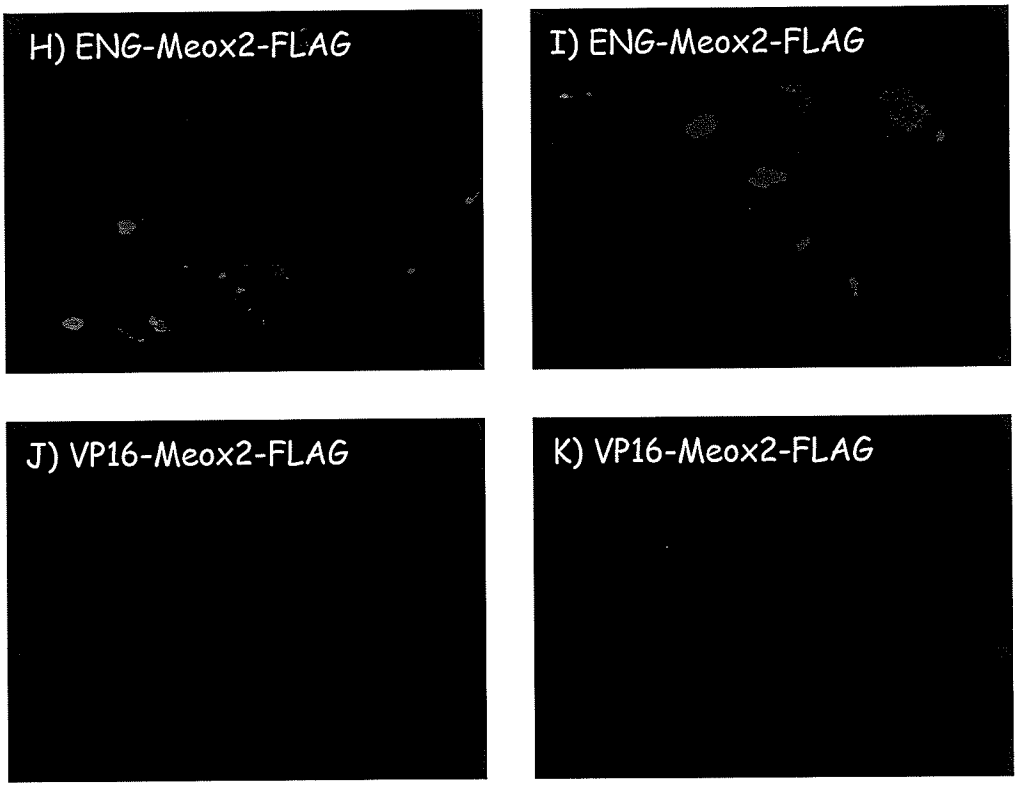

Figure 9: Subcellular distribution of exogenously expressed Meox proteins
Immunocytochemistry of NIH/3T3 cells showing the subcellular location of A) B) Meox1, C) D) Meox2, E) Meox2ΔHD, F) Meox2-N-term, G) Meox2DBD^{mt}, H) I) ENG-Meox2 and J) K) VP16-Meox2 24 hours post-transfection. All constructs contained a carboxyl-terminal FLAG tag that was detected using the anti-FLAG M2 monoclonal antibody. B), D), I) and K) are enlarged views of images A) Meox1, C) Meox2, I) Eng-Meox2 and K) VP16-Meox2, respectively.

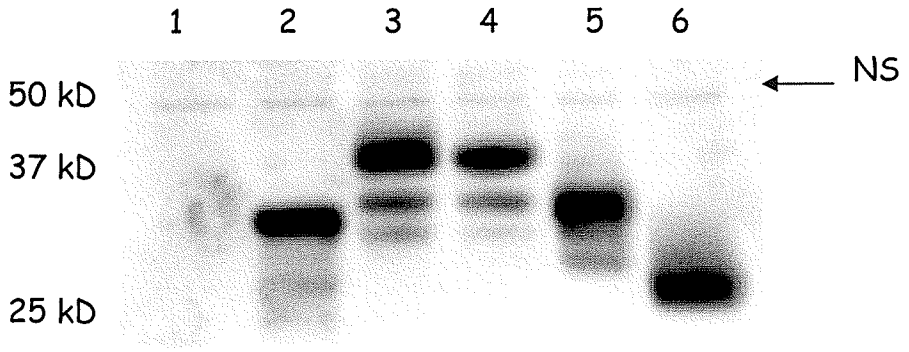

Figure 10: Similar expression levels of the different Meox proteins in HEK293 cells Total cellular proteins derived from cells transfected with 2) Meox1-FLAG, 3) Meox2-FLAG, 4) Meox2-DBD^{mt}-FLAG, 5) Meox2ΔHD and 6) Meox2-N-term-FLAG were separated by SDS-PAGE and analyzed using Western Blot. The negative control for the anti-FLAG monoclonal antibody was proteins derived from cells transfected with the empty pCMV-Tag4A vector (Lane 1). Non-specific bands (NS) were observed in lanes 1-5 and proteolytic degradation products were observed in lanes 3-5.

II) Meox2 DNA binding dependent activation of the *Bapx1* promoter

The human 900 bp *Bapx1* promoter has previously been shown to be activated by Meox1 using luciferase assays. Furthermore, EMSAs provided evidence that this activation was dependent on Meox1 directly binding to DNA [117]. Since the homeodomain of Meox2 is 95% identical to that of Meox1, we predicted that Meox2 would also activate this promoter by directly binding to the promoter sequence and thus provide a model system to verify the activity of our different Meox2 expression constructs. Mouse knockout models supported a role for the redundant regulation of the *Bapx1* promoter by Meox1 and Meox2. In the *Meox1/2* double knockout mice, *Bapx1* expression was completely lost in the somites whereas there was a much less pronounced loss of expression in either of the single *Meox* knockouts [117]. In luciferase reporter assays, a dose dependent activation of the *Bapx1* promoter was seen in NIH/3T3 cells transfected with different levels of *Meox2* expression plasmid (Figure 11). Significant activation of the promoter was observed when 0.5 μg or more of the 4A-Meox2-FLAG plasmid was transfected into the cells (Figure 11).

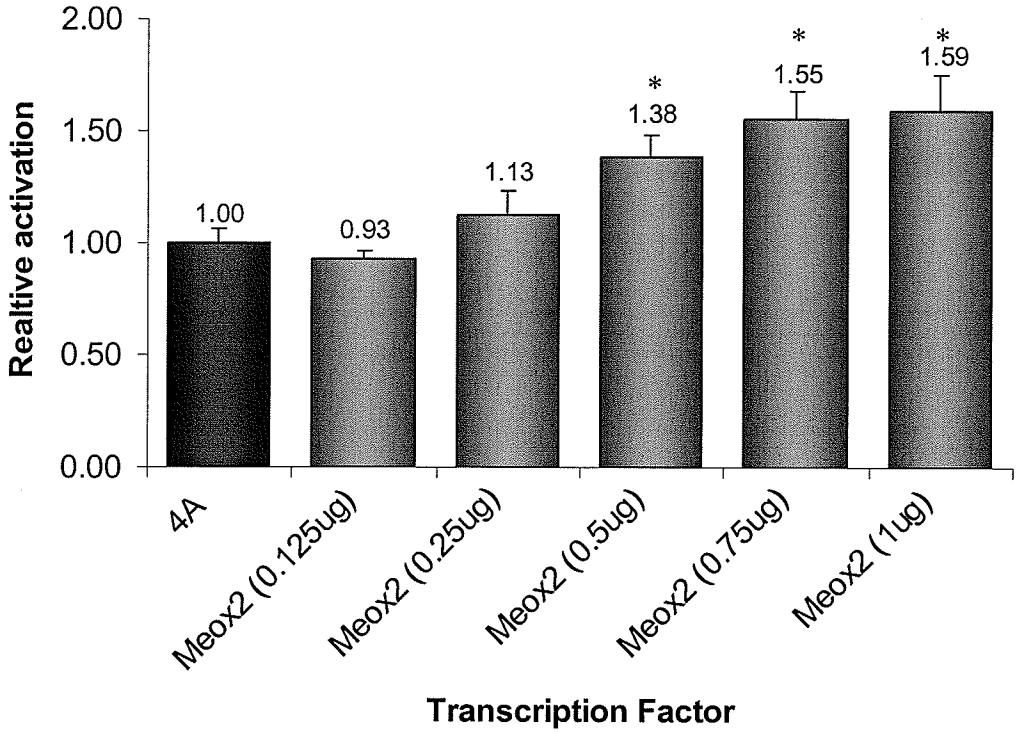

Figure 11: Meox2 activates the *Bapx1* promoter
Luciferase results using NIH/3T3 cells and the 900 bp *Bapx1* promoter demonstrated a dose dependent activation by Meox2. Significant activation of the promoter was seen when at least 0.5 μg of Meox2 expression plasmid was transfected. N=9, P<0.0025.

We used the DNA binding deficient Meox2 expression vectors, 4A-Meox2-DBD^{mt}-FLAG and 4A-Meox2ΔHD-FLAG, to verify that *Bapx1* promoter activation mediated by Meox2 requires DNA binding as had previously been suggested by EMSA results [117]. The DBD mutant has the very well conserved glutamine residue at position 50 of the homeodomain (Q50) mutated to a glutamate (E). This residue has been shown to be important for recognition of TAAT homeobox consensus binding sites and the Q50E mutation has been shown to abolish DNA binding for other homeobox transcription factors such as Siamois [124, 125]. In Meox2ΔHD-FLAG, the entire homeodomain (DNA binding motif of Meox2) was deleted. Both the Meox2-DBD^{mt}-FLAG and the Meox2ΔHD-FLAG mutant proteins were unable to activate the *Bapx1* promoter (Figure 12). These results provided evidence that Meox2 binds and activates the *Bapx1* promoter as was previously suggested by EMSA analysis [117]. Homeodomain proteins recognize similar DNA consensus sequences and binding specificity is imparted by a combination of co-factors and domains flanking the homeodomain [42, 43, 93]. Such binding specificity cannot be fully replicated with *in vitro* assays such as EMSAs and the functional importance of the binding of homeodomain proteins to gene regulatory regions must be validated *in vivo* [93].

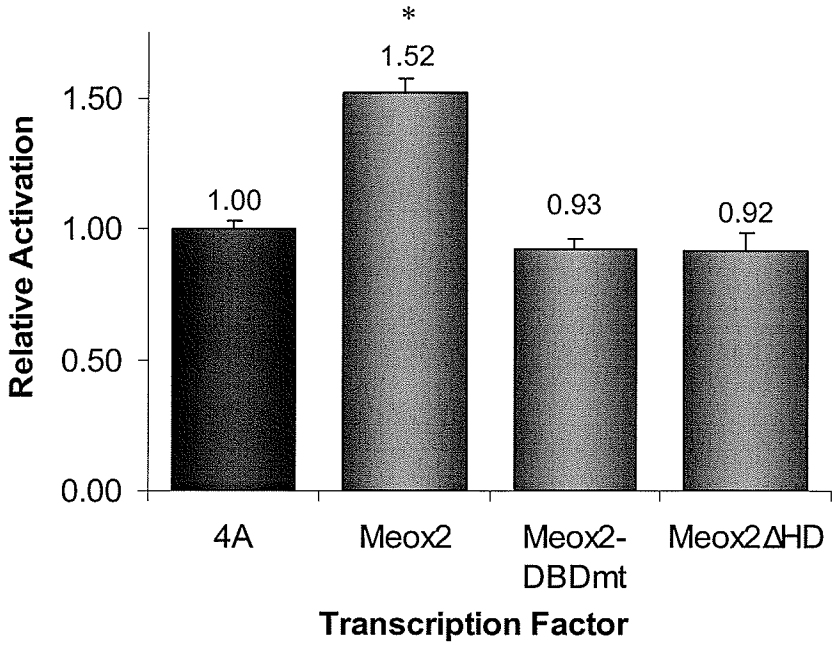

Figure 12: Meox2 DNA-binding dependent activation of the *Bapx1* promoter
Luciferase assay results using 4A-Meox2-DBD^{mt}-FLAG and 4A-Meox2ΔHD-FLAG showing that these mutations abolished Meox2 activation of the *Bapx1* promoter. N=9, P<0.0005.

In order to confirm that Meox2 was indeed acting by binding to DNA and activating transcription rather than inhibiting a protein that repressed expression from the *Bapx1* promoter, chimeric Meox2 proteins were generated (Figure 13). These chimeric proteins have the VP16 Herpes Simplex virus activation domain (a strong activator) or the *Drosophila* Engrailed repressor domain (a strong repressor domain) fused to the carboxyl-terminal region of Meox2 (including the homeodomain) (Figure 8). DNA binding deficient versions of these proteins were generated by mutating the glutamine at position 50 to glutamate as described previously for the full length Meox2 proteins. Chimeric proteins similar to these generated for Meox2 have previously been used to analyze the mechanism of action of various transcription factors [126, 127]. Also, these types of chimeric transcription factors have been used to generate constitutively active proteins or dominant negative proteins [128, 129]. We predicted that the VP16-Meox2 chimeric protein would activate transcription from the *Bapx1* promoter and that this effect would be abolished by the mutation of the glutamine residue. Furthermore we predicted that Engrailed-Meox2 chimeric protein would repress the *Bapx1* promoter in a DNA-binding dependent manner.

The VP16-Meox2-FLAG chimeric protein activated expression from the *Bapx1* promoter 4.2 fold versus the control (Figure 13). This activation was reduced 70% by the DBD mutation (Figure 13). Residual activation seen by VP16-Meox2-DBD^{mt}-FLAG may be due in part to the inability of the Q50E mutation to completely abolish DNA binding. If very minimal or unstable interactions with the DNA were still possible, then this chimeric protein could still significantly activate transcription due to the very strong VP16 activation domain. These results supported our hypothesis that DNA binding is necessary for *Bapx1* promoter activation by Meox2.

Results using the Engrailed-Meox2 chimeric proteins were not as clear as anticipated. Fusion of the Meox2 carboxyl-terminal sequence (including the homeodomain) with this *Drosophila* repressor domain was not sufficient to suppress Meox2-FLAG mediated activation of the *Bapx1* promoter (Figure 13). The activation domain(s) of Meox2 has not yet been mapped. However, this result leads us to consider that either the carboxyl-terminal region or the homeodomain play a role in Meox2-mediated activation. The homeodomain or carboxyl-terminal region may bind other proteins that act as co-factors required for Meox2 mediated activation. The activation observed with Eng-Meox2 was abolished with Q50E mutation further supporting a DNA binding dependent mechanism of activation of the *Bapx1* promoter.

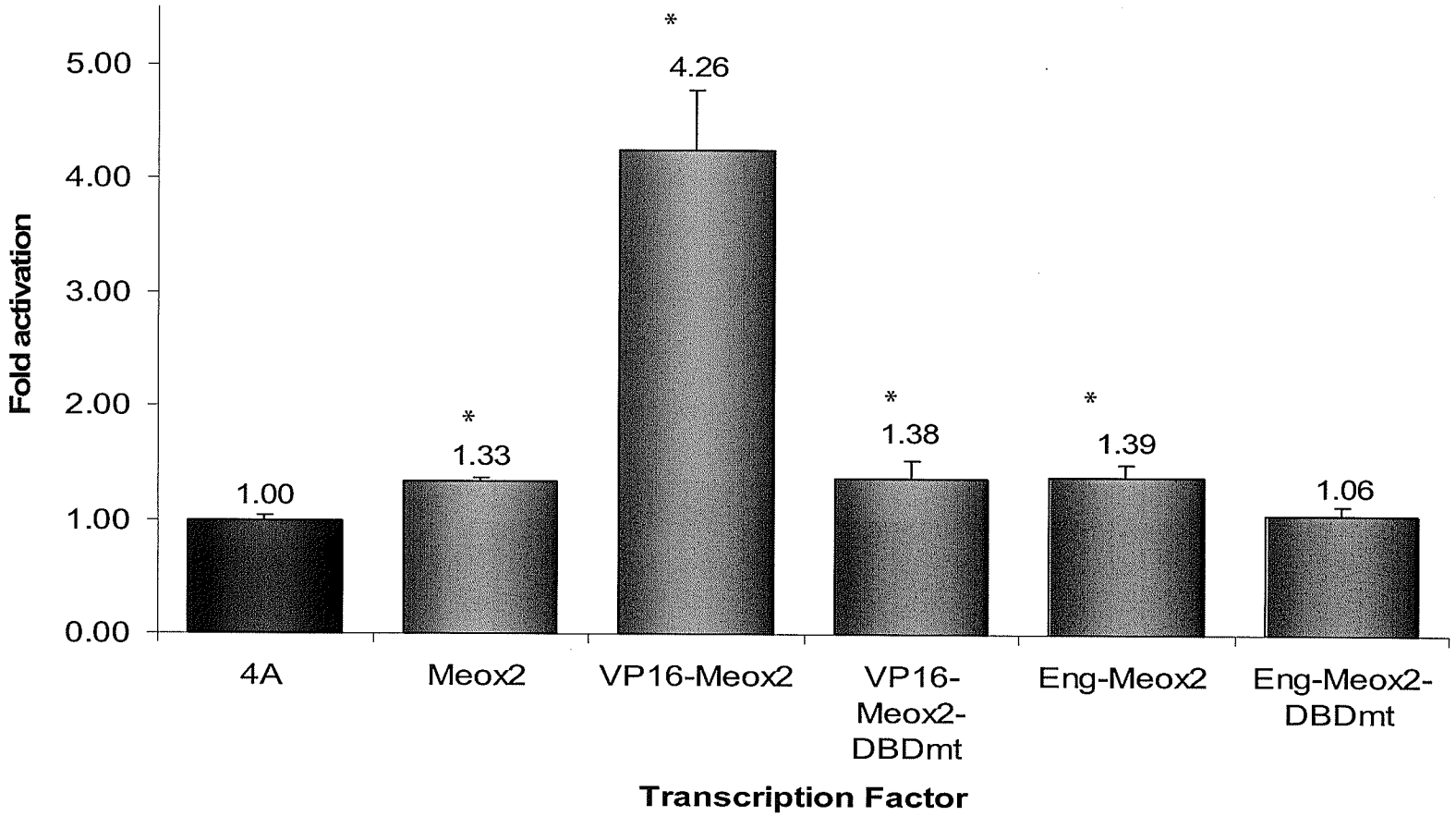

Figure 13: Meox2 activation of *Bapx1* promoter is greatly decreased by the DNA binding domain mutation
Activation of the *Bapx1* promoter by the VP16-Meox2-FLAG and Eng-Meox2-FLAG chimeric proteins was suppressed when the DBD was mutated (VP16-Meox2-DBD^{mt}-FLAG, Eng-Meox2-DBD^{mt}-FLAG). The residual activation seen with the VP16-Meox2-DBD^{mt}-FLAG construct is likely due to transient unstable interactions between the promoter and this fusion protein. N=7, P<0.02.

III) Meox binding to the *Bapx1* promoter

Meox1 and Meox2 have previously been shown to bind a TAAT consensus binding sequence in the *Bapx1* promoter using EMSAs [117]. We have replicated these experiments in order to establish the non-radioactive EMSA system in our lab and to act as a positive control for our EMSA experiments with the *p21* promoter. Furthermore, these experiments allow us to directly test the effect of the Meox DBD mutant proteins on DNA binding.

We were able to show that proteins from nuclear extracts of NIH/3T3 cells transfected with the 4A-Meox1-FLAG expression construct bind specifically to the *Bapx1* oligonucleotide probe (Figure 14A). The shifted band was even more retarded electrophoretically when the anti-FLAG antibody was added to the complex indicating the presence of Meox1-FLAG in the complex, of proteins bound to the probe (Figure 14A). This shifted band was not present when the probe was incubated with nuclear extracts from cells either expressing the Meox1-DBD^{mt}-FLAG protein or cells that were transfected with the empty pCMV-Tag4A vector (Figure 14A and 14B). In this assay, the DBD mutation blocked DNA binding by the mutant Meox1 protein sufficiently to block the detection of the shifted band. The unlabeled mutant probe, in which the consensus homeobox response element had been mutated, was unable to compete for binding with the labeled probe. This finding provided further evidence that the band shift observed was due to a DNA-homeodomain interaction between the probe and Meox1-FLAG and not as a result of other bridging proteins also present in the nuclear extracts. Shifts were observed when either the B5 or B7 (data not shown) *Bapx1* promoter probes were utilized.

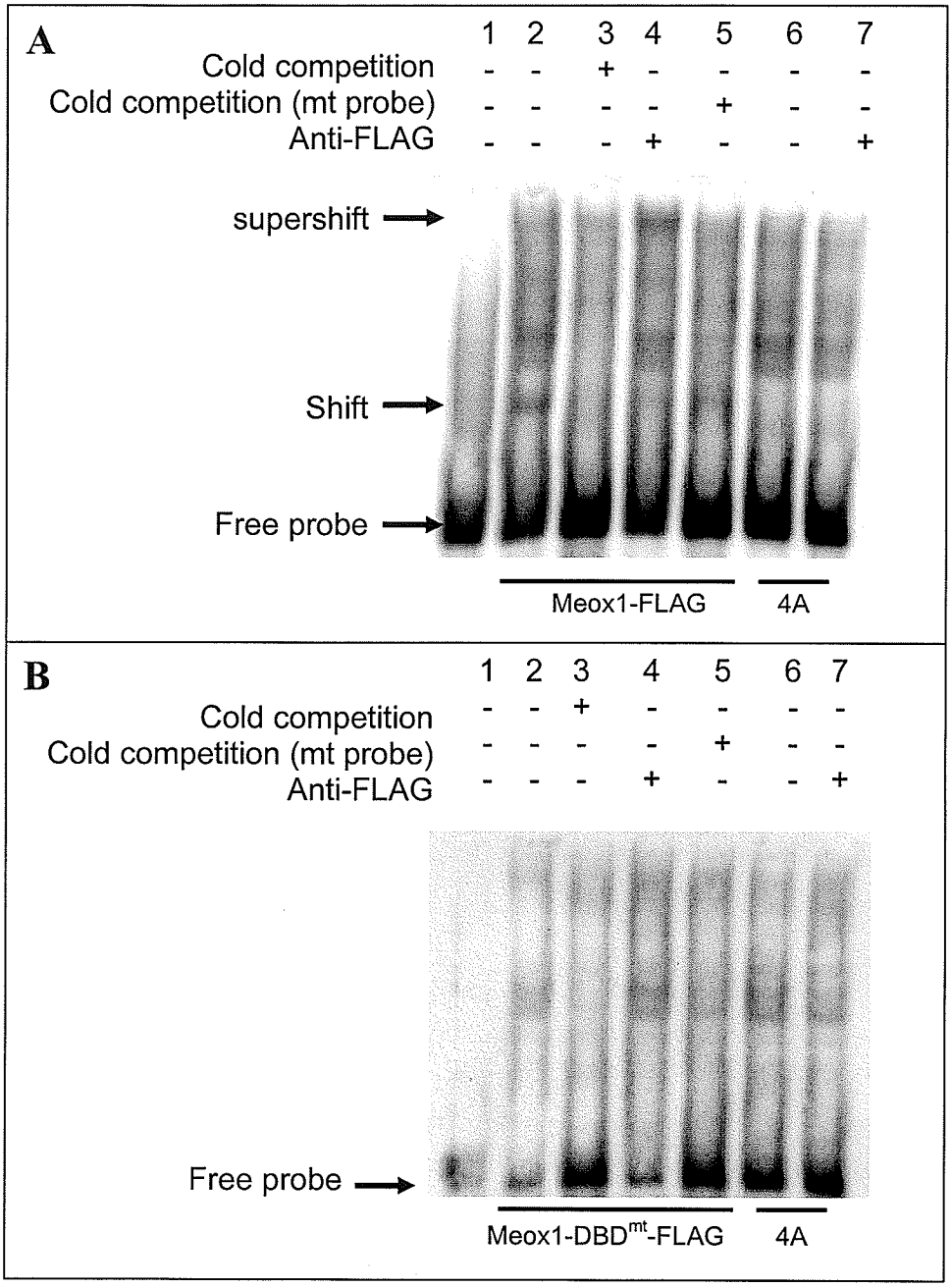

Figure 14: Meox1-FLAG binds to a consensus site within the *Bapx1* promoter
A, Gel shifts obtained using nuclear extracts from cells expressing Meox1-FLAG (lanes 2-5) were compared to shifts obtained from nuclear extracts derived from cells transfected with the empty pCMV-Tag4A vector (lanes 6-7). A specific shift was observed in lane 2. The unlabeled probe was able to compete for binding with the labeled B5 probe (lane 3) and the complex was "supershifted" using the anti-FLAG monoclonal antibody (lane 4). The mutant probe (B7mut) was unable to compete for DNA binding (lane 5). **B**, EMSA using nuclear extracts from cells expressing the Meox1-DBD^{mt}-FLAG protein (lanes 2-5) and cells transfected with the empty pCMV-Tag4A vector (lanes 6-7). There was no difference in the band shifts seen between nuclear extracts obtained from the Meox1-DBD^{mt}-FLAG expressing cells and the control cells.

EMSA experiments were repeated with nuclear extracts from cells expressing the Meox2-FLAG and Meox2-DBD^{mt}-FLAG proteins. In this instance, we were unable to detect a specific shifted band (Figure 15A). Perhaps the complex containing Meox2-FLAG was being obstructed by complexes formed with endogenous proteins. Therefore, we used recombinant MBP-Meox2-FLAG and MBP-Meox2-DBD^{mt}-FLAG proteins which are chimeric proteins containing the maltose binding protein (MBP) fused to Meox2-FLAG and Meox2-DBD^{mt}-FLAG, respectively (Figure 15B). Although, we were able to successfully purify these proteins (Figure 16), we were unable to detect binding of these proteins to the *Bapx1* promoter probes (B5 or B7). Perhaps the recombinant protein was folded incorrectly for DNA binding.

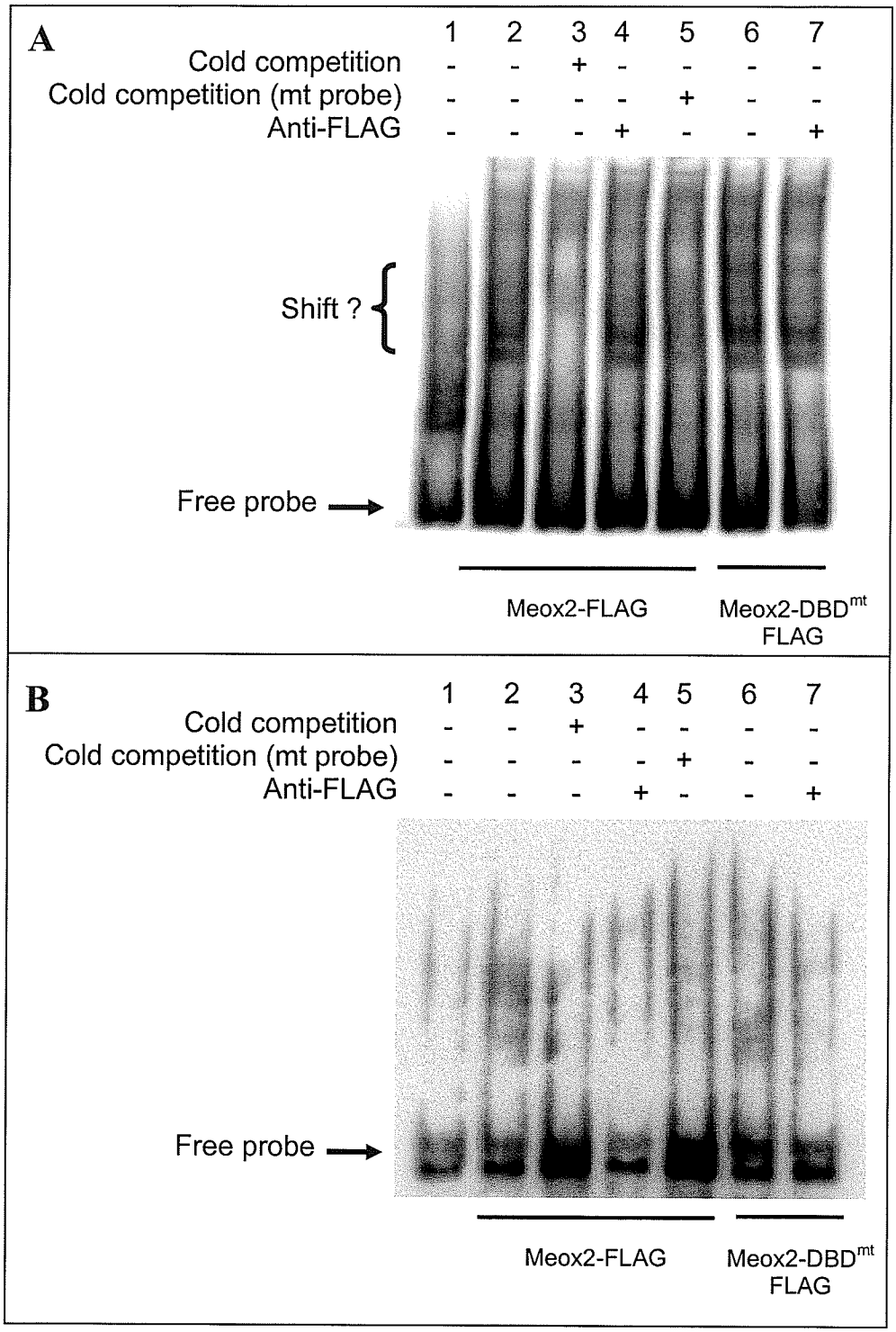

Figure 15: Meox2-FLAG does not bind to the Meox1 DNA consensus binding site in the *Bapx1* promoter

A, EMSAs with nuclear extracts from cells expressing Meox2-FLAG (lanes 2-5) and Meox2-DBD^{mt}-FLAG (lanes 6-7) contained many bands that interfered with our ability to identify any specific bands containing Meox2-FLAG. **B**, EMSAs using Meox2 recombinant proteins did not demonstrate a complex between the Meox2-FLAG protein and the *Bapx1* probe.

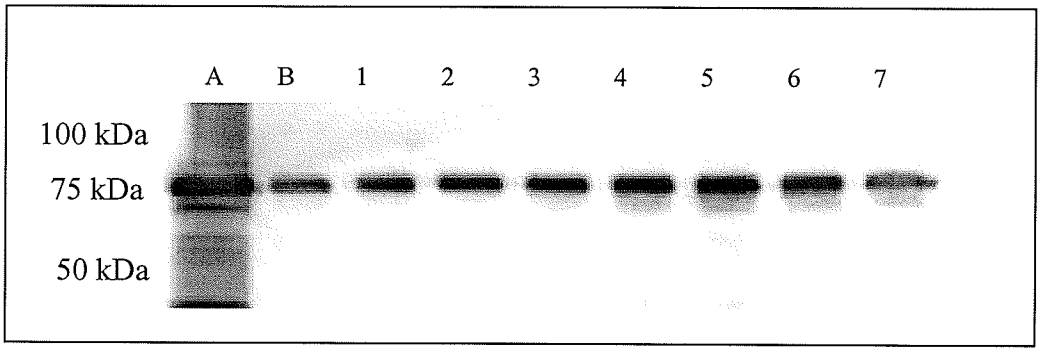

Figure 16: Purification of recombinant MBP-Meox2-FLAG protein
Western Blot analysis of fractions collected during purification of the MBP-Meox2-FLAG recombinant protein on an amylose resin column. **A** indicates the flow through when the sample was initially applied to the amylose resin column. **B** contains the fraction that was eluting from the column at the end of the wash period. **Lanes 1-7** are the first seven 1 ml aliquots eluted from the column. MBP-Meox2-FLAG was detected using the anti-FLAG antibody. Samples 4-5 gave the strongest signal for the fusion protein. The predicted molecular weight of MBP-Meox2-FLAG is 76.5 kDa.

IV) Meox DNA binding independent activation of the *p21* promoter

Since cell cycle arrest induced by Meox2 requires p21, we examined Meox2's regulation of the *p21* promoter. We obtained the 2.4 kb human *p21* promoter [31]. This promoter contains two p53 binding sites at -2270 and -1380 relative to the transcriptional start site (Figure 17) [32]. Thus we used p53 as a positive control for the initial luciferase experiments which were performed in HEK293 cells. p53-EGFP activated expression from the *p21* promoter 3.5 fold versus the empty vector control (pIRES-EGFP) (Figure 18). In comparison, Meox1-EGFP and Meox2-EGFP activated expression from the *p21* promoter 1.80 and 1.78 fold controls. A significant difference was not observed between the activation mediated by Meox1-EGFP versus Meox2-EGFP.

Carboxyl-terminal EGFP tagged Meox constructs were initially used so that the transfection efficiency could be easily monitored and compared using a fluorescent microscope (data not shown). Subsequent experiments were performed using carboxyl-terminal FLAG epitope tagged proteins since this 8 amino acid epitope is much smaller than the 244 amino acid EGFP protein. We reasoned that the EGFP tag could perhaps result in non-physiological or irrelevant interactions due to its large size, possibly affecting the stability and function of the fusion protein.

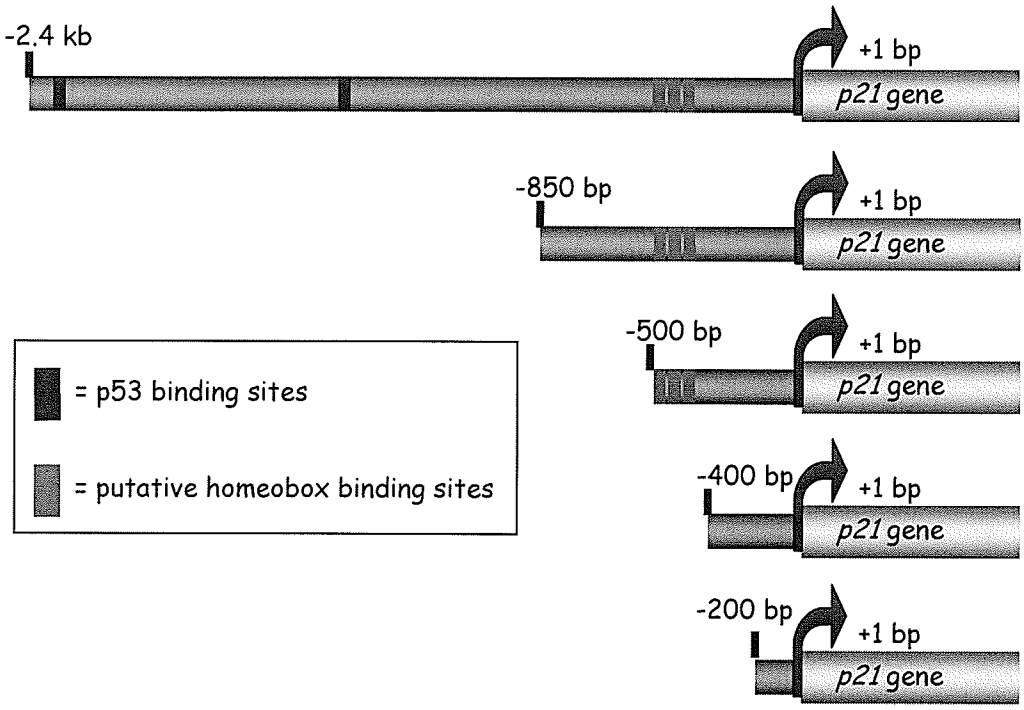

Figure 17: *p21* promoters
The *p21* promoter contains two p53 responsive sites at positions -2270 and -1380. These sites are found in the 2.4 kb construct and have been deleted in all of the truncated constructs. The 400 bp and 200 bp constructs do not contain the three TAAT motifs between positions -434 and -471 which are found in all of the other constructs.

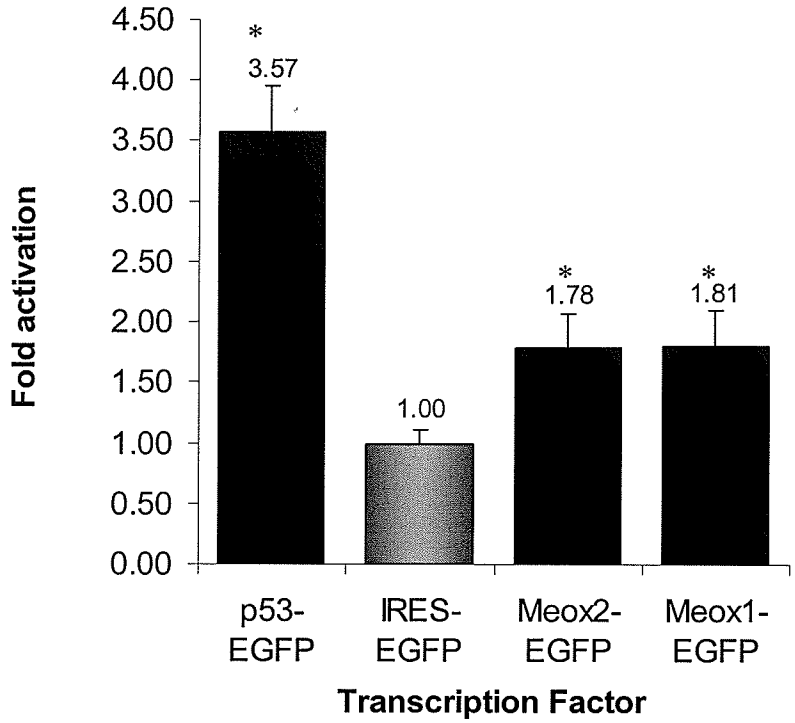

Figure 18: Meox1/2 activate the 2.4 kb *p21* promoter
HEK293 cells were transfected with the indicated vectors and the 2.4 kb *p21* promoter construct using the Ca^{2+} Phosphate method. Meox1-EGFP and Meox2-EGFP activated the *p21* promoter equivalently when compared to the IRES-EGFP control. $N \geq 10$, $p<0.01$.

Transient Ca^{2+} phosphate transfections of HEK293 cells with 4A-Meox1-FLAG and 4A-Meox2-FLAG supported our hypothesis that the Meox1/2 proteins activate the 2.4 kb *p21* promoter equivalently (Figure 19) as previously demonstrated with the Meox-EGFP fusion proteins. In this case, expression was induced approximately 1.3 fold for both the 850 bp and 2.4 kb *p21* promoter reporter constructs versus the 1.8 fold activation seen with the Meox-EGFP fusion proteins. The difference in the level of activation may be due to the particular tag used, FLAG versus EGFP. It was necessary to use tagged versions of the Meox proteins since an antibody for the wild-type proteins was not available to monitor protein expression by immunocytochemistry or western blot analysis.

The homeodomain-deleted and DBD-mutated versions of the Meox proteins were used to determine whether DNA binding was necessary for Meox-mediated activation of the *p21* promoter. Both of these DNA-binding deficient versions of Meox1 and Meox2 were still able to activate the *p21* promoter at levels that were not significantly different from their respective wild-type controls (Figure 19). This result provided evidence to support that Meox1 and Meox2 are mediating their regulation of *p21* transcription independently of DNA binding and therefore are either acting as transcriptional co-activators or transcriptional co-repressors.

We used the 850 bp truncated version of the *p21* promoter (Figure 19, blue bars) to delineate the region of the promoter that is responsive to Meox1 and Meox2. This shorter version of the promoter contains the three putative homeobox binding sites but not the p53 responsive sites located upstream. Meox1/2-mediated activation of the *p21* promoter was not affected by this truncation, further confirming previous reports that Meox2 activation of *p21* gene expression occurs independently of p53 binding [34].

Due to the low transfection efficiencies obtained using the Ca^{2+} Phosphate transfection method, differences between the DNA binding defective and wild-type Meox proteins may not have been evident due to the limited degree of activation obtained for any of the constructs. We therefore optimized the transfection conditions using the Lipofectamine 2000 transfection reagent and achieved higher levels of transfection and a level of *p21* promoter activation that was more comparable (2 fold activation) to those previously obtained with the Meox-EGFP fusion proteins (Figure 20). Similar activation levels were obtained with the different mutant proteins confirming that DNA binding is not necessary for the Meox-mediated activation of the *p21* promoter (Figure 20).

In order to confirm the specificity of Meox2-mediated activation of the *p21* promoter, we verified that a dose dependent increase in activation was observed. Meox2-FLAG did increase the 2.4 kb *p21* promoter activity *in vitro* proportionally to the amount of plasmid encoding the transcription factor used in each experiment (Figure 21). The total amount of DNA in each transfection was kept constant by supplementing with the empty pCMV-Tag4A vector. Experiments conducted in serum starved cells using 3μg of plasmid encoding Meox2 did not show increased activation levels versus those obtained with non-serum starved cells (data not shown).

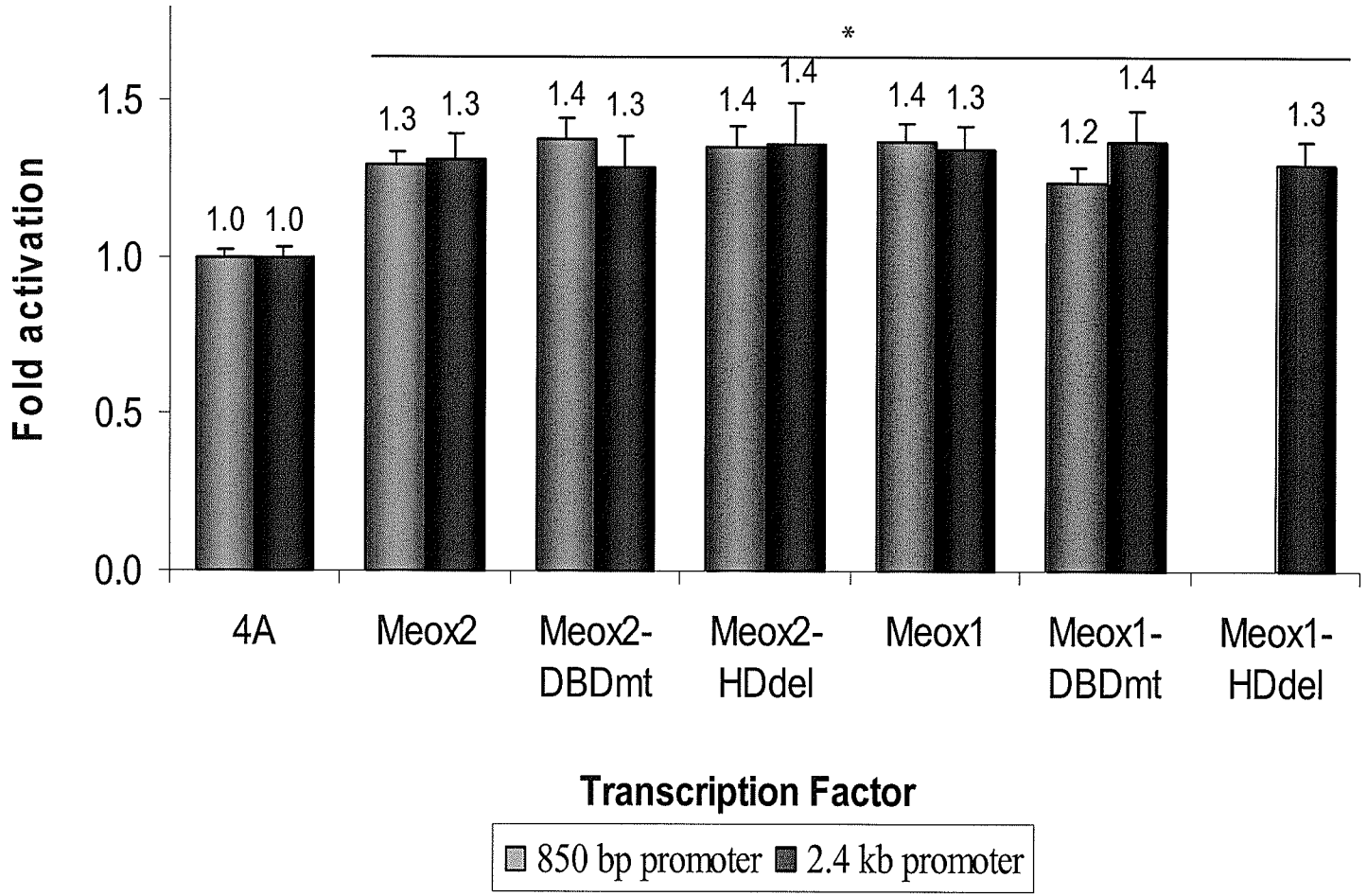

Figure 19: DNA binding independent and p53 independent activation of the *p21* promoter by Meox1/2
Meox2-DBD^{mt}-FLAG, Meox2ΔHD-FLAG, Meox1-DBD^{mt}-FLAG and Meox1ΔHD-FLAG activated the *p21* promoter constructs equivalently to the wild-type proteins indicating that binding to DNA is not necessary for this activation. There were no significant differences in the activation levels between the 850 bp and 2.4 kb promoters supporting that the p53 binding sites are not necessary for the activation observed. $N \leq 6$, $p<0.0005$.

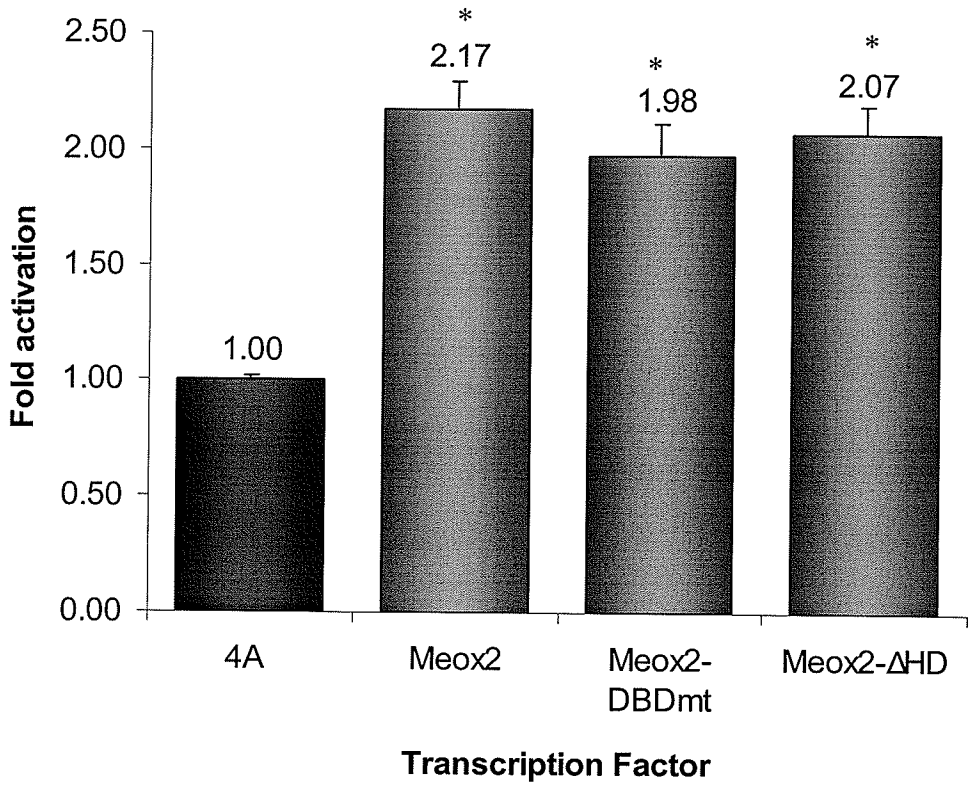

Figure 20: DNA binding independent activation of the *p21* promoter by Meox2
Luciferase assay results from HEK293 cells transfected with different Meox2 plasmids using Lipofectamine 2000 reagent. Meox2-FLAG, Meox2-DBD^{mt}-FLAG and Meox2ΔHD-FLAG all activated the 850 bp *p21* promoter approximately 2 fold versus the 4A control vector. No significant difference was noted between the different Meox2 constructs used. N=18, $p<0.0005$.

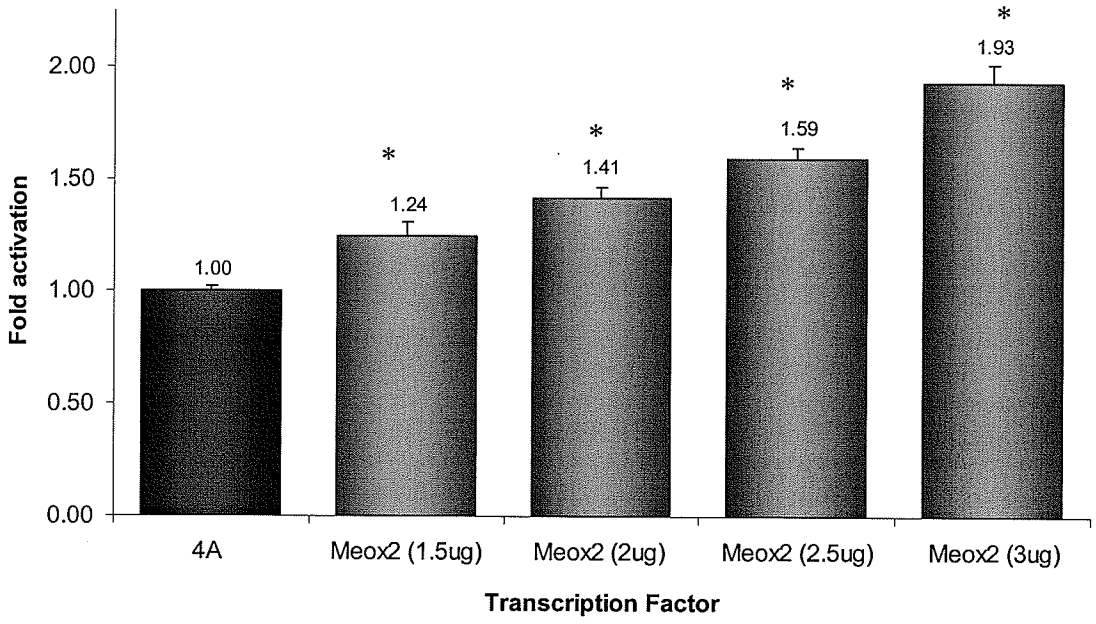

Figure 21: Dose dependent activation of the *p21* promoter by Meox2
Luciferase assay results from HEK293 cells demonstrating Meox2 activation of the 2.4 kb *p21* promoter in a dose-dependent manner. N=10, $p<0.0005$.

To identify the region of Meox2 required for transcriptional activation, HEK293 cells were transfected with the 850 bp *p21* promoter and 4A-Meox2-FLAG, 4A-Meox2ΔHD-FLAG and 4A-Meox2-N-term-FLAG and luciferase assays were performed. We showed that the amino-terminal region of Meox2 was sufficient to mediate transcriptional activation from the *p21* promoter. The activation level with Meox2-N-term-FLAG was not significantly different from those obtained for Meox2ΔHD-FLAG and Meox2-FLAG (Figure 22). 4A-Meox1-FLAG, 4A-Meox2-FLAG, 4A-Meox2-N-term-FLAG and 4A-Meox1-N-term-FLAG had previously been shown to equivalently activate the *p21* promoter (data not shown).

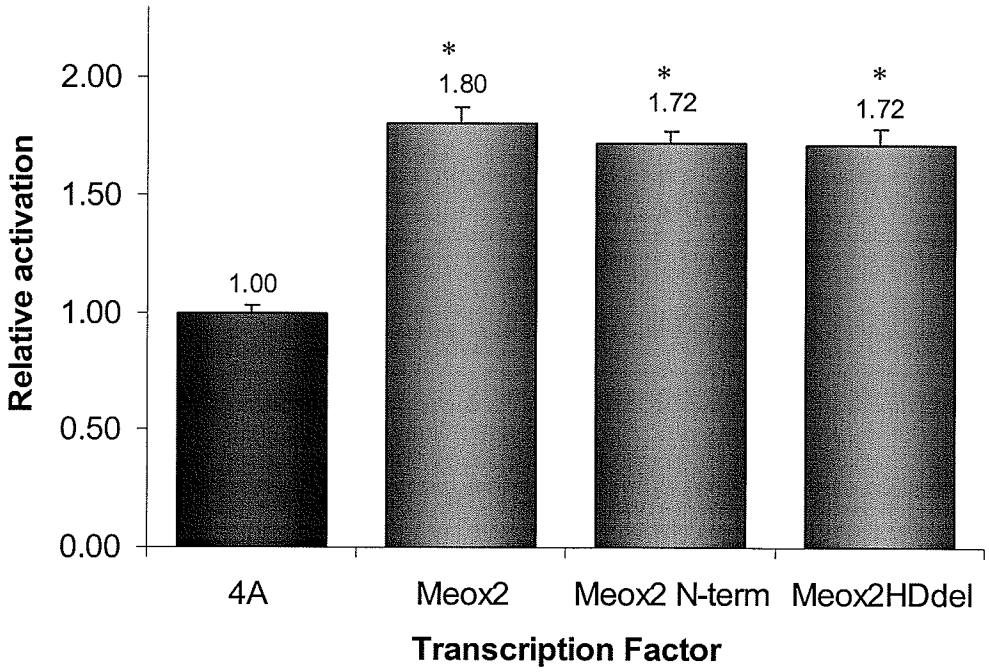

Figure 22: The amino terminal region of Meox2 activates the *p21* promoter
Luciferase assays using Lipofectamine 2000 transfections of HEK293 cells demonstrated that the Meox2-N-term-FLAG protein activated expression from the 850 bp *p21* promoter similarly to the activation obtained with Meox2-FLAG and Meox2ΔHD-FLAG. N ≥15, $p<0.0005$.

As with the *Bapx1* promoter studies, transfections and luciferase assays using the 4A-VP16-Meox2-FLAG and 4A-VP16-Meox2-DBD^{mt}-FLAG plasmids were done to verify that Meox2 was acting as a transcriptional co-activator. Since the DBD mutation and homeodomain deletion did not affect Meox2 activation of the *p21* promoter, we did not anticipate that the DBD mutation would affect the activation mediated by VP16-Meox2-FLAG. Contrary to our expected results, the DBD mutation reduced the activation mediated by the VP16-Meox2-FLAG fusion protein by 48%; this result was statistically significant (Figure 23). These constructs do not contain the amino-terminal region of Meox2 and only include the homeodomain and the carboxyl-terminal region. Two possible reasons were proposed to explain this result. The carboxyl-terminal and homeodomain regions may require DNA binding in order to activate the *p21* promoter whereas the amino-terminal region can activate transcription from the *p21* promoter independent of DNA binding. Alternatively the DBD mutation may be affecting the conformation of Meox2 and thus affecting protein-protein interactions mediated by this region. Evidence supporting this hypothesis is the observation that the DBD mutation alters Meox2 subcellular localization from the nucleus to the cytoplasm (Figure 9). The DBD mutation may also have other unanticipated effects other than simply abolishing DNA binding.

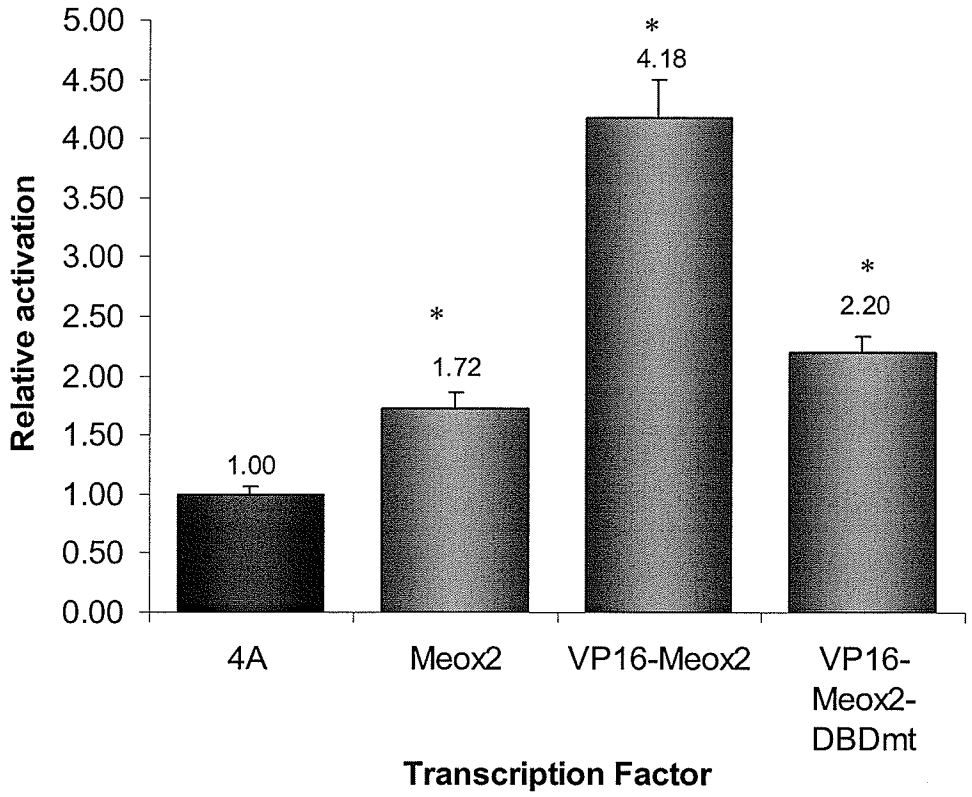

Figure 23: Meox2 induces *p21* transcription by acting as a transcriptional activator
Results from luciferase assays in HEK293 cells demonstrating that the activation mediated by the VP16-Meox2-FLAG fusion protein is significantly reduced by the DBD mutation. The activation mediated by the VP16-Meox2-DBD^{mt}-FLAG construct was significant when compared with controls. N=9, $p<0.0005$.

Results with the 4A-VP16-Meox2-FLAG and 4A-VP16-Meox2-DBD^{mt}-FLAG fusion protein demonstrated that the DBD mutation reduced the activation of the *p21* promoter mediated by this chimeric protein. The mechanism underlying how the mutation was reducing activation of the *p21* promoter was unclear. To address whether this mutation was preventing DNA binding and thus blocking activation of the *p21* promoter, luciferase assays were repeated with the 400 bp and 500 bp truncated versions of the *p21* promoters. VP16-Meox2-FLAG activated the 400 bp *p21* promoter construct lacking the three homeodomain recognition sequences, equivalently to its activation of the 500 bp *p21* promoter construct, which included these homeodomain binding sites (Figure 24). The DBD mutation similarly affected VP16-Meox2-FLAG activation of both these promoters (Figure 24). Taken together, these results demonstrate that the VP16-Meox2-FLAG fusion construct activates the *p21* promoter without binding to the homeodomain binding sites. Also, the effect of the DBD mutation on Meox2 function is more complicated than simply altering Meox2's ability to bind TAAT consensus sequences.

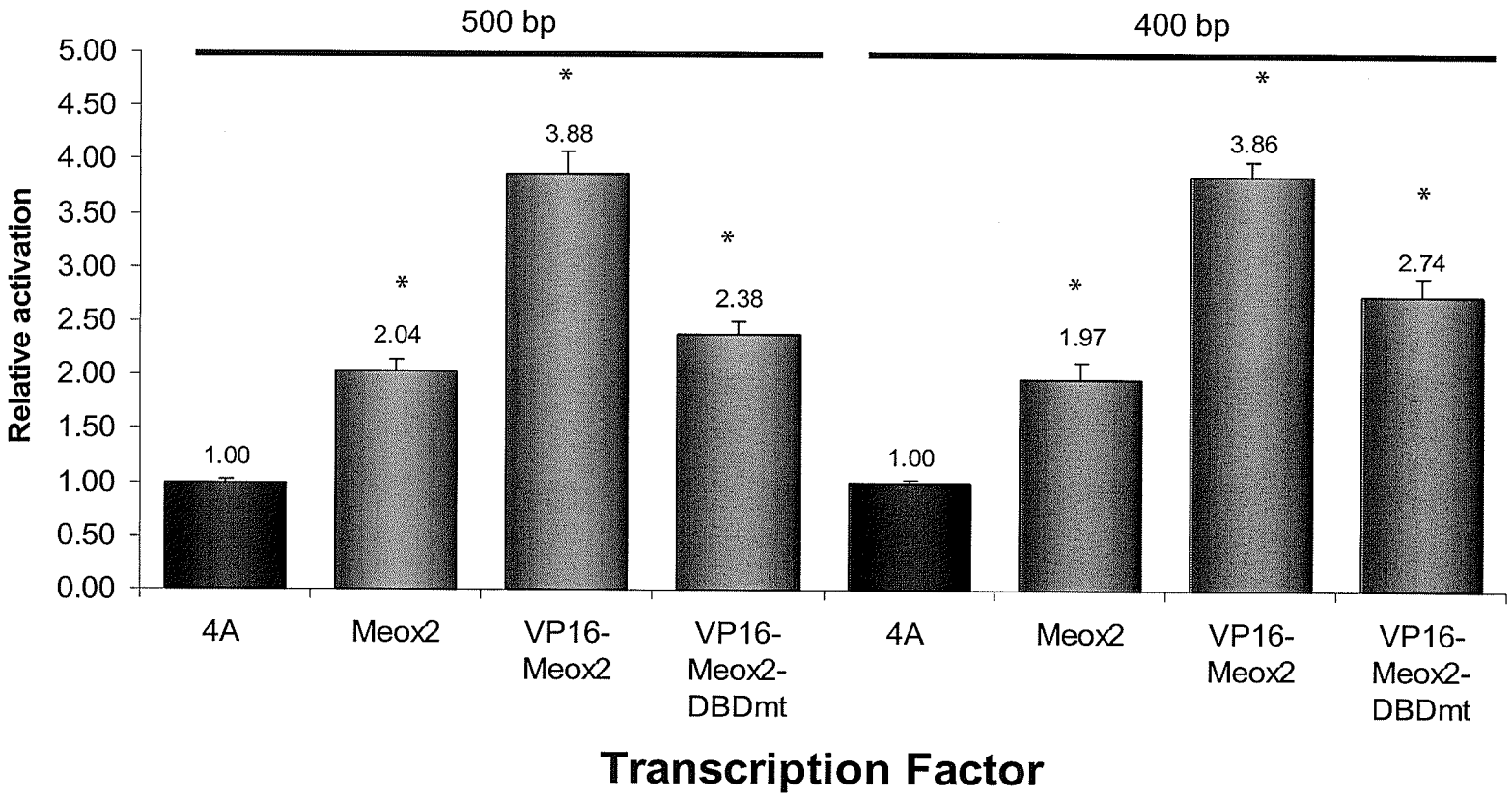

Figure 24: The homeodomain and carboxyl-terminal regions of Meox2 do not require the presence of consensus homeodomain binding sequences to activate the *p21* promoter

Luciferase assay results in HEK293 cells showing that the VP16-Meox2-FLAG fusion protein activated the *p21* promoter independently of the TAAT consensus sequences. Activation levels are equivalent between the 400 bp promoter, which lacks the homeodomain responsive elements, and the 500 bp promoter containing the homeodomain responsive elements. The DBD mutation reduces activation similarly between the 400 and 500 bp promoters. N=9, $p<0.0005$.

In order to determine which region of the *p21* promoter is regulated by Meox2, truncated *p21* promoters including the proximal 500 bp and 400 bp relative to the transcription start site were tested in luciferase assays using HEK293 cells. The pcDNA3 control plasmid and pcDNA3-Meox2 plasmid were used in these experiments rather then the pCMV-Tag4A and 4A-Meox2-FLAG plasmids. The reason for switching plasmids is explained in the subsequent section. Meox2 activated these shorter regions of the promoter similarly to the longer 850 bp and 2.4 kb *p21* promoter constructs (Figure 25). Intriguingly, the 400 bp *p21* promoter does not contain the three consensus homeodomain binding sites through which we originally hypothesized Meox2 would regulate this promoter. Thus, Meox activation of the *p21* promoter is probably not mediated through binding to the TAAT motifs present in the *p21* promoter. The basal activities of these truncated promoters were also determined to ensure that key regulatory regions had not been deleted (Figure 25A). Other experiments determined that the 200 bp *p21* promoter still contained the sequences necessary for Meox2 mediated activation at levels equivalent to those obtained with the 2.4 kb *p21* promoter (data not shown). A single experiment was done with Meox2-N-term-FLAG, Meox2ΔHD-FLAG and the 500 and 400 bp truncated *p21* promoters that determined that the shorter promoters also contained the regions regulated by these mutant Meox2 proteins *in vitro* (data not shown).

Luciferase assays were performed in NIH/3T3 cells to determine whether Meox2 could activate expression from the 2.4 kb *p21* promoter in this fibroblast cell line. A clear trend was not observed when increasing amounts of Meox2 were transfected (Figure 26). Similarly, experiments in NIH/3T3 cells using pcDNA3, pcDNA3-Meox2 and the 850 bp *p21* promoter did not show activation (data not shown). Meox2 did not activate the *p21* promoter in U2OS cells either (data not shown).

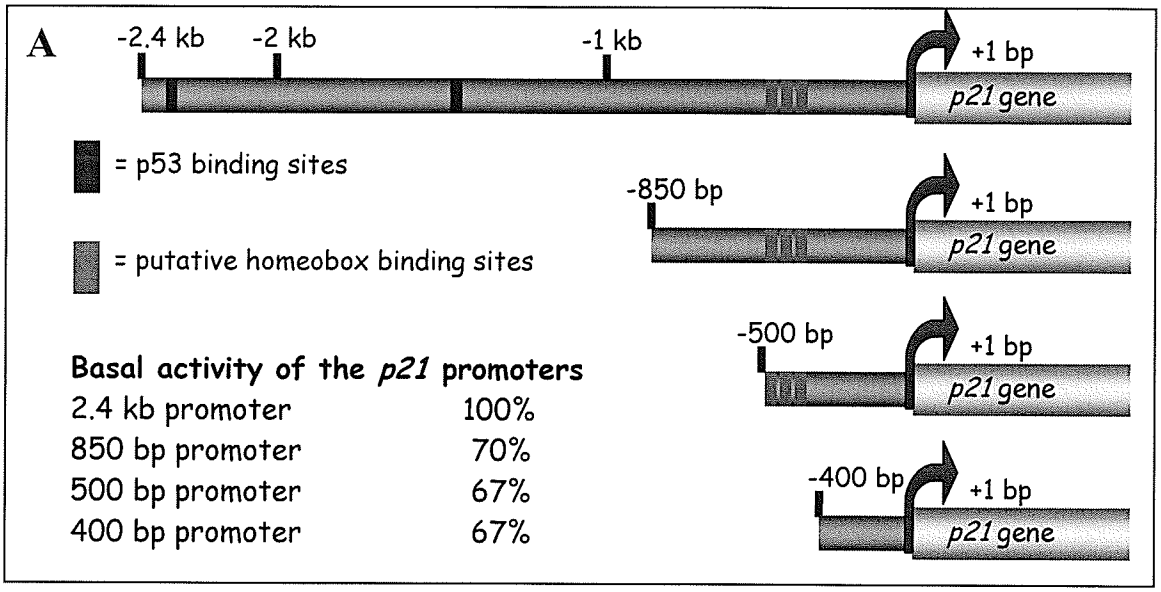

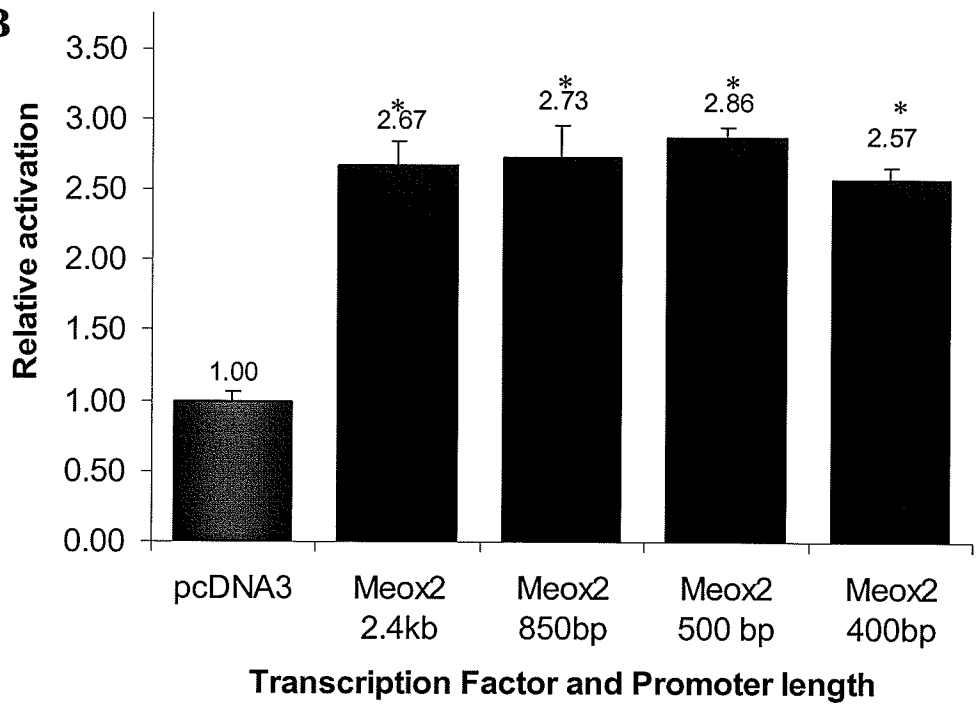

Figure 25: Meox2 activates regions of the truncated *p21* promoter lacking the homeodomain binding consensus sequences

A, Representation of the *p21* promoters used and the basal activity seen without the addition of an exogenous transcription factor. Activation of the full-length 2.4 kb *p21* promoter was set at 100%. B, Luciferase assay results using HEK293 cells transfected with pcDNA3 and pcDNA3-Meox2 and different versions of the *p21* promoter. Meox2 activated the 2.4 kb, 850 bp, 500 bp and 400 bp *p21* promoters equivalently. N $\geq$9, $p<0.0005$.

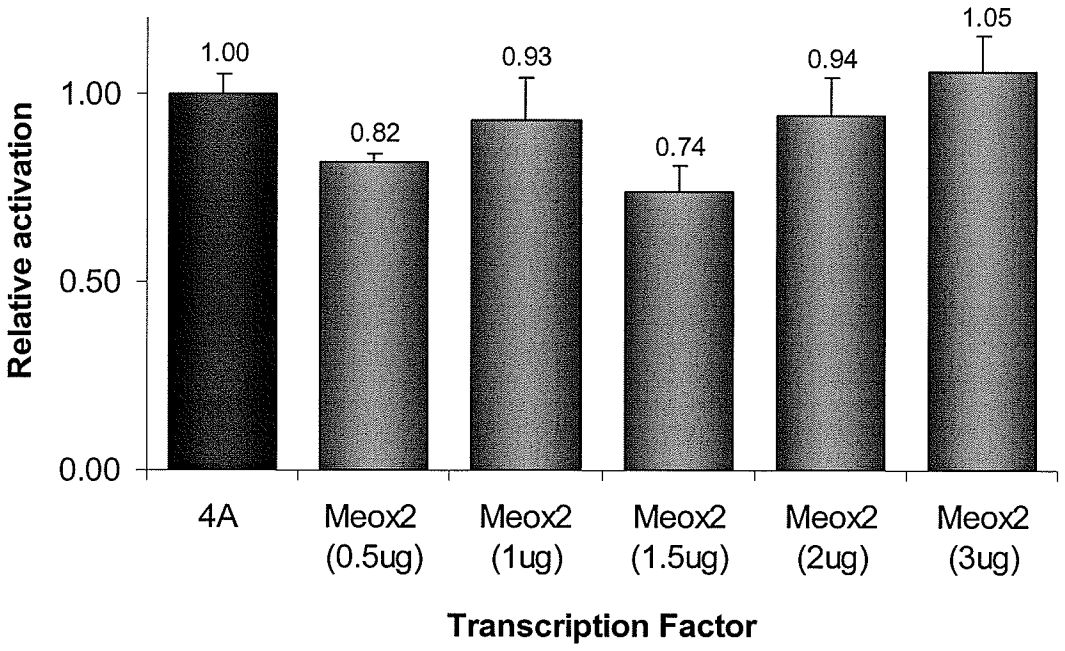

Figure 26: Meox2 does not activate transcription from the 850 bp *p21* promoter in NIH/3T3 cells

Representative experiment demonstrating that a dose dependent activation of the *p21* promoter by Meox2 is not observed in NIH/3T3 cells when 4A-Meox2-FLAG is used. N=3

V) The carboxyl-terminal FLAG tag affects Meox2-mediated transcriptional activation

During the course of this study we suspected that the vectors used to clone our transcription factors were affecting the levels of activation obtained in the luciferase reporter experiment. We therefore performed a series of tests using Meox2 cloned into different vectors (pcDNA3 versus pCMV-Tag4A) with or without the carboxyl-terminal FLAG epitope tag (Meox2 versus Meox2-FLAG). Transfection of pcDNA3-Meox2 into HEK293 cells resulted in a 3.76 fold activation of the 850 bp *p21* promoter compared to the 2.11 fold activation levels obtained when 4A-Meox2-FLAG was transfected (Figure 27). This increase in transcriptional activation was also seen in NIH/3T3 cells when the *Bapx1* promoter was used (Figure 28). In previous experiments using 4A-Meox2-FLAG and the *Bapx1* promoter, activation levels obtained were approximately 1.5 fold with a single experiment yielding an activation level of 1.8 fold (Figure 12). With the pcDNA3-Meox2 construct we obtained a 2 fold activation of the *Bapx1* promoter (Figure 28). Therefore the increased activation using the pcDNA3-Meox2 was seen with both the *p21* and *Bapx1* promoters.

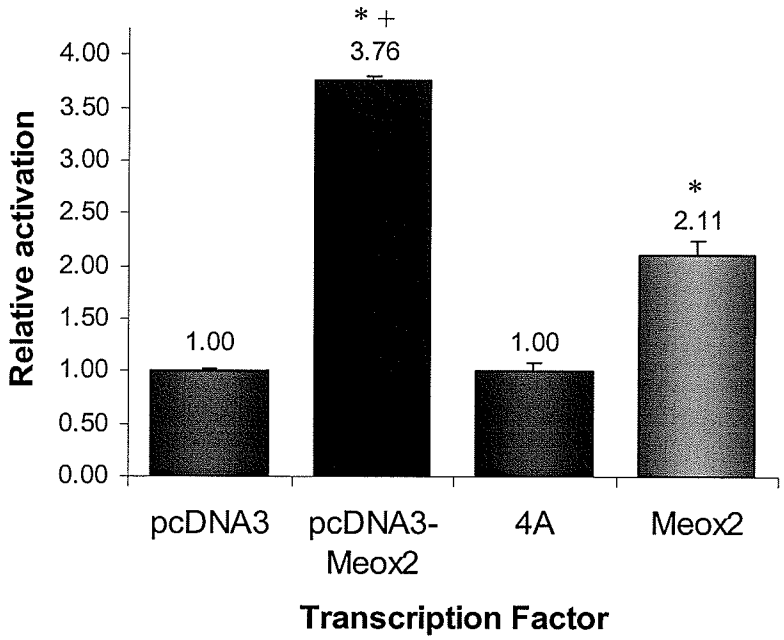

Figure 27: Carboxyl-terminal epitope tagging reduced the transcriptional activation mediated by Meox2

Luciferase assay results demonstrating that transfections with pcDNA3-Meox2 lead to stronger activation of the 850 bp *p21* promoter versus transfections with 4A-Meox2-FLAG. N=3, *$p<0.0005$ versus controls, +$p<0.0005$ versus Meox2-FLAG.

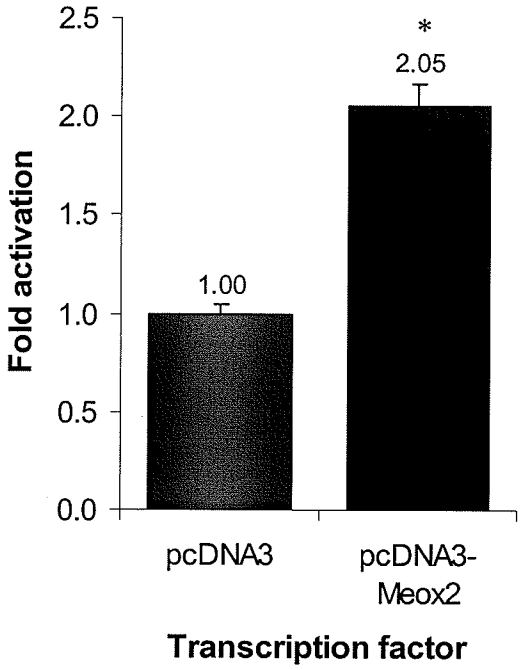

Figure 28: *Bapx1* promoter activation using pcDNA3-Meox2
Bapx1 promoter activation using the pcDNA3-Meox2 construct in NIH/3T3s. N=3, $p<0.0005$.

The enhanced activation seen in both NIH/3T3 cells and HEK293 cells using the pcDNA3-Meox2 construct could either be caused by effects due to the particular plasmid used or due to the presence of the FLAG epitope. In order to determine which factor is responsible, luciferase assays were performed using pcDNA3 as a control and comparing the effects of pcDNA3-Meox2 versus pcDNA3-Meox2-FLAG and pcDNA3-Meox2-DBD^{mt}-FLAG. Both Meox2-FLAG proteins similarly activated the *p21* promoter (1.26 fold for the wild-type and 1.21 for the ΔHD) whereas the non-FLAG tagged Meox2 activated luciferase expression 2.79 fold (Figure 29). The fold induction obtained with pcDNA3-Meox2-FLAG and pcDNA3-Meox2ΔHD-FLAG was lower than when the Meox2 proteins were encoded by the pCMV-Tag4A vector. This reduction is likely due to a lower level of transfection efficiency seen in these experiments as the activation by the non-FLAG tagged Meox2 is also lower than what had been observed previously (Figure 27 versus Figure 29).

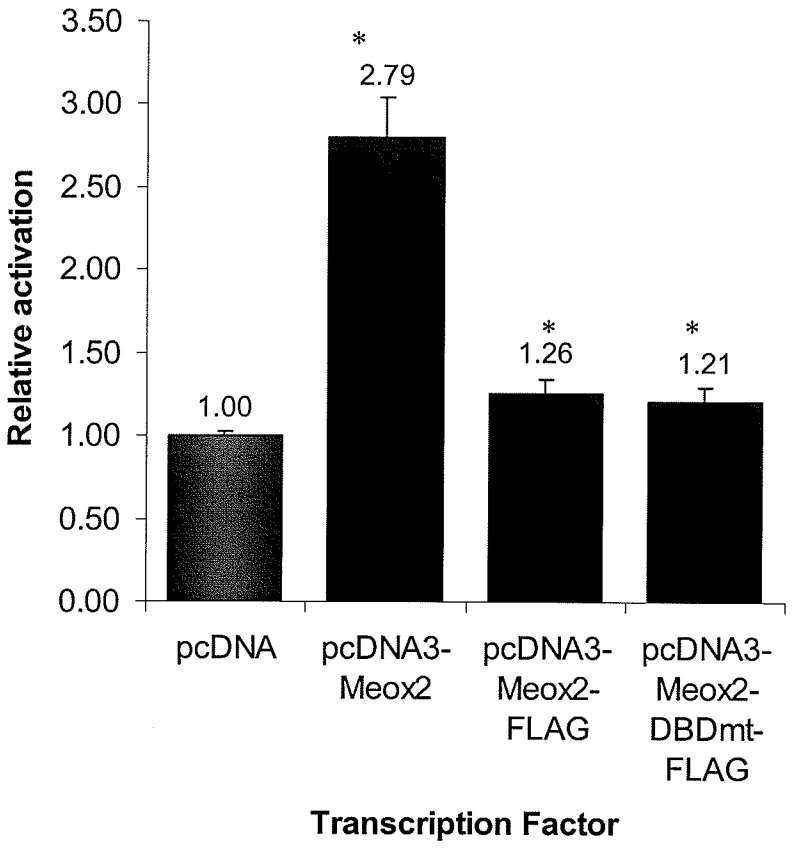

Figure 29: The carboxyl-terminal FLAG epitope reduces Meox2 activation of the *p21* promoter

Luciferase assay results demonstrating that the untagged Meox2 (pcDNA3-Meox2) was a superior transcriptional activator of the 850 bp *p21* promoter than the FLAG epitope tagged versions (pcDNA3-Meox2-FLAG and pcDNA3-Meox2-DBD^{mt}-FLAG). N=9, *$p<0.005$.

E) DISCUSSION

Since Meox2 induces both cell cycle arrest and apoptosis it has been proposed as a potential therapeutic target for the treatment of cardiovascular diseases, such as atherosclerosis and post-balloon angioplasty restenosis that result from excessive cell proliferation. Stimulating these Meox2-mediated functions in the treatment of tumors would be beneficial in inhibiting angiogenesis, a process important for both tumor growth and dissemination [11, 12]. Meox1 and Meox2 contain homeodomains and are therefore thought to function as transcription factors which bind to and regulate transcription from the promoters of target genes. Prior to our investigation, little was known about the mechanisms used by this family of homeodomain proteins to regulate the expression of their downstream target genes.

The main goal of our research is to better understand how Meox2 mediates its anti-proliferative and pro-apoptotic function. Therefore we chose to study the how Meox2 regulates transcription from the *p21* promoter. Originally we hypothesized that Meox2 would use the same mechanism on this promoter as it used to regulate expression from the *Bapx1* promoter. The *Bapx1* promoter was previously shown to be regulated by Meox1. Our study has demonstrated that Meox1 and Meox2 transcription factors can act both as either direct transcription activators or co-activators of transcription. The mechanism of action used by Meox1/Meox2 is promoter specific.

In this study we showed that Meox2 could activate the *Bapx1* promoter in NIH/3T3 fibroblasts and we demonstrated that this activation required Meox2 to be able to bind to DNA. Previously, work by Rodrigo *et al.* had indicated that this promoter was regulated by Meox1 *in vitro* using luciferase assays [117]. Both Meox1 and Meox2 were also shown to bind to a TAAT consensus sequence in the *Bapx1* promoter [117].

However, the functional importance of Meox1 and/or Meox2 direct binding to this promoter was not addressed. We established that Meox2 could activate the *Bapx1* promoter to a level similar to that induced by Meox1 (Figure 11). Using the DNA binding mutant versions of Meox2, we also determined that it was necessary for Meox2 to bind to the *Bapx1* promoter in order to activate expression (Figure 12). Experiments using VP16-Meox2 chimeric proteins showed that Meox2 acts a transcriptional activator to regulate Bapx1 expression (Figure 13).

To our knowledge, this is the first report that Meox1 and Meox2 can activate the same target genes. Given that the homeodomains of these proteins are 95% identical, we predicted that they would recognize similar DNA sequences. Also, this similar target gene specificity supports the mouse gene knockout studies that had indicated the Meox proteins have redundant functions during embryonic development [110]. As we had initially predicted, Meox2 regulates gene transcription by acting as a direct transcription activator and not as a co-activator.

EMSA experiments with the TAAT sequences of the *Bapx1* promoter were used to establish our non-radioactive EMSA assay. This oligonucleotide sequence had previously been shown to bind both Meox1 and Meox2 [117]. These experiments were important because they allowed us to directly establish that the DBD mutation blocked DNA binding by Meox1 (Figure 14). However, we were unsuccessful using EMSA to show that Meox2 bound to this consensus sequence (Figure 15). Our inability to demonstrate Meox2 binding to this site may result from differences in the procedures used to obtain protein samples or the different sensitivities of the available EMSA technologies used. Rodrigo *et al.* used a radioactive EMSA technique and recombinant proteins synthesized with the TNT-coupled wheat germ extract system [117]. We used

the Pierce Lightshift Chemiluminescent EMSA kit and both nuclear extracts and bacterially expressed recombinant protein. It is possible that the amino-terminal MBP domain interfered with Meox2 binding to DNA. In Rodrigo *et al.*'s work, the Meox2 band in the EMSA was unresolved and faint, possibly indicating that there was a weak binding of Meox2 to DNA [117]. Since we could not identify a complex being formed between Meox2 and the *Bapx1* probe, we were unable to directly establish the effect of the DBD mutation on the ability of Meox2 to bind to DNA. However, we believe that this mutation blocks DNA binding by Meox2 as we had shown for Meox1 since the homeodomains of these proteins are 95% identical.

We initially hypothesized that Meox1 and Meox2 would act as direct transcriptional activators of the *p21* promoter. Contrary to our hypothesis, our experiments with the human *p21* promoter revealed that the Meox proteins acted as transcriptional co-activators on this promoter since DNA binding was not necessary for reporter gene expression. Our initial experiments were conducted using the 2.4 kb promoter and we showed that Meox1 and Meox2 equivalently activated transcription from this promoter (Figure 18). To our knowledge, this is the first demonstration that Meox1 activates the *p21* promoter and, thus, has a role in inhibiting cell cycle progression. Experiments using the truncated *p21* promoter constructs showed that Meox2 and Meox1 activation of the *p21* promoter is independent of p53 binding to the promoter (Figure 19). Previously, Smith *et al.* had shown that Meox2 induced *p21* transcription and protein expression in *p53* -/- MEFs [34]. Our experiments were the first to show that Meox1 activated the *p21* promoter in a p53 independent manner.

To determine whether Meox1 or Meox2 require DNA binding, to activate the *p21* promoter, we conducted luciferase assays using DNA binding defective versions of

Meox1/2. Our results using the HD deleted and DBD mutated versions of these proteins indicated that the mutant versions of Meox1/2 were as effective as wild-type in activating the *p21* promoter *in vitro* (Figure 19). Meox1 and Meox2 are not well conserved in regions outside of their homeodomains. Therefore the ability of the HD deleted Meox proteins to equivalently activate a target gene was surprising. The three-dimensional structures of the Meox proteins have not been resolved and thus it is possible that they share conformational similarities that are not easily detectable at the amino acid level.

Transfection efficiencies were low in these experiments so we switched from a Ca^{2+} phosphate to the Lipofectamine 2000 transfection method in order to ensure that differences in activation between the Meox constructs were not being obscured. Since Meox1 and Meox2 appeared to be acting by similar mechanisms, further experiments were conducted only with Meox2. Using Lipofectamine 2000 reagent, Meox2 was shown to activate the *p21* promoter in a dose dependent manner independent of Meox2 binding directly to DNA (Figure 20 and 21). Interestingly, the amino-terminal end of Meox2 was able to activate the *p21* promoter similar to wild-type Meox2 (Figure 22). Basal *p21* promoter activation levels did vary between the different truncated promoter constructs, possible due to the presence of the p53 binding sites only in the 2.4 kb promoter (Figure 25A). However, Meox2 similarly induced expression from all of the truncated promoter constructs including the 200 bp *p21* promoter (Figure 25B and data not shown). Interestingly, the 400 bp and 200 bp *p21* promoter constructs do not contain any homeodomain consensus binding sites. In summary, our data supports a role for Meox2 as a co-activator of the *p21* promoter. This result was intriguing given that we had previously shown that Meox2 acted as a direct transcriptional activator of the *Bapx1* promoter.

We predicted that the DBD mutation of the VP16-Meox2 chimeric protein would have little or no effect on its activation of the *p21* promoter since Meox2 does not need to bind to DNA to activate this promoter. Surprisingly, the DBD mutation reduced the VP16-Meox2 mediated activation of the 850 bp promoter by 48% (Figure 23). How this mutation was affecting *p21* promoter activation remains unclear. The VP16-Meox2-FLAG fusion protein only contains the Meox2 homeodomain and carboxyl-terminal regions. Since the amino-terminal domain was shown to be sufficient to activate the *p21* promoter (Figure 22), we believed that a different mechanism of action may be employed by this fusion construct as it did not contain the amino-terminal region (Figure 8). Perhaps this fusion protein was relying on DNA binding through the homeodomain binding to the TAAT consensus sequences in the *p21* promoter. This hypothesis was tested by comparing the activation levels of the 500 bp and 400 bp versions *p21* promoters with the different VP16-Meox2 chimeric proteins (Figure 24). The same level of activation was observed whether the 850 bp, 500 bp or 400 bp *p21* promoter constructs were used indicating that the VP16-Meox2-FLAG chimeric protein was not targeting the *p21* promoter by binding to the homeodomain response elements since these are missing in the 400 bp *p21* promoter (Figure 23 and 24).

Not only is the 400 bp *p21* promoter activated by the VP16-Meox2-FLAG fusion protein, it is also activated by the wild-type Meox2, Meox2-N-term-FLAG and Meox2ΔHD-FLAG proteins (Figure 25 and data not shown). Furthermore, the activation levels obtained with these proteins were similar to levels obtained when either the 2.4 kb or 850 bp *p21* promoters were used, indicating that the truncated promoter contained the Meox2 responsive sites.

The studies using VP16-Meox2-FLAG complicated our model of how Meox2 activates the *p21* promoter. The following model is proposed to explain how Meox2 can activate the *p21* promoter in HEK293 cells. Firstly, Meox2 may form a complex with other proteins (transcription factors/co-activators or co-repressors) that are bound to the *p21* promoter in this cell line. These interactions could be mediated through both the amino-terminal and carboxyl-terminal regions (including the HD) of Meox2 and may involve one or more distinct accessory proteins (Figure 30). This redundant targeting is suggested since both the amino-terminal Meox2 domain and the VP16-Meox2 (homeodomain/carboxyl-terminal region) could activate the *p21* promoter. Due to the redundant targeting of the *p21* promoter by both the amino-terminal and carboxyl-terminal regions (including the homeodomain), all Meox2 proteins containing at least one of these domains would still be able to target this promoter. Luciferase results with the amino-terminal region of Meox2 showed that this domain contains all of the necessary sequences for activating the *p21* promoter. Thus, the wild-type, HD deleted, DBD^{mt} and amino-terminal Meox2 proteins, which all contain the amino terminal region, would all be able to bind and activate the *p21* promoter indirectly (through an intermediary protein). The same mechanism is hypothesized to occur for similar Meox1 constructs (Figure 19 and data not shown for its amino-terminal construct).

The VP16-Meox2 fusion proteins do not contain the amino-terminal region of Meox2 but they have a strong activation domain. They would therefore be able to bind to the *p21* promoter through interactions with nuclear factors and the Meox2 homeodomain and carboxyl-terminal regions and activate the *p21* promoter through the VP16 activation domain. Why then did the DBD mutation significantly affect activation by this fusion protein? Evidence from our immunocytochemistry experiments suggests that this

mutation has a more complicated effect on Meox2 function than just abolishing DNA binding, since the point mutation was shown to have an effect on the subcellular distribution of Meox2. If this mutation has altered the conformation of the Meox2 protein, it could possibly interfere with the interaction between the Meox2 homeodomain and carboxyl-terminal regions with proteins bound to the *p21* promoter and therefore reduce activation of the *p21* promoter. In our luciferase assays this would result in decreased activation by VP16-Meox2-DBD^{mt}-FLAG when compared to VP16-Meox2-FLAG.

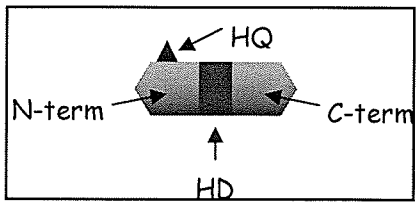

Figure 30: Models of Meox2 protein interactions with the *p21* promoter

Meox2 doesn't require DNA binding to activate the *p21* promoter. The wild-type protein (A) interacts with other proteins bound to the *p21* promoter (shown as hypothetical proteins x and y). Both the amino and carboxyl termini including the homeodomain can target Meox2 to the promoter through these protein-protein interactions. Proteins A, B, C and D activate equally. Protein E is missing the Meox2 AD but contains the VP16 AD and can target the *p21* promoter through the Meox2 HD and carboxyl-terminus binding to protein Y. Proteins C and F contain the DBD mutation which possibly changes the conformation of the Meox2 protein and partially inhibits its interaction with nuclear factors. In the case of protein C, an intact amino-terminus of Meox2 is present therefore targeting as well as activation are still possible. For protein F, targeting is partially inhibited and thus activation levels are lower than with protein E.

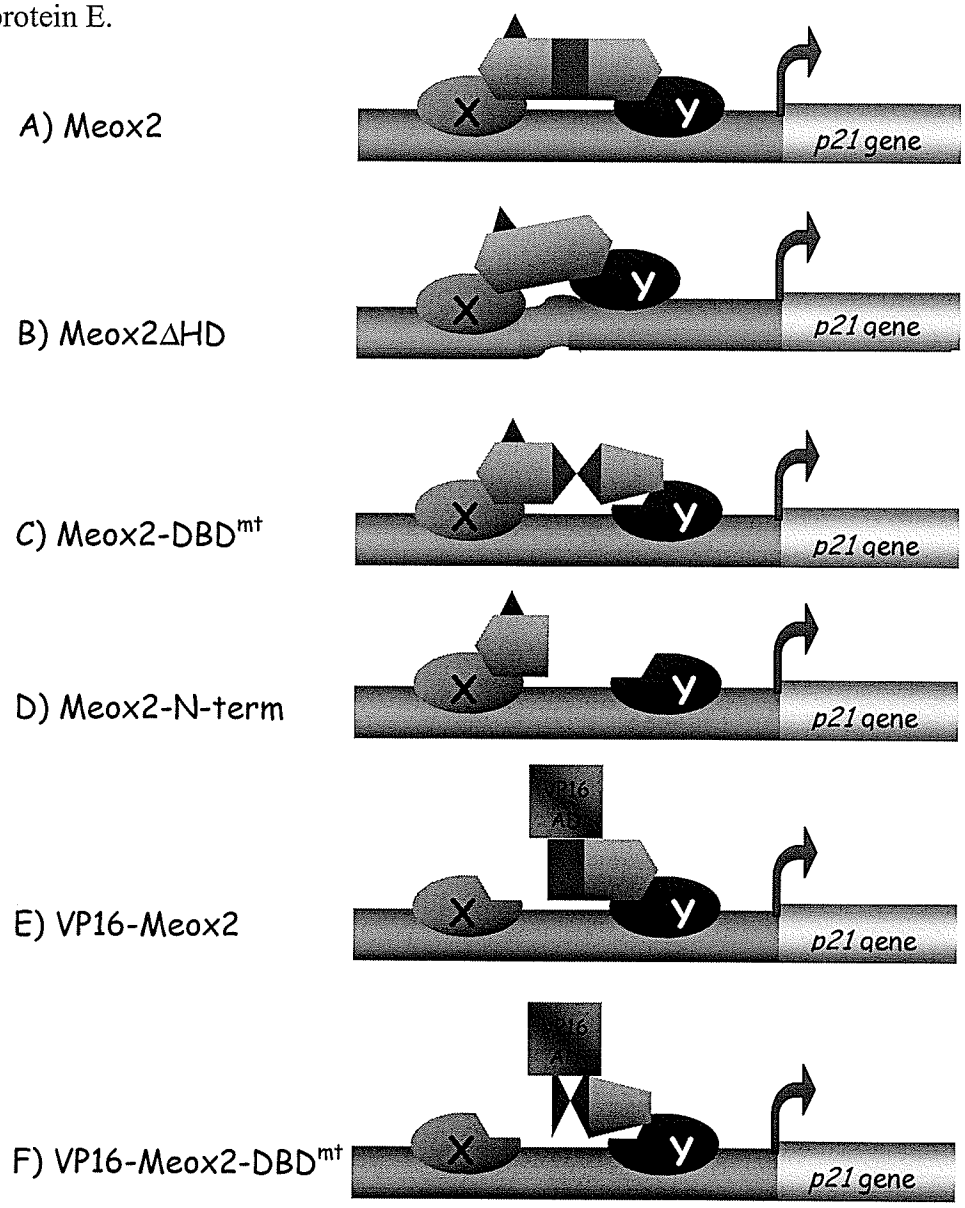

The mechanism of Meox2 activation of the *p21* promoter that we have proposed in this study, through the use of luciferase assays, contrasts with previous results obtained by Smith *et al.* This group determined that Meox2 could up-regulate expression from the *p21* promoter 3.4 fold versus controls and that this activation required the Meox HD [34]. Contrary to our results, their work supports a DNA binding dependent mechanism of Meox2 activation of this promoter. These discrepancies may arise from several differences between our experimental protocols. Smith *et al.* used primary mouse embryonic fibroblasts for their experiments, whereas we used HEK293 cells derived from human embryonic kidney. Luciferase assay results can differ depending on the particular cell line used [106, 107]. This is likely due to the differences in protein expression profiles of each cell line and, thus, potentially different proteins being bound to the promoters studied. Smith *et al.* also performed their experiments under conditions of serum starvation whereas our cells, except during the four hour transfection procedure, were cultured in regular growth media which have high levels of growth factors.

We performed experiments using the NIH/3T3 fibroblast cell line but we were unable to activate the *p21* promoter above basal levels in these cells. Interestingly, the basal *p21* promoter activity was up to 110 fold higher in NIH/3T3 cells compared to HEK293 cells. High levels of *p21* expression have been detected at the mRNA level by RT-PCR in NIH/3T3 cells [130]. In NIH/3T3 cells, the *p21* promoter may be maximally activated and therefore no longer responsive to Meox2 transfection. Alternatively, the DNA binding proteins necessary for mediating Meox2 responsiveness may not be expressed and therefore are not bound to the *p21* promoter in the NIH/3T3 cells. We could not replicate Smith *et al.*'s results using this cell line and, in the future, we will

investigate Meox2-mediated regulation of *p21* expression in primary cultured VSMCs or MEFs.

Future experiments using EMSAs will identify the region of the *p21* promoter that is bound by the nuclear factor complex that includes Meox2. Also, chromatin immunoprecipitation experiments will allow us to determine if the Meox2 mutant proteins are loaded on the endogenous *p21* promoter (via protein-protein interactions) as has been suggested by our luciferase assay results. These experiments will provide more evidence supporting the DNA binding independent activation of the *p21* promoter by Meox2. Western blot analysis of p21 protein levels will also be performed to verify that the forced expression of the various Meox2 proteins results in increased p21 protein levels.

Since our objective is to understand Meox2 mediated cell cycle arrest in VSMCs and cardiomyocytes, we would also like to study Meox2 regulation of $p19^{INK4d}$ and $p57^{kip2}$. Recent work by Patel *et al.* has identified these genes as being differentially regulated when Meox2 is overexpressed in endothelial cells [83].

During this study we also determined that the carboxyl-terminal FLAG tag was inhibiting the ability of Meox2 to activate specific gene promoters. This effect was seen in both HEK293 cells transfected with the *p21* promoter and NIH/3T3 cells transfected with the *Bapx1* promoter (Figures 27-29). Therefore this inhibitory effect does not seem to be cell type or promoter specific. Use of an amino-terminal FLAG tag may reduce this interference while still permitting the detection of proteins by immunocytochemistry and western blot analysis.

Many other observations that warrant further investigation were made during the course of this study. For instance, the immunocytochemistry results demonstrated that

Meox1ΔHD-FLAG, Meox2ΔHD-FLAG and Meox2-N-term-FLAG were found within the cytoplasm of cells whereas the wild type proteins were localized to the nucleus (Figure 9). Whether these mutant proteins are completely excluded from the nuclei remains to be determined using a combination of confocal microscopy and subcellular fractionation. Meox1 and Meox2 contain a nuclear localization sequence (NLS) within their homeodomains that is similar to the NLS of the homeodomain protein PDX1 and HB9 [131, 132]. Mutation or deletion of this NLS altered the subcellular distribution of Meox2 (both Flag and EGFP versions) (Wigle *et al.*, unpublished data). This data supports a functional role for this NLS in controlling Meox2's subcellular distribution. Interestingly, the DBD mutation also changes the localization of Meox2-FLAG from the nucleus to the cytoplasm. The involvement of the DBD in nuclear targeting is not unprecedented and has been demonstrated for other proteins including the homeodomain protein TTF-1 [133, 134]. Also, the HB9 homeodomain protein contains both a bipartite NLS and a PDX-like hexapeptide NLS within its homeodomain [132]. Similar mechanisms of nuclear targeting may be used by the Meox proteins. We predict that the DBD point mutation (Q50E) changes the local conformation of the homeodomain sufficiently to alter the conformation of the immediately adjacent PDX1-like NLS, thus changing the distribution of the mutant Meox2 protein. Characterizing precisely how the DBD mutation affects Meox2 nuclear localization requires further studies into the mechanism underlying the translocation of this protein into the nucleus.

Another observation from the immunocytochemistry experiments was the lack of cells expressing Meox2ΔHD-FLAG and Meox2-DBD^{mt}-FLAG 48 hours post-transfection. At 24 hours post-transfection, the level of expression of these proteins was

comparable to that of staining for Meox2-FLAG (Figure 9). Quantification of these results was beyond the scope of this study.

F) CONCLUSIONS

1) Meox1 and Meox2 activate the same target gene promoters.
2) Meox2 acts as an activator (DNA binding dependent) of the *Bapx1* promoter.
3) The DNA binding domain mutation (Q50E mutation) abolishes Meox1 binding to a *Bapx1* promoter oligonucleotide probe.
4) Meox1 and Meox2 act as co-activators (DNA binding independent) of the *p21* promoter.
5) Expression of the Meox amino-terminal domain is sufficient to activate the *p21* promoter.
6) Expression of the Meox2 homeodomain and the carboxyl-terminal region fused to the VP16 AD is able to activate the *p21* promoter.
7) The Meox2 DNA binding domain mutation alters Meox2 nuclear localization.

G) REFERENCES

1. Berk, B.C., *Vascular smooth muscle growth: autocrine growth mechanisms.* Physiol Rev, 2001. 81(3): p. 999-1030.
2. Gehring, W.J., M. Affolter, and T. Burglin, *Homeodomain proteins.* Annu Rev Biochem, 1994. 63: p. 487-526.
3. Bicknell, K.A., E.L. Surry, and G. Brooks, *Targeting the cell cycle machinery for the treatment of cardiovascular disease.* J Pharm Pharmacol, 2003. 55(5): p. 571-91.
4. Majesky, M.W., et al., *Rat carotid neointimal smooth muscle cells reexpress a developmentally regulated mRNA phenotype during repair of arterial injury.* Circ Res, 1992. 71(4): p. 759-68.
5. Casscells, W., *Migration of smooth muscle and endothelial cells. Critical events in restenosis.* Circulation, 1992. 86(3): p. 723-9.
6. Boehm, M. and E.G. Nabel, *The cell cycle and cardiovascular diseases.* Prog Cell Cycle Res, 2003. 5: p. 19-30.
7. Li, P.F., R. Dietz, and R. von Harsdorf, *Differential effect of hydrogen peroxide and superoxide anion on apoptosis and proliferation of vascular smooth muscle cells.* Circulation, 1997. 96(10): p. 3602-9.
8. Li, C. and Q. Xu, *Mechanical stress-initiated signal transductions in vascular smooth muscle cells.* Cell Signal, 2000. 12(7): p. 435-45.
9. Hu, Y., et al., *Activation of PDGF receptor alpha in vascular smooth muscle cells by mechanical stress.* FASEB, 1998. 12(12): p. 1135-42.

10. Sedding, D.G., et al., *Mechanosensitive p27Kip1 regulation and cell cycle entry in vascular smooth muscle cells.* Circulation, 2003. 108(5): p. 616-22.

11. Folkman, J. and R. Kalluri, *Cancer without disease.* Nature, 2004. 427(6977): p. 787.

12. Dass, C.R., *Tumour angiogenesis, vascular biology and enhanced drug delivery.* J Drug Target, 2004. 12(5): p. 245-55.

13. Oh, H., et al., *Cardiac progenitor cells from adult myocardium: homing, differentiation, and fusion after infarction.* Proc Natl Acad Sci U S A, 2003. 100(21): p. 12313-8.

14. Dowell, J.D., L.J. Field, and K.B. Pasumarthi, *Cell cycle regulation to repair the infarcted myocardium.* Heart Fail Rev, 2003. 8(3): p. 293-303.

15. Itescu, S., M.D. Schuster, and A.A. Kocher, *New directions in strategies using cell therapy for heart disease.* J Mol Med, 2003. 81(5): p. 288-96.

16. Regula, K.M. and L.A. Kirshenbaum, *Breaking down cell-cycle barriers in the adult heart.* Circ Res, 2004. 94(12): p. 1524-6.

17. Pasumarthi, K.B. and L.J. Field, *Cardiomyocyte cell cycle regulation.* Circ Res, 2002. 90(10): p. 1044-54.

18. Hartwell, L.H. and T.A. Weinert, *Checkpoints: controls that ensure the order of cell cycle events.* Science, 1989. 246(4930): p. 629-34.

19. Weinert, T.A., G.L. Kiser, and L.H. Hartwell, *Mitotic checkpoint genes in budding yeast and the dependence of mitosis on DNA replication and repair.* Genes Dev, 1994. 8(6): p. 652-65.

20. Fisher, R.P. and D.O. Morgan, *A novel cyclin associates with MO15/CDK7 to form the CDK-activating kinase.* Cell, 1994. 78(4): p. 713-24.

21. Espinoza, F.H., et al., *A cyclin-dependent kinase-activating kinase (CAK) in budding yeast unrelated to vertebrate CAK.* Science, 1996. 273(5282): p. 1714-7.

22. Morgan, D.O., et al., *Control of eukaryotic cell cycle progression by phosphorylation of cyclin-dependent kinases.* Cancer J Sci Am, 1998. 4 Suppl 1: p. S77-83.

23. Glotzer, M., A.W. Murray, and M.W. Kirschner, *Cyclin is degraded by the ubiquitin pathway.* Nature, 1991. 349(6305): p. 132-8.

24. Cheng, A., et al., *Identification and Comparative Analysis of Multiple Mammalian Speedy/Ringo Proteins.* Cell Cycle, 2005. 4(1).

25. Dinarina, A., et al., *Characterization of a new family of cyclin-dependent kinase activators.* Biochem J, 2005. 386(Pt 2): p. 349-55.

26. Tsai, L.H., et al., *p35 is a neural-specific regulatory subunit of cyclin-dependent kinase 5.* Nature, 1994. 371(6496): p. 419-23.

27. Lew, J., et al., *A brain-specific activator of cyclin-dependent kinase 5.* Nature, 1994. 371(6496): p. 423-6.

28. Tarricone, C., et al., *Structure and regulation of the CDK5-p25(nck5a) complex.* Mol Cell, 2001. 8(3): p. 657-69.

29. Sherr, C.J. and J.M. Roberts, *CDK inhibitors: positive and negative regulators of G1-phase progression.* Genes Dev, 1999. 13(12): p. 1501-12.

30. Mainprize, T.G., et al., *Cip/Kip cell-cycle inhibitors: a neuro-oncological perspective.* J Neurooncol, 2001. 51(3): p. 205-18.

31. el-Deiry, W.S., et al., *WAF1, a potential mediator of p53 tumor suppression.* Cell, 1993. 75(4): p. 817-25.

32. Espinosa, J.M. and B.M. Emerson, *Transcriptional regulation by p53 through intrinsic DNA/chromatin binding and site-directed cofactor recruitment.* Mol Cell, 2001. 8(1): p. 57-69.

33. Perlman, H., et al., *GATA-6 induces p21(Cip1) expression and G1 cell cycle arrest.* J Biol Chem, 1998. 273(22): p. 13713-8.

34. Smith, R.C., et al., *p21CIP1-mediated inhibition of cell proliferation by overexpression of the gax homeodomain gene.* Genes Dev, 1997. 11(13): p. 1674-89.

35. Gorski, D.H. and A.J.M. Leal, *Inhibition of endothelial cell activation by the homeobox gene Gax.* J Surg Res, 2003. 111(1): p. 91-9.

36. Garcia-Bellido, A., *Genetic control of wing disc development in Drosophila.* Ciba Found Symp, 1975. 0(29): p. 161-82.

37. Garcia-Bellido, A., *Homeotic and atavic mutations in insects.* American Zoology, 1977. 17: p. 613-629.

38. Garcia-Bellido, A., *Cell affinities in antennal homoeotic mutants of Drosophila melanogaster.* Genetics, 1968. 59(4): p. 487-99.

39. McGinnis, W., et al., *A homologous protein-coding sequence in Drosophila homeotic genes and its conservation in other metazoans.* Cell, 1984. 37(2): p. 403-8.

40. Kisters-Woike, B., et al., *A model of the lac repressor-operator complex based on physical and genetic data.* Eur J Biochem, 1991. 198(2): p. 411-9.

41. Schevitz, R.W., et al., *The three-dimensional structure of trp repressor.* Nature, 1985. 317(6040): p. 782-6.

42. Wolberger, C., et al., *Crystal structure of a MAT alpha 2 homeodomain-operator complex suggests a general model for homeodomain-DNA interactions.* Cell, 1991. 67(3): p. 517-28.

43. Gros, F., *[Developmental genes].* C R Seances Soc Biol Fil, 1997. 191(1): p. 7-20.

44. Ohto, H., et al., *Cooperation of six and eya in activation of their target genes through nuclear translocation of Eya.* Mol Cell Biol, 1999. 19(10): p. 6815-24.

45. Li, X., C. Murre, and W. McGinnis, *Activity regulation of a Hox protein and a role for the homeodomain in inhibiting transcriptional activation.* EMBO, 1999. 18(1): p. 198-211.

46. Jaynes, J.B. and P.H. O'Farrell, *Active repression of transcription by the engrailed homeodomain protein.* EMBO J, 1991. 10(6): p. 1427-33.

47. Gorski, D.H. and K.M. Walsh, *The role of homeobox genes in vascular remodeling and angiogenesis.* Circ Res, 2000. 87(10): p. 865-72.

48. Kenyon, C., *If birds can fly, why can't we? Homeotic genes and evolution.* Cell, 1994. 78(2): p. 175-80.

49. Abate-Shen, C., *Deregulated homeobox gene expression in cancer: cause or consequence?* Nat Rev Cancer, 2002. 2(10): p. 777-85.

50. Lawrence, P.A. and G. Morata, *Homeobox genes: their function in Drosophila segmentation and pattern formation.* Cell, 1994. 78(2): p. 181-9.

51. Jones, P.L., *Homeobox genes in pulmonary vascular development and disease.* Trends Cardiovasc Med, 2003. 13(8): p. 336-45.

52. Nunes, F.D., et al., *Homeobox genes: a molecular link between development and cancer.* Pesqui Odontol Bras, 2003. 17(1): p. 94-8.

53. Candia, A.F., et al., *Mox-1 and Mox-2 define a novel homeobox gene subfamily and are differentially expressed during early mesodermal patterning in mouse embryos.* Development, 1992. 116(4): p. 1123-36.

54. Gorski, D.H., et al., *Molecular cloning of a diverged homeobox gene that is rapidly down-regulated during the G0/G1 transition in vascular smooth muscle cells.* Mol Cell Biol, 1993. 13(6): p. 3722-33.

55. LePage, D.F., et al., *Molecular cloning and localization of the human GAX gene to 7p21.* Genomics, 1994. 24(3): p. 535-40.

56. Deguchi, Y., et al., *Cloning of a human homeobox gene that resembles a diverged Drosophila homeobox gene and is expressed in activated lymphocytes.* New Biol, 1991. 3(4): p. 353-63.

57. Wharton, K.A., et al., *opa: a novel family of transcribed repeats shared by the Notch locus and other developmentally regulated loci in D. melanogaster.* Cell, 1985. 40(1): p. 55-62.

58. Zhang, N., et al., *Three distinct domains in the HOX-11 homeobox oncoprotein are required for optimal transactivation.* Oncogene, 1996. 13(8): p. 1781-7.

59. Lin, J., et al., *Characterization of Mesenchyme Homeobox 2 (MEOX2) transcription factor binding to RING finger protein 10.* Molecular and Cellular Biochemistry, article in press.

60. Candia, A.F., J.P. Kovalik, and C.V. Wright, *Amino acid sequence of Mox-2 and comparison to its Xenopus and rat homologs.* Nucleic Acids Res, 1993. 21(21): p. 4982.

61. Grigoriou, M., et al., *Isolation of the human MOX2 homeobox gene and localization to chromosome 7p22.1-p21.3.* Genomics, 1995. 26(3): p. 550-5.

62. Degnan, B.M., et al., *A Mox homeobox gene in the gastropod mollusc Haliotis rufescens is differentially expressed during larval morphogenesis and metamorphosis.* FEBS Lett, 1997. 411(1): p. 119-22.

63. Hill, A., A. Wagner, and M. Hill, *Hox and paraHox genes from the anthozoan Parazoanthus parasiticus.* Mol Phylogenet Evol, 2003. 28(3): p. 529-35.

64. Fisher, S.A., et al., *Forced expression of the homeodomain protein Gax inhibits cardiomyocyte proliferation and perturbs heart morphogenesis.* Development, 1997. 124(21): p. 4405-13.

65. Markmann, A., et al., *Expression of transcription factors and matrix genes in response to serum stimulus in vascular smooth muscle cells.* Eur J Cell Biol, 2003. 82(3): p. 119-29.

66. Candia, A.F. and C.V.M. Wright, *Differential localization of Mox-1 and Mox-2 proteins indicates distinct roles during development.* Int J Dev Biol, 1996. 40(6): p. 1179-84.

67. Skopicki, H.A., et al., *Embryonic expression of the Gax homeodomain protein in cardiac, smooth, and skeletal muscle.* Circ Res, 1997. 80(4): p. 452-62.

68. Tallquist, M.D. and P. Soriano, *Epiblast-restricted Cre expression in MORE mice: a tool to distinguish embryonic vs. extra-embryonic gene function.* Genesis, 2000. 26(2): p. 113-5.

69. Rallis, C., et al., *Isolation of the avian homologue of the homeobox gene Mox2 and analysis of its expression pattern in developing somites and limbs.* Mech Dev, 2001. 104(1-2): p. 121-4.

70. Mankoo, B.S., et al., *Mox2 is a component of the genetic hierarchy controlling limb muscle development.* Nature, 1999. 400(6739): p. 69-73.

71. Pasteris, N.G., et al., *Discordant phenotype of two overlapping deletions involving the PAX3 gene in chromosome 2q35.* Hum Mol Genet, 1993. 2(7): p. 953-9.

72. Stamataki, D., et al., *Homeodomain proteins Mox1 and Mox2 associate with Pax1 and Pax3 transcription factors.* FEBS Lett, 2001. 499(3): p. 274-8.

73. Branellec, D., et al., *Regulation of smooth muscle cell migration and integrin expression by the Gax transcription factor.* J Clin Invest, 1999. 104: p. 1469-1480.

74. Branellec, D., et al., *Bax-mediated cell death by the Gax homeoprotein requires mitogen activation but is independent of cell cycle activity.* The EMBO Journal, 1998. 17(13): p. 3576-3586.

75. Chen, D., et al., *Expression of gax, a Growth Arrest Homeobox Gene, Is Rapidly Down-regulated in the Rat Carotid Artery during the Proliferative Response to Ballon Injury.* J Biol Chem, 1995. 270(10): p. 5457-5461.

76. Andres, V., et al., *Embryonic Expression of the Gax Homeodomain Protein in Cardiac, Smooth, and Skeletal Muscle.* Circ Res, 1997. 80(4): p. 452-462.

77. King, R., L. Philipson, and C. Schneider, *Genes Specifically Expressed at Growth Arrest of Mammalian Cells.* Cell, 1988. 54: p. 787-793.

78. Fargnoli, J., et al., *Mammalian Genes Coordinately Regulated by Growth Arrest Signals and DNA-Damaging Agents.* Mol Cell Bio, 1989. 9(10): p. 4196-4203.

79. Maillard, L., et al., *Percutaneous delivery of the gax gene inhibits vessel stenosis in a rabbit model of balloon angioplasty.* Cardiovasc Res, 1997. 35(3): p. 536-46.

80. Yamashita, J., et al., *Opposite regulation of Gax homeobox expression by angiotensin II and C-type natriuretic peptide.* Hypertension, 1997. 29(1 Pt 2): p. 381-7.

81. Saito, T., et al., *Angiotensin II suppresses growth arrest specific homeobox (Gax) expression via redox-sensitive mitogen-activated protein kinase (MAPK).* Regul Pept, 2005. 127(1-3): p. 159-67.

82. Campos, A.H., et al., *DNA microarray profiling to identify angiotensin-responsive genes in vascular smooth muscle cells: potential mediators of vascular disease.* Circ Res, 2003. 92(1): p. 111-8.

83. Patel, S., A.D. Leal, and D.H. Gorski, *The homeobox gene Gax inhibits angiogenesis through inhibition of nuclear factor-kappaB-dependent endothelial cell gene expression.* Cancer Res, 2005. 65(4): p. 1414-24.

84. Thullberg, M., et al., *Distinct versus redundant properties among members of the INK4 family of cyclin-dependent kinase inhibitors.* FEBS Lett, 2000. 470(2): p. 161-6.

85. Lee, M.H., I. Reynisdottir, and J. Massague, *Cloning of p57KIP2, a cyclin-dependent kinase inhibitor with unique domain structure and tissue distribution.* Genes Dev, 1995. 9(6): p. 639-49.

86. Matsuoka, S., et al., *p57KIP2, a structurally distinct member of the p21CIP1 Cdk inhibitor family, is a candidate tumor suppressor gene.* Genes Dev, 1995. 9(6): p. 650-62.

87. Yan, Y., et al., *Ablation of the CDK inhibitor p57Kip2 results in increased apoptosis and delayed differentiation during mouse development.* Genes Dev, 1997. 11(8): p. 973-83.

88. Zhang, P., et al., *Altered cell differentiation and proliferation in mice lacking p57KIP2 indicates a role in Beckwith-Wiedemann syndrome.* Nature, 1997. 387(6629): p. 151-8.

89. Perlman, H., et al., *Bax-mediated cell death by the Gax homeoprotein requires mitogen activation but is independent of cell cycle activity.* EMBO J, 1998. 17(13): p. 3576-86.

90. Perlman, H., et al., *Adenovirus-mediated delivery of the Gax transcription factor to rat carotid arteries inhibits smooth muscle proliferation and induces apoptosis.* Gene Ther, 1999. 6(5): p. 758-63.

91. Witzenbichler, B., et al., *Regulation of smooth muscle cell migration and integrin expression by the Gax transcription factor.* J Clin Invest, 1999. 104(10): p. 1469-80.

92. Weir, L., et al., *Expression of gax, a growth arrest homeobox gene, is rapidly down-regulated in the rat carotid artery during the proliferative response to balloon injury.* J Biol Chem, 1995. 270(10): p. 5457-61.

93. Chariot, A., et al., *The homeodomain-containing proteins: an update on their interacting partners.* Biochem Pharmacol, 1999. 58(12): p. 1851-7.

94. Huang, J.Y., et al., *Functional interaction between nuclear matrix-associated HBXAP and NF-kappaB.* Exp Cell Res, 2004. 298(1): p. 133-43.

95. Harper, J.W., et al., *The p21 Cdk-interacting protein Cip1 is a potent inhibitor of G1 cyclin-dependent kinases.* Cell, 1993. 75(4): p. 805-16.

96. Gartel, A.L. and A.L. Tyner, *The role of the cyclin-dependent kinase inhibitor p21 in apoptosis.* Mol Cancer Ther, 2002. 1(8): p. 639-49.

97. Waga, S., et al., *The p21 inhibitor of cyclin-dependent kinases controls DNA replication by interaction with PCNA.* Nature, 1994. 369(6481): p. 574-8.

98. Luo, Y., J. Hurwitz, and J. Massague, *Cell-cycle inhibition by independent CDK and PCNA binding domains in p21Cip1.* Nature, 1995. 375(6527): p. 159-61.

99. Suzuki, A., et al., *Resistance to Fas-mediated apoptosis: activation of caspase 3 is regulated by cell cycle regulator p21WAF1 and IAP gene family ILP.* Oncogene, 1998. 17(8): p. 931-9.

100. Chai, F., et al., *Involvement of p21(Waf1/Cip1) and its cleavage by DEVD-caspase during apoptosis of colorectal cancer cells induced by butyrate.* Carcinogenesis, 2000. 21(1): p. 7-14.

101. Shin, B.A., et al., *Overexpressed human RAD50 exhibits cell death in a p21(WAF1/CIP1)-dependent manner: its potential utility in local gene therapy of tumor.* Cell Growth Differ, 2001. 12(5): p. 243-54.

102. Dong, Y., et al., *Cytosolic p21Waf1/Cip1 increases cell cycle transit in vascular smooth muscle cells.* Cell Signal, 2004. 16(2): p. 263-9.

103. Zhang, C., et al., *Ets-1 protects vascular smooth muscle cells from undergoing apoptosis by activating p21WAF1/Cip1: ETS-1 regulates basal and and inducible p21WAF1/Cip: ETS-1 regulates basal and inducible p21WAF1/Cip1 transcription via distinct cis-acting elements in the p21WAF/Cip1 promoter.* J Biol Chem, 2003. 278(30): p. 27903-9.

104. Kavurma, M.M. and L.M. Khachigian, *Sp1 inhibits proliferation and induces apoptosis in vascular smooth muscle cells by repressing p21WAF1/Cip1 transcription and cyclin D1-Cdk4-p21WAF1/Cip1 complex formation.* J Biol Chem, 2003. 278(35): p. 32537-43.

105. LaBaer, J., et al., *New functional activities for the p21 family of CDK inhibitors.* Genes Dev, 1997. 11(7): p. 847-62.

106. Bromleigh, V.C. and L.P. Freedman, *p21 is a transcriptional target of HOXA10 in differentiating myelomonocytic cells.* Genes Dev, 2000. 14(20): p. 2581-6.

107. Bai, Y.Q., et al., *CDX2, a homeobox transcription factor, upregulates transcription of the p21/WAF1/CIP1 gene.* Oncogene, 2003. 22(39): p. 7942-9.

108. Gorski, D.H. and A.J. Leal, *Inhibition of endothelial cell activation by the homeobox gene Gax.* J Surg Res, 2003. 111(1): p. 91-9.

109. Smith, R.C., et al., *p21CIP1-mediated inhibition of cell proliferation by overexpression of the gax homeodomain gene.* Genes Dev, 1997. 11(13): p. 1674-89.

110. Mankoo, B.S., et al., *The concerted action of Meox homeobox genes is required upstream of genetic pathways essential for the formation, patterning and differentiation of somites.* Development, 2003. 130(19): p. 4655-64.

111. Tribioli, C. and T. Lufkin, *Molecular cloning, chromosomal mapping and developmental expression of BAPX1, a novel human homeobox-containing gene homologous to Drosophila bagpipe.* Gene, 1997. 203(2): p. 225-33.

112. Azpiazu, N. and M. Frasch, *tinman and bagpipe: two homeo box genes that determine cell fates in the dorsal mesoderm of Drosophila.* Genes Dev, 1993. 7(7B): p. 1325-40.

113. Tribioli, C. and T. Lufkin, *The murine Bapx1 homeobox gene plays a critical role in embryonic development of the axial skeleton and spleen.* Development, 1999. 126(24): p. 5699-711.

114. Hecksher-Sorensen, J., et al., *The splanchnic mesodermal plate directs spleen and pancreatic laterality, and is regulated by Bapx1/Nkx3.2.* Development, 2004. 131(19): p. 4665-75.

115. Lettice, L.A., et al., *The mouse bagpipe gene controls development of axial skeleton, skull, and spleen.* Proc Natl Acad Sci U S A, 1999. 96(17): p. 9695-700.

116. Peters, H., et al., *Pax1 and Pax9 synergistically regulate vertebral column development.* Development, 1999. 126(23): p. 5399-408.

117. Rodrigo, I., et al., *Meox homeodomain proteins are required for Bapx1 expression in the sclerotome and activate its transcription by direct binding to its promoter.* Mol Cell Biol, 2004. 24(7): p. 2757-66.

118. Akazawa, H., et al., *Targeted disruption of the homeobox transcription factor Bapx1 results in lethal skeletal dysplasia with asplenia and gastroduodenal malformation.* Genes Cells, 2000. 5(6): p. 499-513.

119. Rodrigo, I., et al., *Pax1 and Pax9 activate Bapx1 to induce chondrogenic differentiation in the sclerotome.* Development, 2003. 130(3): p. 473-82.

120. Barik, S., *Site-directed mutagenesis by double polymerase chain reaction.* Mol Biotechnol, 1995. 3(1): p. 1-7.

121. Weiner, M.P. and G.L. Costa, *Rapid PCR site-directed mutagenesis.* PCR Methods Appl, 1994. 4(3): p. S131-6.

122. Chen, C. and H. Okayama, *High-efficiency transformation of mammalian cells by plasmid DNA.* Mol Cell Biol, 1987. 7(8): p. 2745-52.

123. Talcott, B. and M.S. Moore, *Getting across the nuclear pore complex.* Trends Cell Biol, 1999. 9(8): p. 312-8.

124. Simon, M.D., et al., *A phage display selection of engrailed homeodomain mutants and the importance of residue Q50.* Nucleic Acids Res, 2004. 32(12): p. 3623-31.

125. Kessler, D.S., *Siamois is required for formation of Spemann's organizer.* Proc Natl Acad Sci U S A, 1997. 94(24): p. 13017-22.

126. Nishizawa, M., et al., *Artificial oncoproteins: modified versions of the yeast bZip protein GCN4 induce cellular transformation.* Oncogene, 2003. 22(39): p. 7931-41.

127. Onda, M., et al., *Analysis of gene network regulating yeast multidrug resistance by artificial activation of transcription factors: involvement of Pdr3 in salt tolerance.* Gene, 2004. 332: p. 51-9.

128. Markel, H., J. Chandler, and W. Werr, *Translational fusions with the engrailed repressor domain efficiently convert plant transcription factors into dominant-negative functions.* Nucleic Acids Res, 2002. 30(21): p. 4709-19.

129. Schmitt, J.F., et al., *Tissue-selective expression of dominant-negative proteins for the regulation of vascular smooth muscle cell proliferation.* Gene Ther, 1999. 6(6): p. 1184-91.

130. Ahn, J.Y., et al., *Transcriptional repression of p21(waf1) promoter by hepatitis B virus X protein via a p53-independent pathway.* Gene, 2001. 275(1): p. 163-8.

131. Moede, T., et al., *Identification of a nuclear localization signal, RRMKWKK, in the homeodomain transcription factor PDX-1.* FEBS Lett, 1999. 461(3): p. 229-34.

132. Kosaka, Y., et al., *Localization of HB9 homeobox gene mRNA and protein during the early stages of chick feather development.* Biochem Biophys Res Commun, 2000. 276(3): p. 1112-7.

133. Christophe-Hobertus, C., et al., *Critical residues of the homeodomain involved in contacting DNA bases also specify the nuclear accumulation of thyroid transcription factor-1.* Eur J Biochem, 1999. 265(1): p. 491-7.

134. LaCasse, E.C. and Y.A. Lefebvre, *Nuclear localization signals overlap DNA- or RNA-binding domains in nucleic acid-binding proteins.* Nucleic Acids Res, 1995. 23(10): p. 1647-56.